Order Number 9429609

Ribozyme-mediated cleavage of a synthetic *tat* gene transcript

Carlos, Ruben, Ph.D.

University of Hawaii, 1994

U·M·I

300 N. Zeeb Rd.
Ann Arbor, MI 48106

RIBOZYME-MEDIATED CLEAVAGE OF

A SYNTHETIC *tat* GENE TRANSCRIPT

A DISSERTATION SUBMITTED TO THE GRADUATE DIVISION OF THE UNIVERSITY OF HAWAII IN PARTIAL FULFILLMENT OF THE REQUIREMENTS FOR THE DEGREE OF

DOCTOR OF PHILOSOPHY

IN

BIOMEDICAL SCIENCES
(BIOCHEMISTRY)

MAY 1994

By

Ruben Carlos

Dissertation Committee:

Tom D. Humphreys, Chairperson
Frederick C. Greenwood
Morton Mandel
Alan F. Lau
Karen Yamaga

ACKNOWLEDGEMENTS

I would like to acknowledge the assistance, support and patience from the members of my dissertation committee. I would especially like to recognize Dr. Tom Humphreys, Dr. Fred Greenwood, and Dr. Morton Mandel for their guidance and advice throughout my tribulation as a graduate student. I thank Drs. Gregory Dolecki and Richard Lum for imparting the scientific homolog of the "green thumb," and Gordon Vansant, Lynn Godfrey, Cheryl Phillipson, and Brian Turano for their help, friendship, and encouragement over the years. I would also like to thank Shelley Ng, Nancy Budding, and the late Jeffrey Laigle for being such great friends. Finally, I would like to acknowledge the tremendous support of my parents, Benjamin and Remedios, and my family, who, although they did not quite understand what I was doing, held great faith in this endeavor.

ABSTRACT

HIV-1 has at least two genes, *tat* and *rev*, encoded by overlapping reading frames, involved in up-regulating HIV-1 transcription and replication. *Tat* encodes a nuclear protein that is a transcriptional *trans*-activator and *rev* encodes a protein regulating RNA splicing. The *tat/rev* RNA transcripts were examined as a target for cleavage by ribozymes, a possible means for "intracellular immunization" to treat HIV disease.

Ribozymes are RNA molecules that cleave other RNA molecules at specific motif sequences using a conserved sequence which folds into a catalytic secondary structure and targeting sequences, which form duplexes with the sequences flanking the cleavable motif in the targeted RNA molecules. Ribozymes RZ1, RZ2, $RZ3_{10}$, $RZ4_{12}$, and $RZ5_{14}$ were designed to cleave the *tat-s* transcript.

Both hammerhead ribozymes, derived from the (+)-strand satellite RNA of tobacco ringspot virus and a hairpin ribozyme, derived from the (-)-strand satellite RNA of tobacco ringspot virus were tested. These ribozymes do not cleave control actin RNA transcripts which possess sixteen cleavage motif sequences but lack flanking complementary ribozyme recognition sequences. The ribozymes cleave at the targeted site of the *tat-s* RNA in experiments performed under near physiological pH and temperature. Substrate cleavage rates show a dependence on both ribozyme and substrate concentrations suggesting that a bimolecular reaction with second order kinetics is the rate limiting reaction. $R_o t$ calculations of expected reactions rates at the lowest ribozyme concentrations indicate a $t_{1/2}$ reaction of ribozyme with substrate of

twenty-one minutes, suggesting that the bimolecular reaction should be completed quickly and not be the rate limiting step of substrate cleavage. It is proposed that the second order reaction rate is due to the continued dissociation and reassociation of the ribozyme:substrate complex before substrate cleavage. For perspective, the number of molecules required in a cell to achieve ribozyme concentrations perfomed in these studies were determined to be about 268 molecules/cell. From this cellular perspective, initial rate reaction experiments predict about 200 *tat-s* molecules/hour are cleaved. This rate may be sufficient to cleave the relatively low amounts of *tat* message in a quiescent HIV-infected cell.

TABLE OF CONTENTS

LIST OF TABLES

LIST OF FIGURES

LIST OF ABBREVIATIONS

AIDS:	Acquired immunodeficiency syndrome
ATP:	adenosine triphosphate
AZT:	3′-azido-2′,3′-dideoxythymidine
bp:	base pair
BRL:	Bethesda Research Laboratories
CAT:	chloramphenicol acetyl transferase
cDNA:	copy DNA
cm:	centimeter
CPM:	counts per minute
CTP:	cytosine triphosphate
°C:	degrees Celsius
DMSO:	dimethylsulfoxide
DNA:	2′-deoxyribonucleic acid
DNase:	deoxyribonuclease
ddH_2O:	doubly-distilled water
dTTP:	2′-deoxythymidine triphosphate
E. coli:	*Escherichia coli*
EDTA:	ethylenediaminetetraacetic acid
EtOH:	ethanol
GTP:	guanosine triphosphate
HIV:	Human immunodeficiency virus

IBI:	International Biotechnologies, Inc.
IFN-γ:	interferon-γ
IPTG:	isopropylthio-β-D-galactoside
kd:	kilodalton
kb:	kilobase pairs
LTR:	long terminal repeat
ml:	milliliter
µl:	microliter
µM:	micromolar
M:	molar
mm:	millimeter
mM:	millimolar
mRNA:	messenger RNA
ng:	nanogram
nt:	nucleotide
P1:	5′ tat-s cleavage product
P2:	3′ tat-s cleavage product
PCR:	polymerase chain reaction
pg:	picogram
pM:	picomolar
RNA:	ribonucleic acid
RNase:	ribonuclease

rNTP	ribonucleotide triphosphate
rpm:	revolutions per minute
RRE:	*rev*-response element
rRNA:	ribosomal RNA
RSV:	Rous sarcoma virus
SEVAG:	chloroform:iso-amyl alcohol 24:1
TAE:	0.04 M Tris-acetate, pH 8.0, 0.001 M EDTA
TAR:	*trans*-activating response (element)
TBE:	0.089 M Tris-borate, pH 8.3, 0.002 M EDTA
TE:	10.0 mM Tris, pH 7.6, 1.0 mM EDTA
tRNA:	transfer RNA
U:	units
UTP:	uridine triphosphate
UV:	ultraviolet
v/v:	volume per volume
w/v:	weight per volume
X-gal:	5-bromo-4-chloro-3-indolyl-β-D-galactoside

CHAPTER 1

INTRODUCTION

The Human Immunodeficiency Virus (HIV)

Acquired immunodeficiency syndrome (AIDS), first observed in the early 1980s in a subset of the human population, became pandemic within a few years, spreading throughout the populations of the world. The result of a depressed immune system, AIDS is characterized by the contraction of a series of opportunistic infections, one of which is the previously rare *Pneumocystis carinii* pneumonia, and the development of Kaposi's sarcoma, another previously rare form of cancer. By 1984, a human retrovirus, the human immunodeficiency virus (HIV), was shown to be the causative agent of AIDS (Barré-Sinoussi *et al.*, 1983; Gallo *et al.*, 1984; Levy *et al.*, 1984). Horizontal transmission of HIV is primarily through sexual or parenteral contact involving the exchange of bodily fluids that contain HIV and/or HIV-infected cells, while vertical transmission involves exposure to an infant through an HIV-infected mother (Blattner, 1991). From its biology, electron microscope morphology, and genomic structure, HIV has been placed into the lentivirus group of retroviruses (Rabson and Martin, 1985). Lentiviruses exhibit cytopathic effects in cultured cells and slowly progressive disease in animals. Two genetically distinct types of HIV have been identified. HIV-1 is responsible for the current worldwide epidemic of AIDS. HIV-2, primarily found in West Africa, seems to be less virulent and has 42% overall homology to HIV-1 at the nucleotide sequence level (Kong *et al.*, 1988; Guyader *et al.*, 1987). Of the two HIV types, this study will focus exclusively on HIV-1.

HIV is tropic for cells which bear the CD4 antigen on the cell surface (Levy, 1989). Among the many cell types vulnerable to HIV infection, it is the particular destruction of the $CD4^+$ T lymphocyte cells which is thought to be the central defect in AIDS (Gallo *et al.*, 1984; Popovic *et al.*, 1984; Klatzmann *et al.*, 1984). The $CD4^+$ T cell plays an important role in the induction of several cell types involved in the immune response (Figure 1.1). Some of the cell types induced by $CD4^+$ T cells are the B lymphocyte cells, which produce antibodies, the $CD8^+$ or cytotoxic T lymphocytes, which destroy virus-infected host cells, and the macrophages, which destroy foreign microorganisms. Thus, the destruction of $CD4^+$ T cells compromises the ability of the immune system to protect the body from harmful pathogens. It has been observed that the cytopathic effects are relatively reduced in infected monocytes and macrophages (Gartner *et al.*, 1986; Ho *et al.*, 1986). It is believed that infected monocytes may serve as a cellular reservoir for the dissemination of HIV to other parts of the body.

Similar in structure to other retroviruses (Varmus, 1988), the HIV particle is composed of two identical RNA molecules wrapped in a viral protein core. Base-paired to each RNA chain is a specific host transfer RNA which serves as a primer for DNA synthesis. The viral core also contains the viral enzymes reverse transcriptase, integrase, and protease, needed for the integration of the viral genome into the host genome. Surrounding the viral core is a hybrid lipid envelope comprised of some of the host cell membrane, acquired during viral budding, and viral glycoproteins.

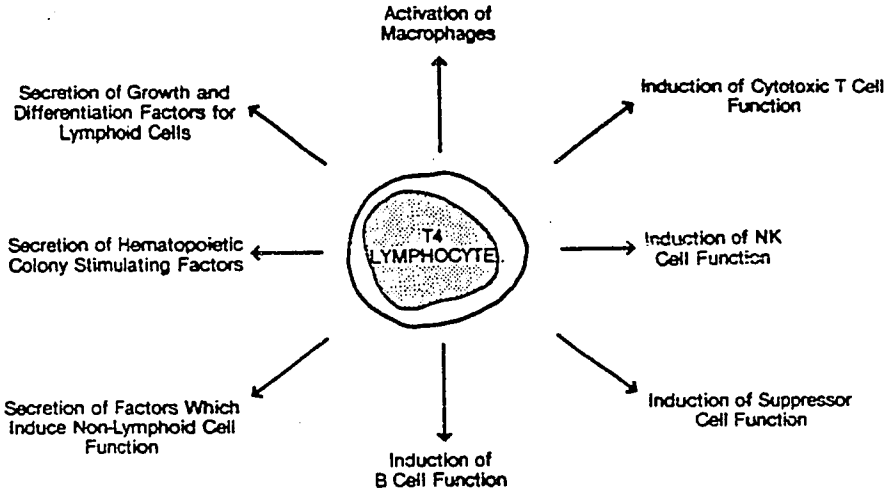

Figure 1.1. Central role of the T4 cell in the human immune response. The T4 cell is directly or indirectly involved in inducing the wide array of the functions of multiple limbs of the immune system. *(Taken from Fauci, 1988).*

The life cycle of HIV is viewed as two stages (Figure 1.2). In the first stage, the HIV envelope glycoprotein, gp120, binds with high affinity to the CD4 molecules located on the host cell surface (McDougal *et al.*, 1986). HIV then enters the cell by either receptor-mediated endocytosis (Maddon *et al.*, 1986) or by virus-mediated endocytosis involving the gp41 transmembrane portion of the viral envelope protein (Stein *et al.*, 1987; McClure *et al.*, 1988; Bedinger *et al.*, 1988). Upon entry of the virus particle into the cell, the virus core is converted into an enzymatically active nucleoprotein complex. The reverse transcriptase transcribes the RNA into double-stranded proviral DNA with complete tandem long terminal repeats (LTR), needed for proviral integration into the host cell's genome. Complete LTR sequences are not present in the HIV RNA genome. After translocation of the provirus to the nucleus, integrase allows the integration of the proviral DNA into the host genomic DNA. An unusual feature of HIV infection compared to most other retroviruses is the observation of large amounts of unintegrated viral DNA in the infected cells, which may be a contributing factor towards the cytopathicity of HIV (Keshet and Tenin, 1979; Shaw *et al.*, 1984). Once the proviral DNA has integrated into the host genome, a latent phase often occurs as the replication cycle is temporarily suspended. Though the mechanism which produces viral latency is not well understood, it is known that the overall activation state of the infected cell is an important factor.

The second stage of the HIV life cycle occurs when the HIV infected cell is activated to produce new virus particles. Factors that up-regulate viral replication after a dormant state fall into three major classes--mitogens and antigens, heterologous viral

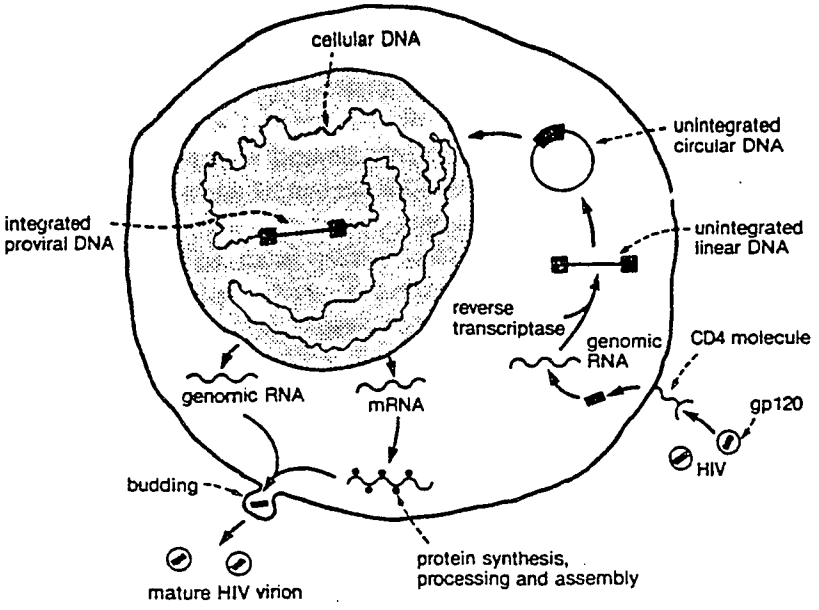

Figure 1.2. The life cycle of HIV. *(Taken from Fauci, 1988).*

genes, and cytokines (Rosenberg and Fauci, 1989). These factors appear to activate host cellular transcription factors or produce *trans*-acting transcription factors from co-infecting viruses. These factors bind to recognition sequences of a promoter element located in the 5′ LTR of HIV (Haseltine, 1991; Cullen, 1991). Viral replication is divided into an early and a late phase. In the early phase, viral regulatory proteins are produced from viral RNA that has been processed into messenger RNA (mRNA). The late phase involves the production of full-length genomic viral RNA and the viral structural proteins. The genomic RNA is packaged and assembled into a viral particle, culminating with the budding of the mature virion from the cell surface (Ho *et al.*, 1987; Cullen and Greene, 1989).

By 1985, the entire HIV-1 proviral genome was cloned and sequenced (Hahn *et al.*, 1984; Shaw *et al.*, 1984; Alizon *et al.*, 1984; Luciw *et al.*, 1984; Ratner *et al.*, 1985; Wain-Hobson *et al.*, 1985; Sanchez-Pescador *et al.*, 1985; Muesing *et al.*, 1985). The HIV-1 provirus is approximately 9.2 - 9.7 kilobase pairs (kb) in size (Figure 1.3). As with other retroviruses, the HIV-1 provirus has LTRs at the proviral ends that contain regulatory elements for replication and the structural genes *gag*, *pol*, and *env* that code for the core proteins, the viral enzymes (reverse transcriptase, integrase, protease), and the envelope glycoproteins, respectively (Rabson and Martin, 1985). HIV-1 also has at least eight additional genes: *vif*, *vpr*, *vpu*, *vpt*, *tev/tnv*, *tat*, *rev*, and *nef*. *vif*, *vpr*, *vpu*, *vpt*, and *tev/tnv* are classified as accessory genes (Vaishnev and Wong-Staal, 1991). Though the exact function of these accessory gene products have not been determined, it has been observed that many of the accessory genes are

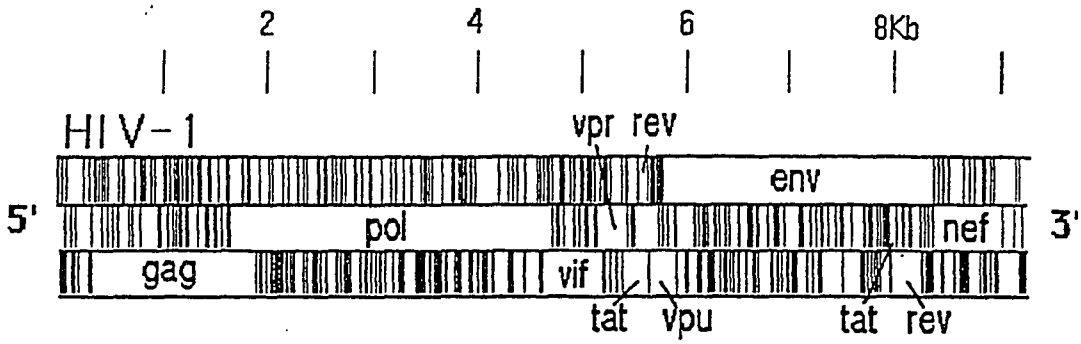

Figure 1.3. Genomic map of HIV-1 representing the integrated provirus. The stop codons in all three reading frames on the coding strand are shown as vertical lines. Open reading frames which have been assign to particular genes are indicated. *(Taken from Hammarskjöld and Rekosh, 1989).*

defective in cultured strains but are highly conserved in natural isolates, suggesting important roles for these genes during viral growth *in vivo*. *Tat*, *rev*, and *nef* are classified as regulatory genes (Sodroski *et al.*, 1985b; Arya *et al.*, 1985; Feinberg *et al.*, 1986; Sodroski *et al.*, 1986; Fisher *et al.*, 1986; Arya and Gallo, 1986; Guy *et al.*, 1987) since it has been shown that they are involved in the regulation of HIV expression. It is possible that other genes exist which have not yet been identified.

The HIV-1 regulatory genes and their products

Cytoplasmic HIV-1 mRNA analyses of infected cells showed the presence of RNAs at 9.3, 4.3, and 1.8 kb in size. The largest species of RNA is the full-length non-spliced RNA that is used to transcribe the *gag* and *pol* proteins as well as being packaged into virus particles. Copy DNA (cDNA) clones that were able to hybridize to subgenomic DNA probes derived from the 5′ end, the *env* region, and the 3′ end of the virus, and not to the *gag-pol* region of the virus, were isolated and characterized by DNA sequence analysis (Muesing *et al.*, 1985). Northern blots of the HIV-1 mRNAs probed with subgenomic viral DNA fragments were also performed (Arya *et al.*, 1985). Results indicate that the intermediate species of RNA (~4.3 kb), from which the *env* proteins are derived, is generated by the removal of a single intron consisting of the *gag-pol* region of the genome. The smallest species of RNA (~2.0 kb) is shown to be doubly spliced. The RNAs of this size class represent the processed products of the *tat*, *rev*, and *nef* genes. The *tat* and *rev* genes both contain two coding exons (Arya *et al.*, 1985; Sodroski *et al.*, 1985a; Sodroski *et al.*, 1986; Feinberg *et al.*, 1986). The first exon of *rev* lies totally within the first exon of *tat*, although different reading

frames are used. There is also a partial overlap between the second exons of *tat* and *rev*, as well as part of the *env* exon. Again, different reading frames are used. The *nef* gene is located 3′ of the *env* gene (Arya and Gallo, 1986; Allan *et al.*, 1985). The first splice removes the *gag-pol* region while the second splice removes most of the *env* region, resulting in the linkage of sequences from the 5′ end of the genome to the corresponding two exons of each respective gene (Figure 1.4).

Activation of infected cells from latency results in the initial production of the doubly spliced mRNAs that encode the regulatory gene products Tat, Rev, and Nef (Feinberg *et al.*, 1986). RNA from long-term infected cells were used to synthesize cDNA using the polymerase chain reaction (PCR) technique and primers that would hybridize at the 5′ and 3′ ends of the transcripts (Robert-Guroff *et al.*, 1990). The amplified mRNAs were electrophoresed and analyzed by Southern blotting and probing with specific oligonucleotide probes corresponding to the *tat*, *rev*, or *nef* exons. Populations of M13 clones, produced from the PCR-amplified RNAs, were also examined by hybridization to the same probes used in the Southern analysis. The results of these experiments show that the *nef* transcript is predominant, while the *rev* transcript makes up an intermediate fraction, and the *tat* transcript is present in low abundance.

Using a chloramphenicol acetyl transferase (CAT) assay, it has been demonstrated that the HIV LTR is able to act as a transcriptional promoter. CAT activity is increased in HIV-infected H9 lymphocytes and relative to uninfected H9

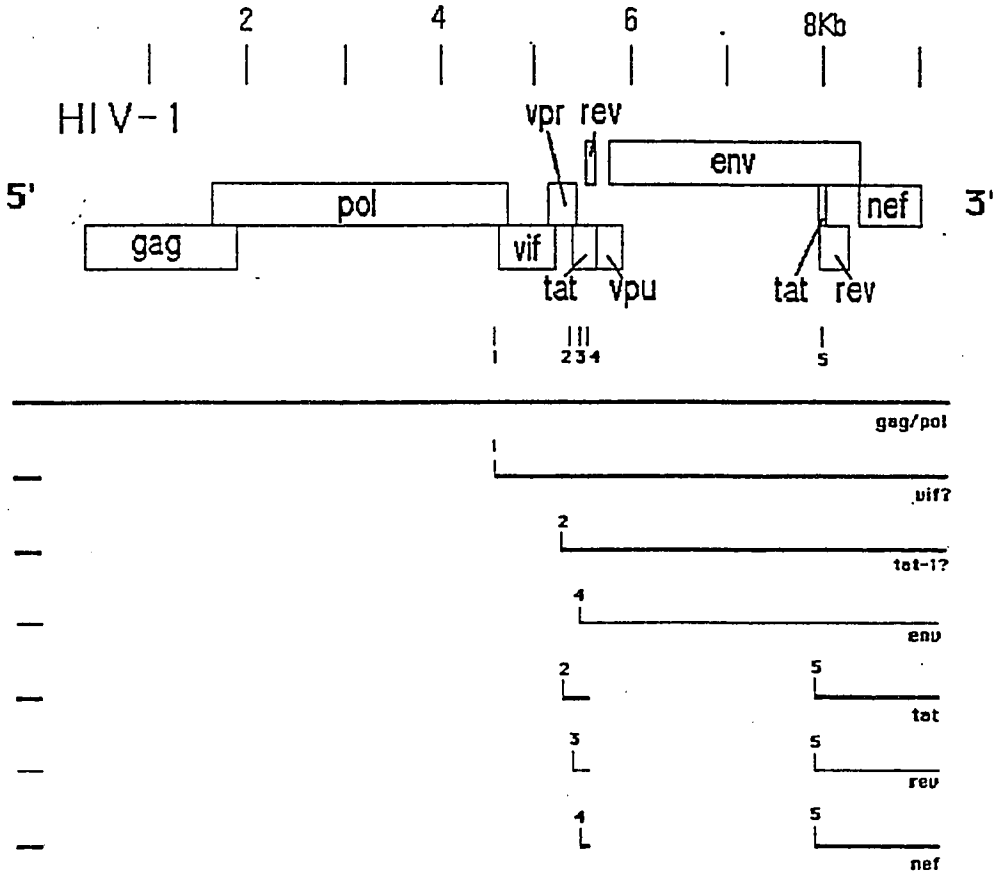

Figure 1.4. Structure of known and postulated HIV-1 mRNAs. The diagram at the top shows the positions of the open reading frames assigned to known viral genes. The thick lines represent mRNAs corresponding to sequenced cDNAs. The thin lines represent mRNAs that are postulated to exist but which have not yet been verified by cDNA cloning. The sites numbered 1 - 5 represent positions of known splice acceptors. *(Taken from Hammarskjöld and Rekosh, 1989).*

cells, indicating the presence of a *trans*-acting activation factor (Sodroski *et al.*, 1985b). Deletion studies have identified that the *trans*-activating factor is encoded by the *tat* gene (Sodroski *et al.*, 1985a; Arya *et al.*, 1985). Deletion analysis of the HIV LTR initially revealed that nucleotides -17 to +80 of the RNA initiation site are needed for Tat activation. The region has been called the TAR element for *trans*-acting responsive element (Rosen *et al.*, 1985). Subsequent deletion and mutation analyses indicate that the region at +19 to +42 of the RNA initiation site is important for Tat *trans*-activation and that TAR functions only in its native orientation and only when it is downstream of the transcription initiation site (Hauber and Cullen, 1988; Jakobovits *et al.*, 1988; Selby *et al.*, 1989). Secondary structure analysis of the HIV leader mRNA by nuclease S1 and ribonuclease T1 mapping show the formation of stable stem-loop structures under native conditions (Muesing *et al.*, 1987). Mutagenesis experiments specific for RNA secondary structure, where the sequence at region +19 to +42 is not altered at either the DNA or RNA level, were performed. 5′ RNA sequences, which, during transcription, disrupt the formation of the wild-type TAR structure even before the formation of the TAR hairpin, showed reduced levels of Tat-induced *trans*-activation of a CAT reporter gene. A 3′ antisense mutation, with modified sequences after the +19 to +42 region, also disrupts the TAR secondary structure, but *only* after the TAR hairpin has had a chance to form. This 3′ antisense mutation allowed Tat *trans*-activation of the CAT reporter gene, suggesting Tat interacts transiently with TAR and that this interaction occurs concurrently with transcriptional elongation (Berkhout *et al.*, 1989). These observations and other

evidence to be reported, also suggest TAR acts in a RNA form. Because of its location, TAR is a part of all HIV gene transcripts, and are thus potentially subject to Tat regulation.

Tat is a 15.5 kilodalton (kd) protein which is localized in the nucleus (Hauber *et al.*, 1987). It contains a series of seven cysteine residues enabling it to form metal-linked homodimers (Frankel *et al.*, 1988), although the existence of Tat homodimers *in vivo* has not been observed. A COS cell culture was transfected with a plasmid containing an IL-2 indicator gene under the control of the HIV LTR. Another COS cell culture was co-transfected with both the IL-2 indicator gene plasmid and a *tat* expression construct. Both cultures were also transfected with a reference plasmid that contains the rat insulin II gene under the control of the Rous sarcoma virus (RSV) LTR, which is not affected by *tat* co-expression. Seventy-two hours after transfection, the cultures were supplemented with actinomycin D to prevent *de novo* RNA synthesis. Total RNA was isolated from cultures at different times after the addition of the antibiotic and the levels of the IL-2 indicator mRNA and the insulin reference mRNA were quantitated using an S1 nuclease assay (Hauber *et al.*, 1987). Cultures that co-expressed the *tat* expression plasmid showed an 8-fold higher steady-state level of the indicator mRNA relative to the *tat*$^-$ culture. However, when the IL-2 indicator mRNA was compared against the insulin reference mRNA over time, no stabilization of the indicator mRNA was observed.

The transfected COS cultures were also used in nuclear run-off experiments to investigate the effects of Tat on the rate of transcription from the HIV LTR. Instead

of the rat insulin reference gene, a human interferon γ (IFN-γ) gene under the control of the RSV LTR was used as an internal control. In these experiments, nuclei from the transfected cells were isolated, and the transcripts that were initiated *in vivo* were allowed to elongate *in vitro* in the presence of [α-^{32}P]UTP. The labeled mRNAs were then hybridized to IL-2 DNA and IFN-γ DNA fragments immobilized on nitro-cellulose filters. In the presence of Tat, a significant amount of the HIV LTR IL-2 mRNA hybridized to its corresponding DNA fragment when compared to the hybridization of the IFN-γ mRNA. Thus, the observed increase in the level of steady-state HIV LTR transcripts with *tat* co-expression is due to the increase in the rate of gene transcription.

It has been demonstrated through mobility shift and filter binding assays that a highly basic domain, of lysine and arginine residues, of Tat is able to bind to the TAR hairpin (Dingwall *et al.*, 1989; Weeks *et al.*, 1990; Roy *et al.*, 1990), placing Tat into a class of sequence-specific RNA binding proteins that have an arginine-rich motif (Lazinski *et al.*, 1989). Mutations in a 3 nucleotide bulge of TAR (+23 to +25) reduced Tat binding and Tat *trans*-activation of a CAT reporter. Mutations in the loop or the stem of TAR, while reducing Tat *trans*-activation, had no effect on Tat binding (Roy *et al.*, 1990). This finding, as well as the identification of several proteins, from HeLa nuclear extracts, which are able to bind to TAR (Gatignol *et al.*, 1989; Gaynor *et al.*, 1989; Marciniak *et al.*, 1990b) and the identification of a Tat-binding protein (Nelbock *et al.*, 1990) suggest that the direct binding of Tat to TAR is only one of the elements involved in Tat-TAR *trans*-activation. Marciniak's group has identified a

68 kd nuclear protein that binds to the terminal loop sequence of TAR. A partially purified p68 protein preparation was shown to enhance Tat *trans*-activation *in vitro* (Marciniak *et al.*, 1990a) leading to the suggestion that the p68 protein may confer the specific binding of Tat to TAR (Figure 1.5).

The mechanism by which Tat enhances the rate of transcription remains unclear. One hypothesis proposes that Tat functions to suppress the premature termination of transcription by stabilizing the transcriptional polymerases (Laspia *et al.*, 1990; Marciniak *et al.*, 1990a). An alternative hypothesis proposes that the rate of gene transcription is due to an increase in the rate of transcription initiation (Hauber *et al.*, 1987). Sharp and Marciniak (1989) also noted that Tat enhancement can be roughly divided into a 20-fold increase in viral mRNA and a 5-fold increase in the amount of protein synthesized per mRNA molecule. The observation that there is an increase in protein synthesis per mRNA molecule provides evidence that Tat may also serve to increase the efficiency of translation of TAR-containing mRNA. Since these hypotheses are supported with numerous valid experiments, it is probable that Tat functions on all three levels.

Rev is a 19 kd phosphorylated nuclear protein (Felber *et al.*, 1989) which also belongs to the class of sequence-specific RNA binding proteins that have an arginine-rich motif (Lazinski *et al.*, 1989; Malim *et al.*, 1989a; Perkins *et al.*, 1989). This arginine-rich region may also contain sequences that target Rev to the nucleolus (Cochrane *et al.*, 1990). Rev induces the expression of the viral structural genes while it simultaneously decreases the expression of the regulatory genes (Feinberg *et al.*,

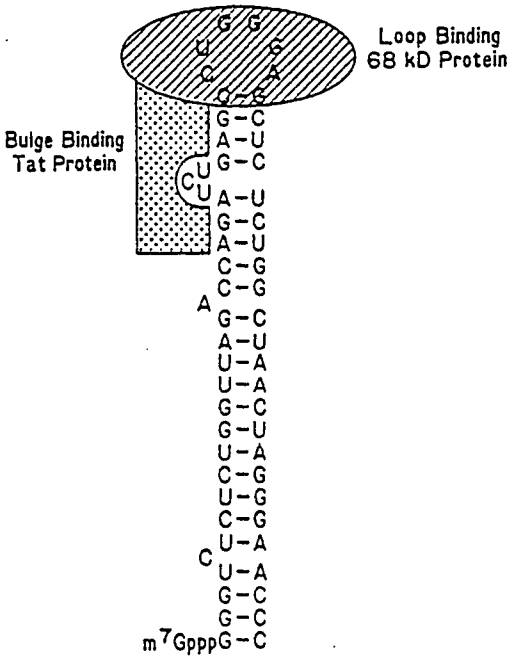

Figure 1.5. Schematic representation of the interaction of Tat with TAR. *(Taken from Cullen, 1990).*

1986; Sodroski *et al.*, 1986; Malim *et al.*, 1988; Felber *et al.*, 1989; Hammarskjöld *et al.*, 1989; Chang and Sharp, 1989). Rev acts in *trans* by binding to RNA transcripts that contain a Rev-responsive element (RRE). The RRE, a complex stem-loop structure comprised of 234 nt, is located in the 5′ region of the *env* gene, and thus targets the unspliced and singly-spliced RNAs (the *gag-pol* and *env* mRNAs) for export from the nucleus to the cytoplasm (Malim *et al.*, 1989b; Hammarskjöld *et al.*, 1989; Felber *et al.*, 1989). Chang and Sharp (1989) have demonstrated that recognition of even one splice site by cellular spliceosomal components can retain the RNA in the nucleus. They suggest that Rev helps the dissociation of unspliced RNA from splicing components, thus freeing the RNA for export.

Unlike Tat and Rev, the 27 kd myristylated and phosphorylated Nef protein is found in the cytoplasm (Allan *et al.*, 1985; Franchini *et al.*, 1986; Guy *et al.*, 1987). Its myristylation suggests that Nef probably associates with factors in the cytoplasmic membrane. Nef also has GTP-binding, GTP-hydrolyzing, and autophosphorylating activities (Allan *et al.*, 1985; Guy *et al.*, 1987), which suggests that Nef belongs in the family of signal transducing G-proteins. Indeed, Nef shows some homology with the *ras* family of proteins (Guy *et al.*, 1987; Gilman, 1987). Nef has been reported to down-regulate viral transcription and has been implicated in maintaining HIV-1 latency (Luciw *et al.*, 1987; Terwilliger *et al.*, 1986; Ahmed and Venkatesan, 1988; Niederman *et al.*, 1989). However, two groups have provided evidence that Nef has no effect on the inhibition of transcription, questioning whether Nef is indeed a negative factor (Kim *et al.*, 1989; Hammes *et al.*, 1989). Although *nef's* role in viral replication is

unclear, the conservation of the *nef* open reading frame argues for a significant role in HIV replication.

Since the HIV life cycle is known, antiretroviral agents can be created that target critical stages of HIV replication (Table 1.1)(Mitsuya *et al.*, 1990). Current investigations of anti-HIV agents range from the development of vaccines that block HIV binding to the target cell to the use of nucleoside analogs, particularly 3′-azido-2′,3′-dideoxythymidine (AZT or zidovudine), which inhibit the transcription of RNA to DNA (Mitsuya *et al.*, 1985). A series of modest experiments were performed that use anti-RNA agents called ribozymes against an HIV regulatory gene product. Of the three HIV-1 regulatory genes, *tat* is the most powerful effector. Targeting *tat* and incapacitating Tat function should be detrimental to viral replication. Additionally, since the *rev* gene shares sequences with the *tat* gene, it is possible to target both the *tat* and the *rev* gene products simultaneously.

Catalytic RNA Molecules

Examples of catalytic RNA molecules are numerous. In what is now called group I intron self-splicing, *Tetrahymena* produces a ribosomal RNA (rRNA) subunit that accurately excises its 400 bp intron in the absence of any protein (Kruger *et al.*, 1982). Other group I introns occur in rRNA and mRNA genes in yeast mitochondria, some transfer RNA (tRNA), rRNA and mRNA genes in chloroplasts, and in mRNA genes in bacteriophages (Waring and Davies, 1984; Cech, 1988).

Small RNAs found in plants have the ability to self-cleave (Buzayan *et al.*, 1986; Prody *et al.*, 1986). These small RNAs fall into two groups:

Table 1.1. Selected stages of HIV replication that are potential targets for therapeutic intervention. *(Taken from Mitsuya* et al., *1990).*

Stage	Possible Intervention
Binding to target cell	Antibodies to virus or cellular receptors; genetically engineered soluble CD4 proteins
Fusion of virus with target cell	Antibodies or drugs that block the fusogenic domain of virus
Entry into target cell and uncoating of RNA	Drugs (by analogy with uncoating inhibitors against rhinoviruses and related picornaviruses)
Transcription of RNA to DNA by reverse transcriptase	Reverse transcriptase inhibitors (for example, AZT and other dideoxy- or didehydro-dideoxy nucleoside congeners)
Degradation of RNA by RNase activity (encoded by viral *pol* gene	RNase H inhibitors
Migration of viral DNA to nucleus	Agents that block viral DNA migration into nucleus (as yet unidentified)
Integration of DNA into host genome	Agents that inhibit *pol*-encoded integrase function (as yet unidentified)
Transcriptional-translational efficiency of viral RNA	Inhibitors of Tat protein; mutant Tat protein molecules; TAR inhibitors; "pseudo-TAR" molecules; Rev protein inhibitors; antisense constructs against *tat* or *rev* mRNAs; activator of the *nef* gene (?)
Ribosomal frameshifting	Ribosomal frameshift inhibitors (as yet unidentified)
Viral component maturation Gag•Pol fusion polyprotein cleavage	Viral protease inhibitors (for example, transition state mimetics, synthetic peptides)
Myristoylation and glycosylation	Myristoylation and glycosylation inhibitors (for example, castanospermine and inhibitors of trimming glucosidase)
Packaging	Antisense construct against the packaging sequence
Viral budding	Interferons or interferon inducers; antibodies to viral antigens that may be associated with viral release; inhibitors of the *vpu* gene (?)

viroids and virusoids/satellite RNAs. Viroids are self-replicating infectious single-stranded circular RNAs that are not encapsidated. Virusoids or satellite RNAs can be circular or linear molecules, are encapsidated by plant viruses, and are also dependent on plant viruses for replication. These plant RNAs appear to replicate using a rolling circle model (Figure 1.6), where self-cleavage of the unit length RNA genome occurs as a last step. The displaced strand folds back upon itself, binding to form an active tertiary cleavage site (see the hammerhead and hairpin secondary structures in Figure 1.7).

Ribozymes are catalytic RNA molecules that are able to break not intramolecular covalent bonds but instead covalent bonds located in other RNA molecules. The development of ribozymes is a direct result of studies of self-splicing RNA molecule in *Tetrahymena*, viroids and virusoids. Initial ribozyme studies focused on the ability of the ribozyme to recognize its substrate and the chemistry of the cleavage reaction (Zaug *et al.*, 1986; Forster and Symons, 1987). It has been demonstrated that a portion of the ribozyme active site requires base-pairing with the substrate RNA molecule while the ribozyme's tertiary structure confers its ability to cleave covalent bonds. Since bond cleavage is a function of tertiary structure and requires a small sequence motif at the site of cleavage, attention shifted to the development ribozymes that were able to recognize and cleave specific sequences in target RNA molecules (Uhlenbeck, 1987; Haseloff and Gerlach, 1988).

Three predominant ribozyme classes are based on the *Tetrahymena* ribosomal RNA self-splicing intron (Kruger *et al.*, 1982), and the self-splicing (+)-strand and

Figure 1.6. Rolling circle model of viroid/virusoid replication. The rolling circle generates a multimeric single-stranded tail (which folds back on itself to form a self-cleaving splice complex; not shown). *(Taken from Lewin, 1990).*

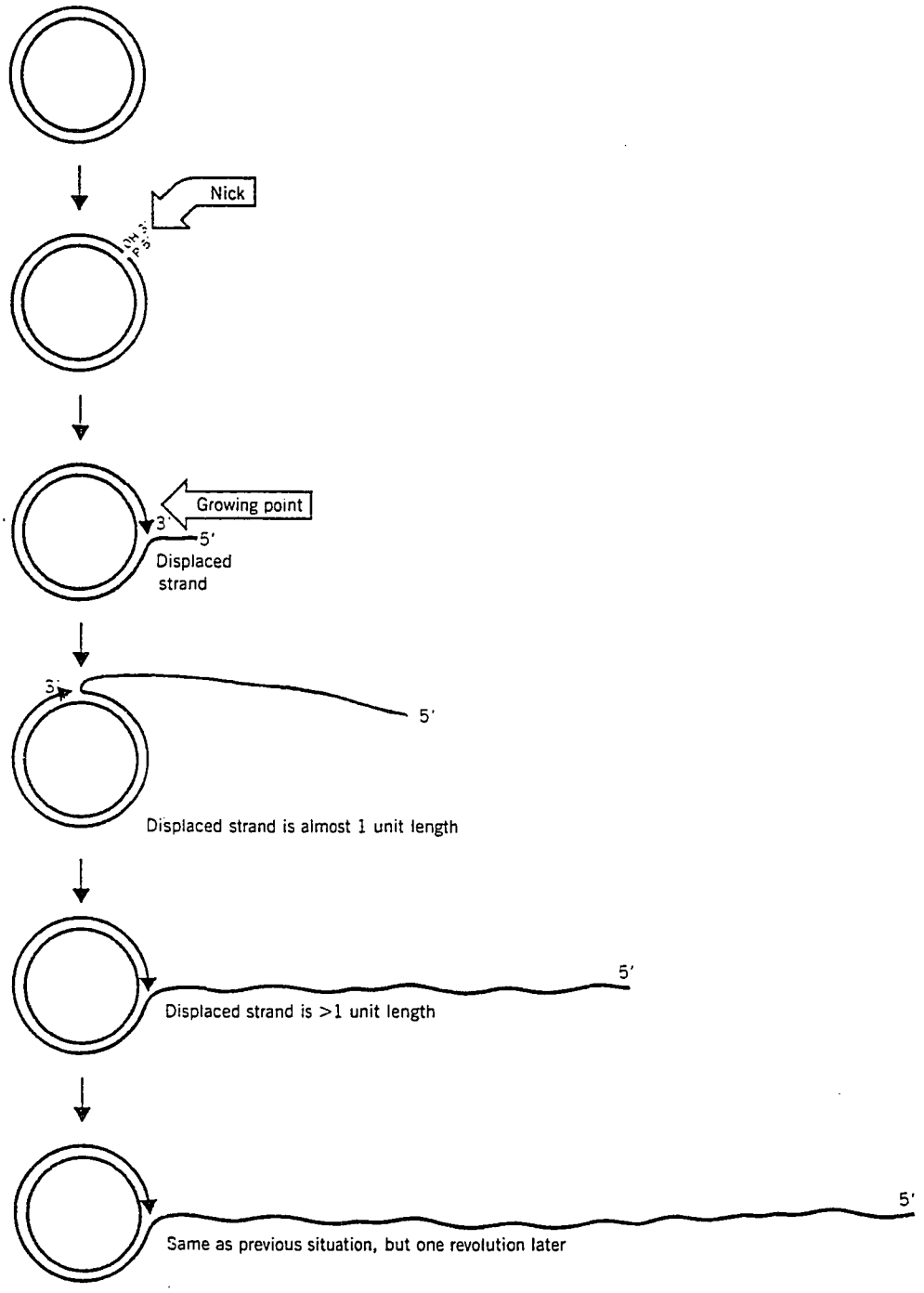
Nick
3'
5'
Growing point
3'
5'
Displaced
strand
3'
5'
Displaced strand is almost 1 unit length
5'
Displaced strand is >1 unit length
5'
Same as previous situation, but one revolution later

(-)-strand virusoid RNAs of the tobacco ringspot virus, which have either a hammerhead-shaped secondary structure (Prody *et al.*, 1986; Forster and Symons, 1987) or a hairpin-type secondary structure at the active site (Hampel and Tritz, 1989) (Figure 1.7). The *Tetrahymena* intron ribozyme is a relatively large molecule (300-400 nt in size) that can be designed to cleave after the substrate sequence motif 5′-NNNU-3′ (where N represents a nucleotide position on the substrate RNA) by incorporating into the ribozyme's primary structure sequences complementary to the target sequence. The hairpin ribozyme, intermediate in size (50-60 nt), can target the sequence 5′-N_4(G or C)N↑GUCN_6-3′ (Hampel and Tritz, 1990). The hammerhead ribozyme, the smallest of the three motifs (19-38 nt), can target the sequence 5′-N_6GUH↓N_8-3′, where H can be A, C, or U, and the arrow represents the cleavage site. Since the *Tetrahymena* ribozyme has a four-base recognition sequence, mRNA molecules would contain more *Tetrahymena* ribozyme cleavage sites relative to the hammerhead (~17-base recognition site) and the hairpin (~15-base recognition site) cleavage sites. Thus, the *Tetrahymena* ribozyme is more suited to the specific cleavage of an uncharacterized RNA molecule, while the hammerhead and hairpin ribozymes is more suited to the cleavage of well-characterized RNA molecules.

Preliminary studies using hammerhead ribozymes for the down-regulation of specific genes have already begun (Cotten and Birnstiel, 1989; Cameron and Jennings, 1989; Sarver *et al.*, 1990). Sarver *et al.* (1990) have demonstrated the hammerhead ribozyme cleavage of HIV-1 *gag* RNA in a cell-free system. Additionally, when human cells stably expressing anti-*gag* RNA ribozymes were challenged with HIV-1, a

Figure 1.7. Base-paired nucleotide sequences of three ribozyme-substrate constructs derived from self-splicing and self-cleaving RNA molecules. The bases indicated by an "N" can be A, G, C, or U and N′ is complementary to N by Watson-Crick rules. The arrows indicate the sites of cleavage in the substrate RNAs. The projections of these structures on paper are arbitrary and do not represent any experimentally determined aspects of three dimensional structure. *(Taken from Holt and Lechner, 1990).*

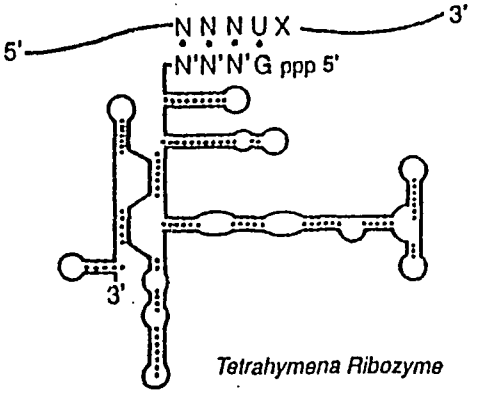

Tetrahymena Ribozyme

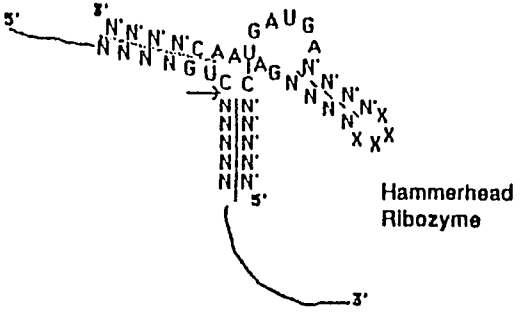

Hammerhead
Ribozyme

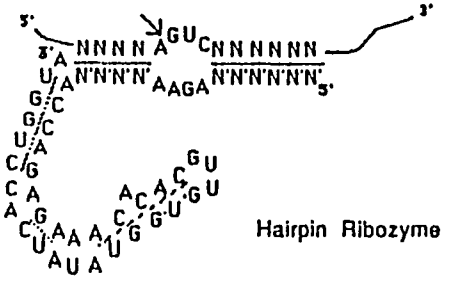

Hairpin Ribozyme

reduction in antigen p24 was observed relative to nonribozyme-expressing cells. Chang *et al.* (1990) have designed ribozymes that target two sites in the HIV-1 *gag* gene and one site in the 5′ LTR. Another group has demonstrated the *in vitro* cleavage of *vif* RNA by a synthetic ribozyme (Lorentzen *et al.*, 1991). These ribozyme studies have also noted the need for a high molar excess of ribozymes to effectively elicit biological effects (Cotten *et al.*, 1989; Cameron and Jennings, 1989). In an effort of improve the cleavage efficiency of ribozymes, Goodchild and Kohli (1990) have studied the effects of several hammerhead ribozymes that cleaved a 28 nt sequence from HIV-1 RNA. They have demonstrated that reducing the extent of base-pairing between ribozyme and substrate from 20 to 12 base pairs increased the cleavage rate and that deletions in the stem/loop structure in the ribozyme increased the initial rate of the cleavage reaction.

Four hammerhead ribozymes and one hairpin ribozyme were designed which cleave a 390 nt synthetic *tat* RNA (*tat-s*) transcript into two fragments *in vitro*. The inability of these ribozymes to recognize and cleave an actin control RNA transcript, which lack ribozyme recognition sequences is also demonstrated. Various cellular parameters which affect ribozyme activity were studied *in vitro* to test ribozyme technology as a possible means of "intracellular immunization" (Baltimore, 1988) for HIV therapy.

CHAPTER 2

MATERIALS AND METHODS

Restriction Endonuclease Digestion of DNA

The restriction enzymes used in this study were purchased from various manufacturers of molecular biology reagents. Single and double digestions of DNA were performed according to the respective manufacturer's instructions.

Extraction of Nucleic Acid Reactions with PHENOL/SEVAG

Equal volumes of phenol, which contains 0.1% (w/v) 8-hydroxyquinoline equilibrated with 0.1 M tris, pH 8.0, and SEVAG (chloroform:iso-amyl alcohol 24:1) were added to the reactions and the samples were mixed vigorously for 15 seconds. For reactions containing polyethylene glycol, the aqueous and organic phases were separated by centrifugation at maximum speed for 5 minutes at room temperature in an Eppendorf microcentrifuge model 5414. For reactions that did not contain polyethylene glycol, the reactions were transferred into tubes containing Phase Lock Gel I™ purchased from 5 Prime → 3 Prime, Inc. before the addition of phenol and SEVAG. The aqueous phase was isolated by centrifugation at maximum speed for 30 seconds at room temperature in an Eppendorf microfuge model 5414.

Preparation of Sephadex G-50 Spin Columns

Sephadex G-50-80 beads were suspended and autoclaved in a solution of 10 mM Tris, pH 7.6, 0.1% sodium dodecyl sulfate. A spin column was prepared by plugging the bottom of a 1 ml disposable syringe with a small amount of sterile

siliconized glass wool. The syringe was then filled with the Sephadex slurry, inserted into a 15 ml Corex tube, and centrifuged at room temperature for 2 minutes at 2000 rpm using a Sorvall H-1000B rotor in a Sorvall RT6000B centrifuge. More resin was added and packed down by further centrifugation until the volume of the packed column reached the 1 ml mark on the syringe. A microfuge tube with its cap removed was then placed in the 15 ml Corex tube followed by the prepared spin column. The phenol extracted RNA sample was layered onto the column and centrifuged for 2 minutes at 2000 rpm. The collected effluent was transferred to a capped microfuge tube.

Precipitation of Nucleic Acids with Ethanol (EtOH)

The nucleic acid solution was brought to a final concentration of 2.5 M ammonium acetate (NH_4Acetate, NH_4CH_3COO) by the addition of a half volume of sterile 7.5 M NH_4Acetate. Two volumes of 95% EtOH were then added and the tube was incubated at -20°C for at least 2 hours. The precipitated nucleic acids were recovered by centrifugation at maximum speed for 15 minutes at 4°C in an Eppendorf microcentrifuge model 5414. After centrifugation, the supernatant was carefully decanted and discarded. The remaining pellet was carefully rinsed with 70% ice cold EtOH and dried at room temperature in a Savant Speed Vac Concentrator.

Preparation of Synthetic Oligodeoxynucleotides

Oligodeoxynucleotides were synthesized on an Applied Biosystems 380B DNA synthesizer at the University of Hawaii Biotechnology-Molecular Biology

Instrumentation Facility. The synthesized oligonucleotides were resuspended in sterile doubly-distilled H_2O (ddH_2O). Sample aliquots were removed to which loading dye at a final concentration of 50% formamide, 0.0025% (w/v) bromophenol blue, 0.0025% (w/v) xylene cyanol FF, 5 mM EDTA was added. The oligonucleotides were then electrophoresed through a TBE (0.089 M Tris-borate, pH 8.3, 0.002 M EDTA) buffered 7 M urea/12% polyacrylamide gel at 500 volts until the xylene cyanol dye had migrated ~3/4 of the length of the gel. A Bio-Rad Protean II vertical electrophoresis cell was used. The cast gel was 1.0 mm thick by 16 cm wide by 20 cm long. The separated oligonucleotides were visualized via UV-shadowing, the slowest migrating bands were excised and eluted as described in Sambrook *et al.*, 1989. The purified oligonucleotides were stored in sterile ddH_2O at -20°C.
The sequence of the oligonucleotides are:

T7 primer (18 nt):

5′-TAATACGACTCACTATAG-3′

RZ1 oligomer (54 nt):

5′-CATCAAGTTTCGTCCTCACGGACTCATCAGAGCTTACTATA-
GTGAGTCGTATTA-3′

RZ2 oligomer (67 nt):

5′-TACCAGGTAATATACCACAACGTGTGTTTCTCTGGTAGGCT-
TCTAGACTCTATAGTGAGTCGTATTA-3′

$RZ3_{10}$ oligomer (53 nt):

5′-AGAACAGTTTCGTCCTCACGGACTCATCAGAGACTCTATAG-

TGAGTCGTATTA-3′

$RZ4_{12}$ oligomer (51 nt):

5′-GGCAGTTTCGTCCTCACGGACTCATCAGAGACTCTATAGTG-

AGTCGTATTA-3′

$RZ5_{14}$ oligomer (53 nt):

5′-AAGGCAGTTTCGTCCTCACGGACTCATCAGAGACTCTATAG-

TGAGTCGTATTA-3′

Partially double-stranded ribozyme templates were prepared by annealing the T7 primer with each ribozyme oligomer at equimolar concentrations in 10 mM tris, pH 8.0 for 3 minutes at 65°C and cooling the samples on ice (Milligan *et al.*, 1987). The ribozyme transcription templates were stored at -20°C until ready for use.

Synthesis of Ribozyme Molecules

Ribonucleotide solutions, each at 100 mM in concentration, were purchased from Pharmacia P-L Biochemicals and were combined to form either an rNTP (CTP^-) mixture composed of GTP, ATP, and TTP, at a concentration of 2.5 mM/NTP to be used for radiolabeling RNA, or an rNTP mixture composed of CTP, GTP, ATP, and TTP, at a concentration of 25 mM/NTP to be used for large scale synthesis of RNA. The rNTP mixtures were stored at -20°C. T7 RNA polymerase, RNAsin®, and RQ1 RNase-free DNase were purchased from Promega Corporation. The [α-^{32}P]-CTP

(3000 Ci/mmol) used for labeling RNA was purchased from the Du Pont Company, NEN Research Products.

For radiolabeled ribozymes, transcription reactions and removal of the DNA template and unincorporated nucleotides were performed as described in the standard transcription protocol from the Promega Protocols and Applications Guide, 2nd edition (Promega Corporation, 1991) for the synthesis of high specific activity RNA probes using [α-^{32}P]-CTP and T7 RNA polymerase. The transcription reactions were scaled up to a final volume of 50 µl and contained 100 nM partially double-stranded ribozyme DNA template. After a phenol/SEVAG extraction and precipitation with EtOH, the radiolabeled ribozymes were resuspended in 7 µl RNA loading buffer (95% formamide, 10 mM EDTA, 0.1% bromophenol blue, 0.1% xylene cyanol FF), heated at 70°C for 3 minutes and immediately cooled on ice. The samples were electrophoresed through a TBE buffered 7 M urea/20% polyacrylamide gel (0.4 mm thick) in a Bethesda Research Laboratories (BRL) Sequencing Gel Apparatus Model SO for 1.5 hours at 1600 volts. The ribozymes were visualized by exposing the gel to x-ray film for 3 to 15 minutes. The developed film was aligned with the gel and the slowest migrating bands were excised and eluted in 300 µl of RNA elution buffer (0.1% SDS, 0.5 M NH_4CH_3COO, 0.01 M $MgCH_3COO$) at 37°C for 12 to 16 hours with occasional gentle agitation. The eluted ribozymes were EtOH precipitated, resuspended in sterile ddH_2O and stored at -20°C until ready for use.

For the synthesis of large amounts of ribozyme (Milligan *et al.*, 1987), transcription reactions were performed at 40°C for 2 to 3 hours and contained 40 mM

tris, pH 8.1, 20 mM $MgCl_2$, 1 mM spermidine, 50 μg/ml bovine serum albumin, 80 mg/ml polyethylene glycol (8000 MW), 5 mM dithiothreitol, 1 U/μl RNAsin®, 0.01% (v/v) Triton X-100, 100 nM appropriate partially double-stranded ribozyme DNA template, 4 mM of each NTP, and 2 units (U)/μl T7 RNA polymerase. The reactions were terminated by the addition of 1.5 U RQ1 RNase-free DNase and incubation at 37°C for 15 minutes. The *in vitro* synthesized ribozymes were extracted twice with phenol/SEVAG, passed through a Sephadex G-50 spin column and precipitated with EtOH. The samples were resuspended in 20 μl sterile ddH_2O and stored at -20°C. The RNA concentrations were determined by measuring the A_{260} of the final solution.

Preparation of ^{32}P-Labeled RNA Size Markers

Labeled RNA size markers were synthesized using linear control DNA templates. Plasmid pT7-0 contains a T7 RNA polymerase promoter and was purchased from the United States Biochemical Corporation as a mixture of plasmid pT7-0 DNA linearized with *Ban II*, *Sal I*, and *Pvu II*. Transcription with T7 RNA polymerase produces transcripts of 146 nt, 315 nt, and 1728 nt. The Riboprobe® Gemini Positive Control Template from the Promega Corporation is derived from a transcription vector which contains a T7 and an SP6 RNA site. The Riboprobe® control template was obtained as a mixture of plasmid DNA linearized with *Hind III*, *Eco RI*, and *Hinc II*. Although the control template can be used by both T7 and SP6 RNA polymerase to produce transcripts of known size and sequence, transcription with this particular template was performed using only SP6 RNA polymerase.

Transcription of the Riboprobe® control template with SP6 RNA polymerase results in transcripts of 11 nt, 172 nt, and 1386 nt.

Using pT7-0 linear DNA and T7 RNA polymerase and the Riboprobe® transcription control template and SP6 RNA polymerase, RNA transcripts were labeled using [α-^{32}P]-CTP as described in the standard transcription protocol from the Promega Protocols and Applications Guide, 2nd edition (Promega Corporation, 1991) for high specific activity RNA probes. Both the T7 and the SP6 RNA polymerase were purchased from Promega Corporation.

Preparation of Double-Stranded 11/2B2 DNA

Plasmid 11/2B2 is an M13 bacteriophage subclone containing part of a sea urchin actin gene (Wang, 1987). Single-stranded 11/2B2 DNA was provided by Dr. Allan Wang. 10 ng single-stranded 11/2B2 DNA was used to transform *Escherichia coli* JM101 using the calcium chloride/rubidium chloride transformation procedure described in Maniatis *et al.* (1982). Transformants were selected on YT plates containing 2.5 µg/ml isopropylthio-β-D-galactoside (IPTG) and 2.5 µg/ml 5-bromo-4-chloro-3-indolyl-β-D-galactoside (X-gal). A well-isolated colorless plaque was picked with a sterile toothpick and placed in a flask containing 12 ml YT medium (0.8% bacto-tryptone, 0.5% bacto-yeast extract, 0.25% NaCl, pH 7.0) and 60 µl *E. coli* JM101 overnight culture. The culture was incubated for 6 hours at 37°C with constant vigorous shaking. The double-stranded form of 11/2B2 DNA was prepared as described in the heading entitled "Small-scale Preparations of the Replicative Form of Bacteriophage M13 DNA" in Sambrook *et al.* (1989), however, the isolation of the

aqueous phase after phenol/SEVAG extraction was performed as described elsewhere in this chapter. The 11/2B2 double-stranded DNA was resuspended in 30 µl TE (10.0 mM Tris, pH 7.6, 1.0 mM EDTA) containing DNase-free RNase A (20 µg/ml) and stored at 4°C. Typical DNA yields ranged from 1 µg to 7 µg.

Construction and Preparation of Plasmid p616EX2 DNA

The vector DNA, plasmid pGEM®-1, and T4 DNA ligase were purchased from Promega Corporation. SeaKem® ME agarose used in agarose gel electrophoresis was purchased from FMC®. Plasmid p616EX2 construction was performed as described in Maniatis *et al.* (1982). Both pGEM®-1 DNA and 11/2B2 DNA were digested with *Bam HI* and *Hinc II* for 3 hours at 37°C. The digestions were terminated by heating the reactions at 70°C for 10 minutes and cooling immediately on ice. The pGEM®-1 digestion reaction was stored at -20°C until ready for use. 0.1 volume of DNA loading solution (80% glycerol, 0.05 M EDTA, 0.25% bromophenol blue) was added to the 11/2B2 DNA digestion reaction, heated to 70°C for 3 minutes and quick-chilled on ice. The 11/2B2 cleavage products were electrophoresed through a TAE (0.04 M Tris-acetate, pH 8.0, 0.001 M EDTA) buffered 1.0% agarose gel for 1 hour at 100 volts in an International Biotechnologies, Inc. (IBI) Model QSH horizontal gel electrophoresis apparatus. The gel was stained in 0.5 mg/ml ethidium bromide and visualized over ultraviolet (UV) illumination. The 256 bp band was excised and purified with QIAEX, an agarose gel extraction kit purchased from QIAGEN Inc. Purification with QIAEX was performed according to the manufacturer's instructions.

A 1:3 molar ratio of pGEM®-1:insert DNA was used in the ligation reaction. Ligation was performed at 15°C overnight. The resulting plasmid construct, p616EX2, was used to transform *E. coli* JM101 using the calcium chloride/rubidium chloride transformation procedure described in Maniatis *et al.* (1982). Transformants were selected on LB plates containing 50 μg/ml ampicillin. A well-isolated bacterial colony was then used to inoculate 12 ml LB medium (1% bacto-tryptone, 0.5% bacto-yeast extract, 1% NaCl, pH 7.0) containing 50 μg/ml ampicillin. The culture was incubated overnight at 37°C with continuous vigorous shaking. Plasmid p616EX2 DNA was isolated essentially as described in the heading entitled "Small-scale Preparations of the Replicative Form of Bacteriophage M13 DNA" in Sambrook *et al.* (1989), however, the isolation of the aqueous phase after phenol/SEVAG extraction was performed as described earlier in this chapter. The p616EX2 DNA was resuspended in 30μl TE containing DNase-free RNase A (20 μg/ml) and stored at 4°C. Typical p616EX2 DNA yields ranged from 1μg to 12 μg.

Preparation of Plasmid pSP6-TAT-S DNA

Plasmid pSP6tat-s DNA was kindly provided by B.Q. Ferguson *et al.* (1989). pSP6tat-s DNA was used to transform *E. coli* SK1592 using the calcium chloride/rubidium chloride transformation procedure described in Maniatis *et al.* (1982). Yuanxin Zhang, a graduate student, performed the transformation and prepared a glycerol stock (0.7% dimethylsulfoxide, DMSO) of the transformed bacteria as part of a laboratory rotation project. 2 ml LB medium containing 50 μg/ml ampicillin was inoculated with the glycerol stock. The bacteria were allowed to

propagate overnight at 37°C with continuous vigorous shaking. The culture was streaked out onto a LB plate containing 50 μg/ml ampicillin and incubated at 37°C for 12 hours. A well isolated bacterial colony was then used to inoculate 12 ml LB medium containing 50 μg/ml ampicillin. The culture was incubated overnight at 37°C with continuous vigorous shaking. Plasmid pSP6tat-s DNA was then isolated essentially as described in the heading entitled "Small-scale Preparations of the Replicative Form of Bacteriophage M13 DNA" in Sambrook *et al.* (1989), however, the isolation of the aqueous phase after phenol/SEVAG extraction was performed as described elsewhere in this chapter. The pSP6tat-s DNA was resuspended in 30μl TE containing DNase-free RNase A (20 μg/ml) and stored at 4°C. Typical pSP6tat-s DNA yields ranged from 2 μg to 14 μg.

Preparation of RNA Substrates

Plasmids pSP6tat-s and p616EX2 were respectively cleaved with *Pvu II* and *Hinc II* for 2 hours at 37°C. A 0.1 volume of DNA loading solution was added to the digestion reaction, heated to 70°C for 5 minutes, and quick-chilled on ice. Linear plasmid DNA was separated from any remaining circular plasmid DNA by electrophoresis through a TAE buffered 0.8% agarose gel for 2 hours at 80 volts in an IBI Model QSH horizontal gel electrophoresis apparatus. The gel was stained in 0.5 mg/ml ethidium bromide and visualized over UV illumination. The linear DNA bands were excised from the gel and subsequently purified with QIAEX according to the manufacturer's instructions.

The linearized DNAs from plasmids pSP6tat-s and p616EX2 were used as templates to produce ^{32}P-labeled RNA transcripts as described in the standard transcription protocol from the Promega Protocols and Applications Guide, 2nd edition (Promega Corporation, 1991) for high specific activity RNA probes. SP6 RNA polymerase and linear plasmid pSP6tat-s were used to produce *tat-s* RNA, while T7 RNA polymerase and linear plasmid p616EX2 were used to produce actin RNA. The transcription reactions for the production of the substrate RNAs were scaled up to a final volume of 50 µl. The labeled *tat-s* and actin transcripts were EtOH precipitated, resuspended in 7µl RNA loading buffer, heated to 70°C for 3 minutes and quick-chilled on ice. The samples were then electrophoresed through a TBE buffered 7 M urea/5% polyacrylamide gel (0.4 mm thick) for 2 hours at 1600 volts. The transcripts were visualized by exposing the gel to x-ray film for 3 to 10 minutes. The developed film was aligned with the gel and the slowest migrating bands were excised and eluted in 300 µl RNA elution buffer at 37°C for 12 to 16 hours with occasional gentle agitation. The eluted RNAs were ethanol precipitated, resuspended in sterile ddH_2O, and stored at -20°C until ready for use.

Additionally, large amounts of unlabeled *tat-s* RNA were synthesized using the conditions described in the Promega Protocols and Applications Guide, 2nd edition (Promega Corporation, 1991) for the synthesis of large amounts of RNA. After a phenol/SEVAG extraction, the unlabeled *tat-s* RNA transcripts were purified by passage through a Sephadex G-50 spin column, precipitated with EtOH, and

resuspended in sterile ddH_2O and stored at -20°C until ready for use. The RNA concentration was determined by an A_{260} measurement of the final solution.

Ribozyme-Mediated Cleavage Reactions of Substrate RNA

Cleavage reactions were performed in cleavage buffer (50 mM Tris, 20 mM $MgCl_2$) at 37°C. The cleavage reactions were performed at either pH 8.0, pH 7.5, or pH 7.2 as indicated in each experiment described in Chapter 3. The substrate RNA and the ribozyme RNA were heated in water to 70°C for 3 minutes and immediately quick-chilled on ice before being combined in the following order: a) appropriate volumes of a 5X concentrated cleavage buffer and sterile ddH_2O, such that a 1X concentration of cleavage buffer is obtained in the final reaction volume, were combined in a tube and allowed to reach 37°C; b) the labeled substrate RNA (and in some experiments, unlabeled substrate RNA) was added next; c) followed by the addition of ribozyme. In the case of cleavage reactions using ribozyme RZ2, instead of the substrate RNA being the second reagent added, RZ2 RNA was added to allow for the formation of the ribozyme's tertiary active structure, followed by the addition of the substrate RNA. In both cases, the reactions were initiated upon the addition of the final component of the reaction. Cleavage was allowed to proceed at 37°C. At various time points, 5 µl aliquots of the cleavage reaction were removed, transferred to tubes that contained 3 µl RNA loading buffer and immediately frozen in liquid nitrogen. The aliquots were stored on dry ice until all samples from the time points were obtained. The samples were heated at 70°C for 3 minutes and cooled on ice before electrophoresis in TBE-buffered 7 M urea/5% polyacrylamide gels (0.4 mm

thick) for 2 hours at 1600 volts in a BRL Sequencing Gel Apparatus Model SO. The gels were placed in fixing solution (12% methanol, 10% glacial acetic acid in ddH_2O) for 15 minutes before drying and autoradiography.

Quantifying the Extent of Substrate Cleavage

In the initial reaction kinetics experiments using ribozymes $RZ3_{10}$, $RZ4_{12}$, and $RZ5_{14}$, the quantity of full-length substrate and resulting cleavage products were determined using two methods. With both methods, it was only necessary to measure the intact substrate band and the 5′ product band to determine the extent of substrate cleavage.

Method I

The autoradiograph was aligned with the dried gel, and the regions on the gel that corresponded to the intact substrate and the 5′ cleavage product as well as a background control strip from a section of the gel with little or no radioactivity were excised in strips of approximately equal size. The strips were placed in a 7% BBS-3 cocktail [7% (v/v) Beckman Bio-Solv® 3, 0.32% 2,5-diphenyloxazole (PPO) in toluene] and measured in a Beckman LS 7000 liquid scintillation counter. The resulting radioactive value from the intact substrate band is defined as ***CPM Uncut***. The resulting radioactive value from the 5′ cleavage band is defined as ***CPM P1***. The resulting radioactive value from the background control strip is defined as ***CPM Background***. The following equations were used to obtain values that are corrected for background error:

$$\text{CPM(c) Uncut}_{t=n} = \text{CPM Uncut}_{t=n} - \text{CPM Background} \quad \textbf{(Equation 2.1)}$$

$$\text{CPM(c) Pl}_{t=n} = \text{CPM Pl}_{t=n} - \text{CPM Background} \quad \textbf{(Equation 2.2)}$$

Since the intact tat-s message is 390 nt and the 5′ cleavage product is 205 nt, the ***CPM(c) Pl*** value must be normalized to reflect molar stoichiometry relative to the ***CPM(c) Uncut*** value. The size ratio of *Pl* to *tat-s* is derived below and is used as a coefficient in subsequent calculations:

$$\frac{\text{length Pl}}{\text{length tat-s}} = \frac{205 \text{ nt}}{390 \text{ nt}} = 0.53 \quad \textbf{(Equation 2.3)}$$

Thus normalizing the CPM value for the amount of 5′ labeled cleavage product present at time $t = n$ relative to labeled tat-s is therefore:

$$\text{CPM(c) Pl}_{\text{normal, } t=n} = \frac{\text{CPM(c) Pl}_{t=n}}{0.53} \quad \textbf{(Equation 2.4)}$$

the fraction of tat-s cleavage would be:

$$\text{fraction tat-s cleaved}_{t=n} = \frac{\dfrac{\text{CPM(c) Pl}_{t=n}}{0.53}}{\dfrac{\text{CPM(c) Pl}_{t=n}}{0.53} + \text{CPM(c) Uncut}_{t=n}}$$

$$= \frac{\text{CPM(c) Pl}_{\text{normal, } t=n}}{\text{CPM(c) Pl}_{\text{normal, } t=n} + \text{CPM(c) Uncut}_{t=n}}$$

(Equation 2.5)

So far, ***fraction tat-s cleaved***$_{t=n}$ represents only the labeled population of the tat-s in the timecourse experiment. Assuming the labeled population of tat-s reflects the behavior of the entire tat-s population in the reaction, the actual amount of tat-s cleaved can be determined using the equation below

$$\text{mol tat-s}_{\text{cleaved, } t=n} = (\text{fraction tat-s cleaved}_{t=n}) \cdot (\text{mol tat-s}_{\text{total, } t=0})$$

(Equation 2.6)

and since stoichiometrically,

$$1 \text{ mol tat-s} \rightarrow 1 \text{ mol P1} + 1 \text{ mol P2} \qquad \textbf{(Equation 2.7)}$$

the amount of tat-s substrate that has been cleaved in a reaction at time $t = n$ can be expressed as

$$\text{mol tat-s}_{\text{cleaved, } t=n} = \text{mol P1}_{t=n} = \text{mol P2}_{t=n} \qquad \textbf{(Equation 2.8)}$$

Therefore the amount of the 5′ cleavage product can be determined:

$$\text{mol P1 present}_{t=n} = (\text{fraction tat-s cleaved}_{t=n}) \cdot (\text{mol tat-s}_{\text{total, } t=0})$$

(Equation 2.9)

Method II

The autoradiograph was scanned on a Gilson Spectrophotometer at a wavelength of 425 nm. The baseline for each scan was normalized and the peaks corresponding to the substrate (called *Peak A*) and product (called *Peak B*) were

excised from the resulting profile printout and weighed on a Mettler Balance. The resulting weight measurements were used in the determination of the extent of substrate cleavage. Using a variants of some earlier equations, the weight values were normalized as follows:

$$\text{grams Peak } B_{\text{normal, } t=n} = \frac{\text{grams Peak } B_{t=n}}{0.53} \qquad \textbf{(Equation 2.10)}$$

and the fraction of tat-s cleavage is

$$\text{fraction tat-s cleaved}_{t=n} = \frac{\text{grams Peak } B_{\text{normal, } t=n}}{\text{grams Peak } B_{\text{normal, } t=n} + \text{grams Peak } A_{t=n}}$$

(Equation 2.11)

Using Equation 2.9, the amount of P1 present in the reaction at $t = n$ can be determined. Since the amount of ribozyme for each reaction is also known, the amount of 5′ product produced per ribozyme molecule at time $t = n$ can be determined:

$$\frac{\text{mol P1}_{t=n}}{R \cdot n} = \text{turnover rate} \qquad \textbf{(Equation 2.12)}$$

Since the calculations were numerous and repetitive, data analysis was performed using the Excel 3.0 Spreadsheet program. The tabulated data are presented in spreadsheet form in Appendices A - J.

CHAPTER 3

RESULTS

Ribozyme Design

The design of ribozymes followed the sequence requirements and constraints described by Haseloff and Gerlach (1988) for the hammerhead ribozymes, and by Hampel *et al.* (1990) for the hairpin ribozyme. Both types of ribozymes have similar requirements for proper substrate recognition and activity:

1) The ribozyme requires that the substrate have a particular nucleotide sequence at or near the cleavage site. For the hammerhead ribozyme, the cleavage site on the substrate RNA must have the sequence 5′-GUH-3′ (H = any nucleotide except G) preceding the cleavage site. For the hairpin ribozyme, the sequence 5′-GUC-3′ must precede the cleavage site on the substrate RNA.

2) The ribozymes must have sequences complementary to the nucleotides flanking the required "GUH" or "GUC" sequence of the substrate RNA in order to allow proper recognition and binding of the ribozyme to the substrate RNA.

3) The ribozyme must contain sequences which aid in the formation of the ribozyme's tertiary structure and activity. These sequences are highly conserved in some of the naturally occurring self-cleaving RNAs. The hammerhead ribozymes use the sequence described in Haseloff and Gerlach (1988), derived from the (+)-strand satellite RNA of tobacco ringspot virus. The hairpin ribozyme uses the sequence presented in Hampel *et al.* (1990), derived from the (-)-strand satellite RNA of tobacco ringspot virus. From these constraints, it is evident that in order to design a ribozyme

that cleaves a specific RNA molecule, knowledge of the nucleotide sequence of the substrate RNA is an absolute requirement.

As noted in Chapter 1, the *tat* gene mRNA was targeted as a substrate for the ribozymes. For these experiments, a chemically synthesized *tat* gene, *tat-s*, which encodes a functional Tat protein (Ferguson *et al.* 1989) was chosen because it was available in an *in vitro* transcription vector. The *tat-s* gene was assembled as four oligonucleotide subfragments with sequences which introduced five restriction enzyme sites (*Nco I, Sph I, Stu I, Hind III*, and *Bam HI*) into the gene sequence. The restriction enzyme sites, though not present in the native (wild-type) gene, do not alter the wild-type amino acid sequence of the Tat protein (Figure 3.1). To produce the *in vitro* transcription vector, the *Bam HI-Nco I* fragment containing the synthetic Tat coding sequence was inserted into plasmid pSP6polyA. The resultant plasmid, pSP6tat-s, can be used for the SP6 promoter-directed transcription of full-length, polyadenylated *tat-s* RNA (Figure 3.2). Cell-free translation of the *tat-s* transcript produces a protein with similar SDS-PAGE behavior as native Tat protein expressed in bacteria, mouse cells and HIV-infected cells. To demonstrate Tat-s protein activity, the *tat-s* gene was placed into an SV40-derived expression plasmid. The resulting *tat-s* expression plasmid and either plasmid pLTR-CAT or pLTR-β-gal, reporter gene plasmids for chloramphenicol acetyl transferase and β-galactosidase, respectively, were used to co-transfect HeLa cells. The transfected HeLa cells produced CAT or β-galactosidase activity, establishing the ability of the synthetic TAT protein to induce LTR expression of the reporter genes *in trans*.

Figure 3.1. Nucleotide sequence and corresponding encoded amino acid sequence for the synthetic HIV-1 Tat coding sequence. The row labeled **"tat-s"** corresponds to the synthetic *tat* coding sequence. Differences between the synthetic *tat* coding sequence and the HIV-1 isolate IIIB *tat* coding sequence is indicated by the appearance of the naturally occurring nucleotide in the row labeled **"tat."** The row labeled **"TAT"** presents the amino acid sequence encoded by both nucleic acid sequences. The nucleotide substitutions at positions 39 and 42 were introduced to remove dyad symmetry to prevent formation of an internal hairpin structure during gene assembly. All other base substitutions were made to introduce the restriction endonuclease cleavage sites (*Nco I, Sph I, Stu I, Hind III,* and *Bam HI*) to facilitate gene assembly. *(Taken from Ferguson* et al., *1989).*

```
          Nco I                15                  30
tat-s  ccATG GAG CCA GTA GAT CCT AGA CTA GAG CCC TGG AAG CAC
tat                                                      T
TAT      MET Glu Pro Val Asp Pro Arg Leu Glu Pro Trp Lys His

               45                  60  Sph I           75
tat-s    CCT GGA AGT CAG CCT AAA ACT GCA TGC ACC AAT TGC TAT
tat        A                         T   T
TAT      Pro Gly Ser Gln Pro Lys Thr Ala Cys Thr Asn Cys Tyr

                     90                  105
tat-s    TGT AAA AAG TGT TGC TTT CAT TGC CAA GTT TGT TTC ATA
tat
TAT      Cys Lys Lys Cys Cys Phe His Cys Gln Val Cys Phe Ile

         120   Stu I          135                 150
tat-s    ACA AAG GCC TTA GGC ATC TCC TAT GGC AGG AAG AAG CGG
tat          A
TAT      Thr Lys Ala Leu Gly Ile Ser Tyr Gly Arg Lys Lys Arg

                  165                 180                 195
tat-s    AGA CAG CGA CGA AGA GCT CCT CAA GGC AGT CAG ACT CAT
tat
TAT      Arg Gln Arg Arg Arg Ala Pro Gln Gly Ser Gln Thr His

               Hind III  210                 225
tat-s    CAA GTA AGC TTA TCA AAG CAA CCC ACC TCC CAA TCC CGA
tat            T TCT C
TAT      Gln Val Ser Leu Ser Lys Gln Pro Thr Ser Gln Ser Arg

             240                 255         Bam HI
tat-s    GGG GAC CCG ACA GGC CCG AAG GAA TAG ggatcc
tat                                         ------
TAT      Gly Asp Pro Thr Gly Pro Lys Glu END
```

The plasmid map of pSP6tat-s is also shown in Figure 3.2. The available plasmid map of pSP6tat-s was not detailed enough to predict the exact sequence of the mRNA transcript. The fullest approximation of the sequence is shown in Figure 3.3. Although base position 1 on the *tat-s* transcript has been arbitrarily designated as the first base encoding the Tat-s protein sequence, the transcript may contain several nucleotides 5′ of this sequence. Additionally, unknown nucleotides may exist between the stop codon and the poly-A region as well as between the poly-A region and the *Pvu II* site used to linearize the plasmid for *in vitro* transcription. Because the exact size of the transcript is not known, the size of the *tat-s* transcript as well as the *tat-s* cleavage products must be empirically determined.

The target site picked for ribozyme RZ1 spans bases 193 to 207, with the sequence 5′-CAUCAAGUa↑AGCUUA-3′ containing a required GUA cleavage sequence at position 199 to 201. Cleavage should occur after position 201 as indicated by the arrow. The *tat-s* transcript is targeted by flanking the ribozyme conserved sequences with bases complementary to the nucleotides that flank the intended cleavage site on the substrate RNA. The lowercase letter marks the nucleotide within the target sequence of the substrate that is unable to form a basepair with the ribozyme. The primary sequence of ribozyme RZ1 is:

5′-gUAAGCU**CUGAUGAGUCCGUGAGGACGAA**ACUUGAUG-3′

The Haseloff and Gerlach conserved hammerhead ribozyme sequence is in bold and the flanking underscored sequences represent the nucleotides that basepair with the substrate RNA. Note that the first nucleotide of this particular ribozyme is not

Figure 3.2. SP6 promoter-directed transcription of *tat-s* RNA. Plasmid pSP6tat-s is linearized by *Pvu II* digestion. The linear DNA was isolated by electrophoresis and purified by binding to a solid support. The linear DNA was used as template for SP6 RNA polymerase. Transcription initiates at the SP6 promoter site and terminates as the enzyme "runs off" the template, producing an RNA molecule of discrete length. The pSP6tat-s plasmid map is not to scale and only shows the relative positions of the major features. Amp = β-lactamase gene; ori = *E. coli* origin of replication.

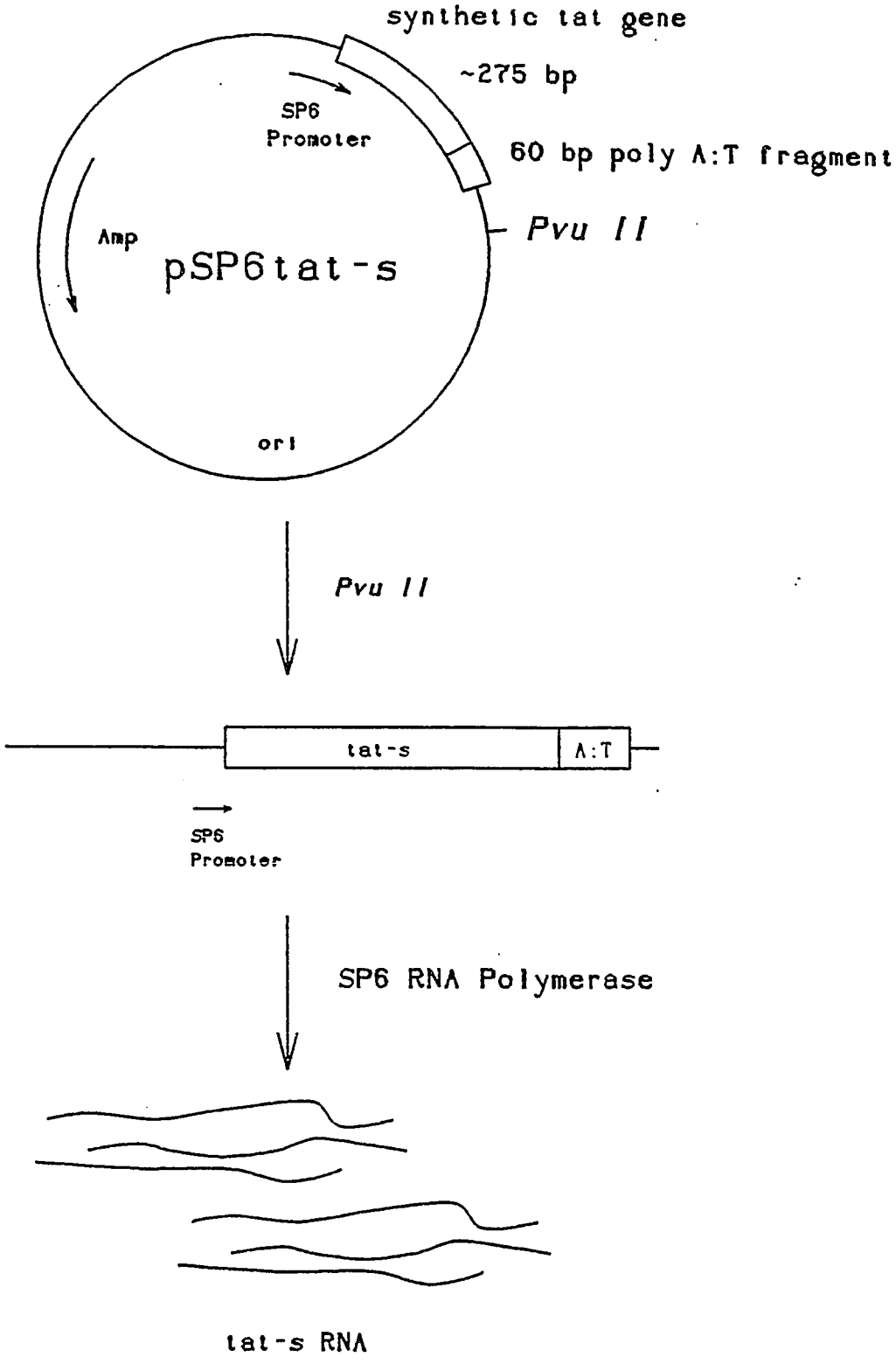
synthetic tat gene
~275 bp
SP6
Promoter
60 bp poly A:T fragment
Amp
pSP6tat-s
Pvu II
ori
Pvu II
tat-s
A:T
SP6
Promoter
SP6 RNA Polymerase
tat-s RNA

Figure 3.3. Sequence of the HIV-1 *tat-s* transcript. The plasmid map of pSP6tat-s did not provide detailed information to predict the exact sequence of the *tat-s* transcript, hence the appearance of $(NNNN)_7$ denoting the positions of nucleotides of unknown sequence and number.

```
                  1       10          20          30          40
(NNNN)₂ (C or U) AUGGAGCCAG UAGAUCCUAG ACUAGAGCCC UGGAAGCACC

         50          60          70          80          90
CUGGAAGUCA GCCUAAAACU GCAUGCACCA AUUGCUAUUG UAAAAAGUGU

        100         110         120         130         140
UGCUUUCAUU GCCAAGUUUG UUUCAUAACA AAGGCCUUAG GCAUCUCCUA

        150         160         170         180         190
UGGCAGGAAG AAGCGGAGAC AGCGACGAAG AGCUCCUCAA GGCAGUCAGA

        200         210         220         230         240
CUCAUCAAGU AAGCUUAUCA AAGCAACCCA CCUCCCAAUC CCGAGGGGAC

        250         260    266
CCGACAGGCC CGAAGGAAUA GGGAUC (A or G) (NNNN)₂ (AAA)₂₀ (NNNN)₂
```

involved in basepairing with the substrate. This is a by-product of the method used to synthesize the ribozyme molecule, where the T7 RNA polymerase always initiates transcription with a G residue (Milligan *et al.*, 1987). Figure 3.4 shows a conceptual scheme of the ribozyme bound to its substrate at the target sequence.

Subsequent ribozymes were designed based on alternative cleavage sites in the substrate RNA which allowed for the basepairing of the initial G residue of each ribozyme. This new target site chosen for ribozyme RZ2 spans bases 180 to 193 and has the sequence 5′-AGGCa↑gucAGACUC-3′. The cleavage site, which should occur after position 184, is indicated by the arrow. The lowercase letters mark nucleotides that do not basepair with the ribozyme while the underscored letters mark the nucleotides that basepair with the ribozyme. Ribozyme RZ2, which employs the hairpin structure, has the following primary sequence:

5′-GAGUCUAGAAGCCUACCAGAGAAACACACGUU-

GUGGUAUAUUACCUGGUA-3′

Except for the underscored sequences, which represent the nucleotides that basepair with the substrate RNA, this ribozyme sequence is composed primarily of the Hampel conserved hairpin sequence. Figure 3.5 shows a conceptual scheme of the ribozyme bound to its substrate at the target sequence.

In order to test the effect of varying the length of the sequences that basepair between ribozyme and target, hammerhead ribozymes $RZ3_{10}$, $RZ4_{12}$, and $RZ5_{14}$, were designed based on the GUC sequence present at positions 185 to 187 of the *tat-s*

Figure 3.4. Ribozyme RZ1 binding to the *tat-s* RNA transcript. The ribozyme sequence is shown using characters without serifs and the target sequence on the *tat-s* RNA transcript is shown using characters with serifs. The small arrow seen in the ribozyme:substrate complex indicates the site of *tat-s* cleavage.

5' - GUAAGCUCUGAUGAGUCCGUGAGGACGAAACUUGAUG - 3'

Ribozyme RZ1

+

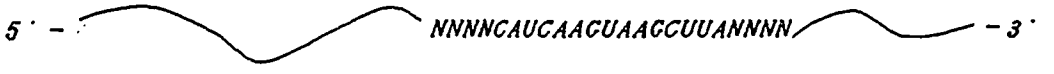

tat-s RNA

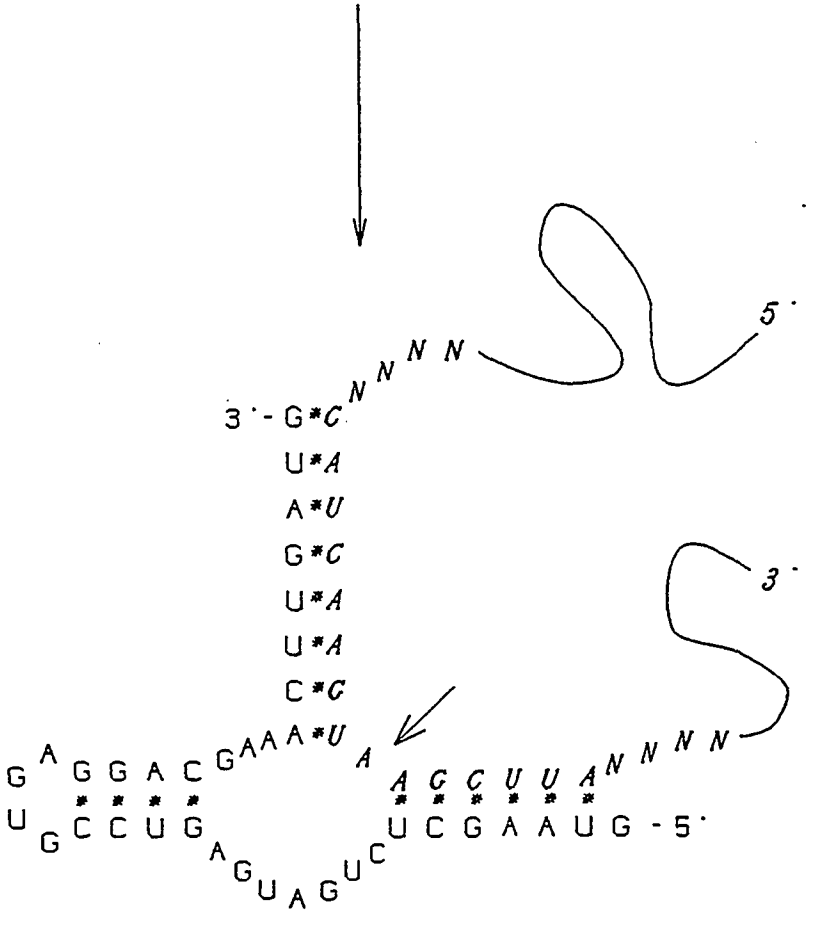

Ribozyme:tat-s complex

Figure 3.5. Ribozyme RZ2 binding to the *tat-s* RNA transcript. The ribozyme sequence is shown using characters with serifs and the target sequence on the *tat-s* RNA transcript is shown using characters without serifs. The small arrow seen in the ribozyme:substrate complex indicates the site of *tat-s* cleavage.

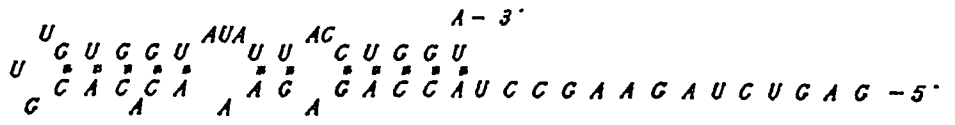

Ribozyme RZ2

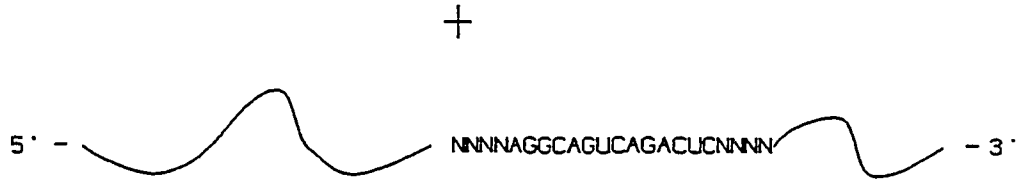

tat-s RNA

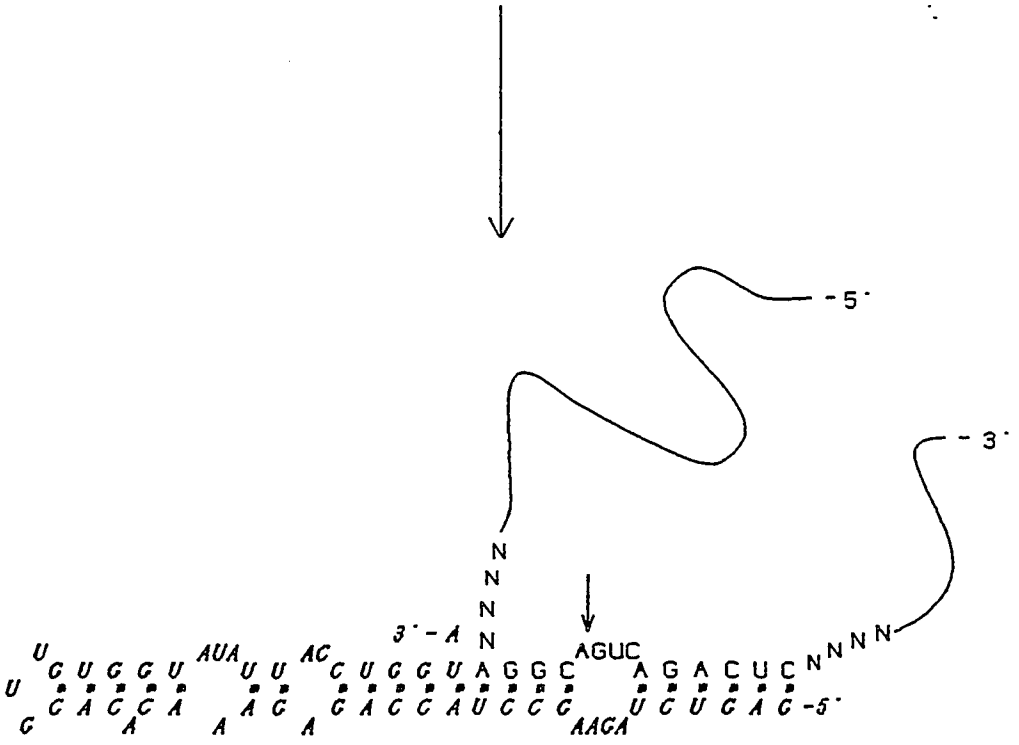

Ribozyme:tat-s complex

transcript. The targets vary by the number of basepairs included in the 5′ complementary sequence and are:

$RZ3_{10}$ target site – 5′-CAGUc↑AGACUC-3′

$RZ4_{12}$ target site – 5′-GGCAGUc↑AGACUC-3′

$RZ5_{14}$ target site – 5′-AAGGCAGUc↑AGACUC-3′

The cleavage site using ribozymes $RZ3_{10}$, $RZ4_{12}$, and $RZ5_{14}$ occurs after base 187 and the sizes of the *tat-s* RNA 5′ and 3′ cleavage fragments produced by the three ribozymes will be identical. Since the ribozyme target sequences are very similar, differing only in the number of basepairs formed upstream from the cleavage site, the nomenclature of these particular hammerhead ribozymes also includes a subscript that indicates the extent of basepair formation with the substrate. The primary sequence of ribozymes $RZ3_{10}$, $RZ4_{12}$, and $RZ5_{14}$ are as follows:

$\underline{RZ3_{10}}$

5′-GAGUCU**CUGAUGAGUCCGUGAGGACGAA**ACUGuucu-3′

$\underline{RZ4_{12}}$

5′-GAGUCU**CUGAUGAGUCCGUGAGGACGAA**ACUGCC-3′

$\underline{RZ5_{14}}$

5′-GAGUCU**CUGAUGAGUCCGUGAGGACGAA**ACUGCCUU-3′

The bolded sequences represent the Haseloff and Gerlach conserved hammerhead sequence, while the underscored sequences represent the nucleotides that basepair with the substrate RNA. Note that ribozyme $RZ3_{10}$ also contains some sequence at its 3′

region that is not involved in substrate recognition and binding. Schematic illustrations of the different ribozymes bound at the *tat-s* RNA target sequence is shown in Figure 3.6.

To allow easy comparison of the five ribozymes designed for use in these studies, the relevant features of each ribozyme are summarized in Table 3.1 and the relative positions of the target sites for each ribozyme are indicated on aligned sequences in Figure 3.7.

Ribozyme Synthesis

The ribozyme RNA molecule was synthesized *in vitro* following the scheme of Milligan *et al.* (1987) as diagrammed in Figure 3.8. Two complementary oligonucleotides are chemically synthesized to produce a template for T7 RNA polymerase. Only the T7 RNA polymerase recognition sequence must be double-stranded while the portion encoding the actual RNA may be single-stranded. One oligonucleotide contains both the polymerase recognition site and the negative strand encoding the ribozyme, while the second oligonucleotide contains only the complement of the recognition sequence. Both molecules are annealed to form a molecule that is partially double-stranded at the T7 promoter site. With the promoter portion of the molecule being double-stranded, the T7 RNA polymerase is able to initiate transcription and uses the single-stranded negative strand as a template for the ribozyme. Upon reaching the end of the template molecule, the polymerase dissociates from the transcription complex and releases the RNA molecule. This strategy was used to synthesize all ribozymes.

Figure 3.6. Ribozymes $RZ3_{10}$, $RZ4_{12}$ and $RZ5_{14}$ bound to the *tat-s* RNA transcript. The ribozyme sequences are shown using characters without serifs and the target sequence on the *tat-s* RNA transcript is shown using characters with serifs. The small arrow seen in each ribozyme:substrate complex indicates the site of *tat-s* cleavage.

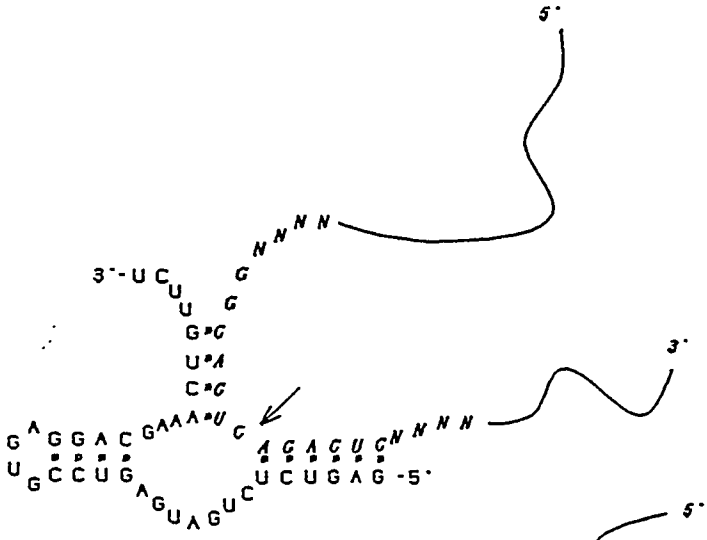

Ribozyme $RZ3_{10}$: tat-s complex

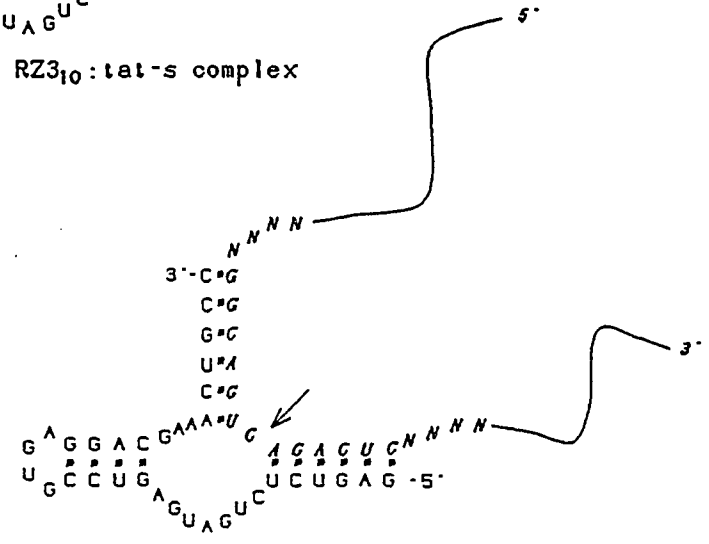

Ribozyme $RZ4_{12}$: tat-s complex

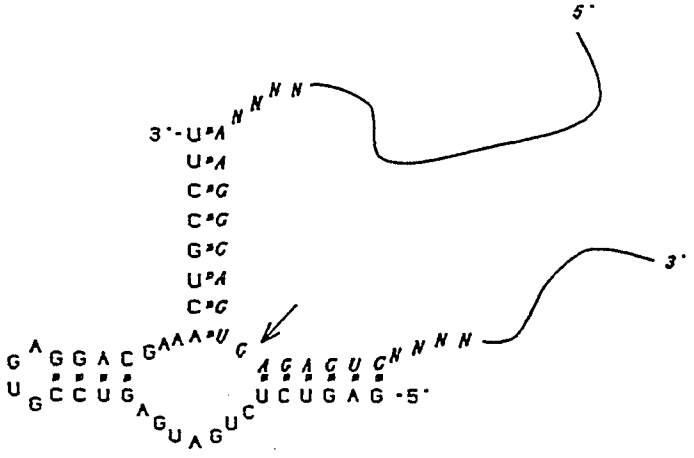

Ribozyme $RZ5_{14}$: tat-s complex

Table 3.1. Major features of the ribozyme constructs and their corresponding substrate cleavage products.

Ribozyme	RZ1	RZ2	$RZ3_{10}$	$RZ4_{12}$	$RZ5_{14}$
length	37 nt	50 nt	36 nt	34 nt	36 nt
calculated molecular weight	12,210 MW	16,500 MW	11,880 MW	11,220 MW	11,880 MW
secondary structure motif	hammer-head	hairpin	hammer-head	hammer-head	hammer-head
target size	15 nt	14 nt	11 nt	13 nt	15 nt
bp formed with substrate	14 bp	10 bp	10 bp	12 bp	14 bp
size of 5′ cleavage product	218 nt	202 nt	205 nt	205 nt	205 nt
size of 3′ cleavage product	172 nt	188 nt	185 nt	185 nt	185 nt

Figure 3.7. Relative positions of the *tat-s* RNA cleavage site for ribozymes RZ1, RZ2, $RZ3_{10}$, $RZ4_{12}$ and $RZ5_{14}$. The topmost set of rows the alignment of the *tat-s* and *tat* coding region along with the corresponding amino acid sequence. The target site for each ribozyme is presented in the subsequent rows. The bold letters indicate the nucleotides involved in basepairing with the corresponding ribozyme with the arrow marking the site of cleavage. Note that with the exception of ribozyme RZ1, all the ribozymes have the potential of binding and cleaving the naturally occurring *tat* RNA transcript. *Hind 3* = *Hind III* restriction site in *tat-s*.

```
                  180         190         200 Hind 3 210
tat-s       AGCTCCTCAA  GGCAGTCAGA CTCATCAAGT AAGCTTATCA
tat                                           TTCTC
TAT          AlaProGln  GlySerGlnThr HisGlnVal SerLeuSer
```

Ribozyme RZ1:

```
                  180         190         200 ⬇       210
            AGCUCCUCAA GGCAGUCAGA CUCAUCAAGU A AGCUUAUCA
```

Ribozyme RZ2:

```
                  180      ⬇  190         200         210
            AGCUCCUCAA GGCA GUCAGA CUCAUCAAGU AAGCUUAUCA
```

Ribozyme $RZ3_{10}$:

```
                  180         ⬇190        200         210
            AGCUCCUCAA GGCAGUC AGA CUCAUCAAGU AAGCUUAUCA
```

Ribozyme $RZ4_{12}$:

```
                  180         ⬇190        200         210
            AGCUCCUCAA GGCAGUC AGA CUCAUCAAGU AAGCUUAUCA
```

Ribozyme $RZ5_{14}$:

```
                  180         ⬇190        200         210
            AGCUCCUCAA GGCAGUC AGA CUCAUCAAGU AAGCUUAUCA
```

Figure 3.8. T7 promoter-directed synthesis of RNA using a partially double-stranded molecule as a template. Two chemically synthesized oligonucleotides are annealed to form a partially double-stranded dimer. The double-stranded region of the molecule serves as the T7 RNA polymerase recognition and initiation site while the single-stranded region of the molecule serves to encode the ribozyme. The oligonucleotides are shown using characters with serifs and the RNA transcript produced is shown using characters without serifs.

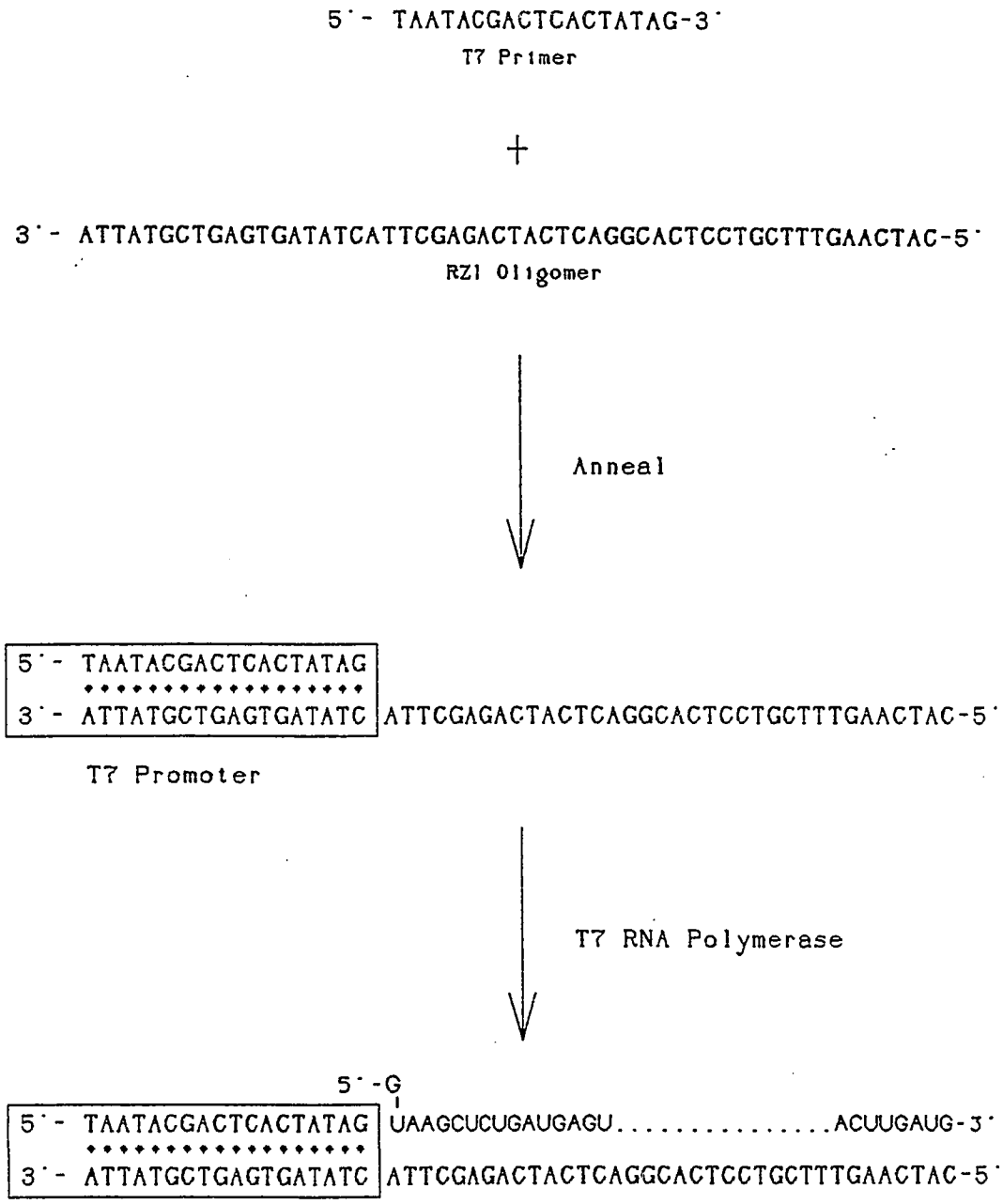
5'- TAATACGACTCACTATAG-3'
T7 Primer
+
3'- ATTATGCTGAGTGATATCATTCGAGACTACTCAGGCACTCCTGCTTTGAACTAC-5'
RZ1 Oligomer
Anneal
5'- TAATACGACTCACTATAG
3'- ATTATGCTGAGTGATATC
ATTCGAGACTACTCAGGCACTCCTGCTTTGAACTAC-5'
T7 Promoter
T7 RNA Polymerase
5'-G
5'- TAATACGACTCACTATAG
UAAGCUCUGAUGAGU.....ACUUGAUG-3'
3'- ATTATGCTGAGTGATATC
ATTCGAGACTACTCAGGCACTCCTGCTTTGAACTAC-5'

Control RNA Substrate

As a control for ribozyme substrate specificity, a transcription plasmid was constructed which encoded a partial actin mRNA sequence that would not be recognized by any of the *tat-s* ribozymes. A *Bam HI* to *Hinc II* fragment from double-stranded bacteriophage p11/2B2 DNA (Wang, 1987), containing the terminal 326 bp coding region of exon 2 and 30 bp of the second intron of the *Tg616* sea urchin actin gene was inserted into the *Bam HI* to *Hinc II* multiple cloning sites of plasmid pGEM®-1 (Figure 3.9). The resulting plasmid, p616EX2, contains the 356 bp actin subfragment in the 5′ to 3′ sense orientation relative to the T7 RNA polymerase promoter of the plasmid. Plasmid p616EX2 was linearized with *Hinc II* and used as the template for T7 RNA polymerase transcription of the actin control RNA. The actin transcript has a predicted size of 385 nt. The transcript is larger than the 356 bp actin gene DNA subfragment because 38 bases of the pGEM®-1 multiple cloning site, located between the T7 promoter and the *Bam HI* site of insertion, are also transcribed. The predicted sequence for the actin transcript is shown in Figure 3.10. Computer analysis of the actin transcript sequence against the ribozyme sequences revealed no apparent homology such that the ribozymes should not be able to bind and cleave the actin transcript at any site.

Size Determination of RNA Substrates and Products

Tat-s, actin and size standard RNA substrates were transcribed *in vitro* from the appropriate transcription vectors using ^{32}P-labeled precursors, incubated with various

Figure 3.9. Plasmid map of the control plasmid p616EX2. A 356 bp *Bam HI-Hinc II* DNA fragment comprising the terminal 326 bp coding region of exon 2 and initial 30 bp of the second intron of the *Tg616* sea urchin actin gene (Wang, 1987) was inserted into the *Bam HI* and *Hinc II* sites of plasmid pGEM®-1. The actin gene subfragment is in the sense orientation relative to the T7 promoter. The plasmid map of p616EX2 is not to scale and only shows the relative positions of the major features. Amp = β-lactamase gene; ori = *E. coli* origin of replication.

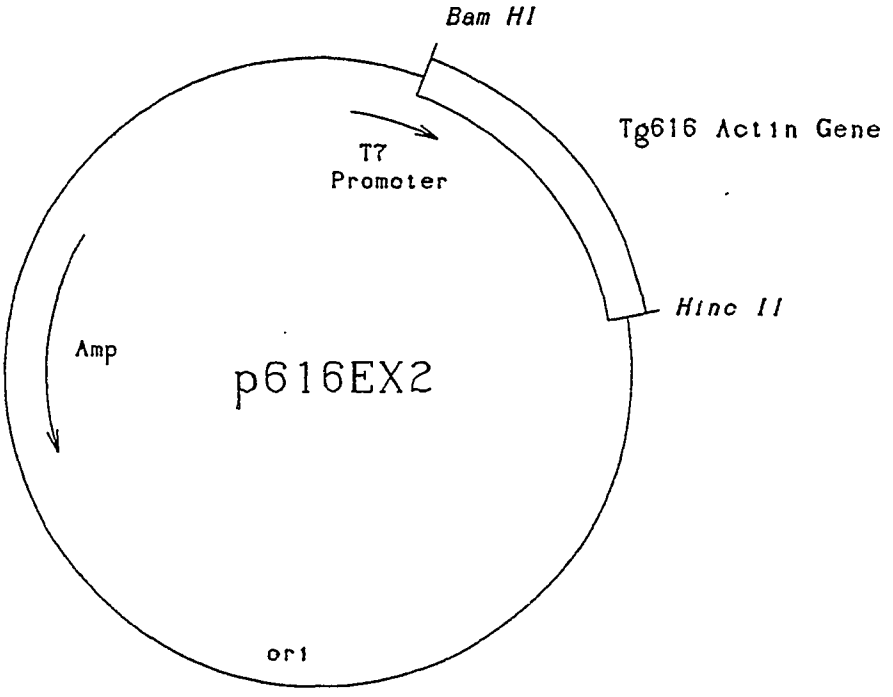
Bam HI
Tg616 Actin Gene
T7
Promoter
Hinc II
Amp
p616EX2
ori

Figure 3.10. Predicted sequence of the p616EX2 actin transcript. The sequence is based on the linearization of p616EX2 with *Hinc II* and subsequent T7 promoter-directed synthesis using T7 RNA polymerase. The lowercase letters represent part of the pGEM®-1 multiple cloning site present between the T7 promoter and the *Bam HI* actin subfragment cloning site.

```
        10          20          Bam  HI     40          50
gggagaccgg aauucgagcu cgcccgggGG AUCCGGUAUG GUGAAGGCCC

        60          70          80          90          100
GAUUCGCCGG AGACGAUGCC CCAAGGGCUG UCUUCCCAUC CAUUGUUGGC

       110         120         130         140         150
AGGCCCCGUC ACCAGGGUGU CAUGGUUGGU AUGGGACAGA AGGACAGCUA

       160         170         180         190         200
CGUCGGAGAC GAGGCUCAGA GCAAGAGAGG UAUCCUCACC CUGAAGUACC

       210         220         230         240         250
CCAUCGAGCA CGGUAUCGUC ACCAACUGGG ACGAUAUGGA GAAGAUCUGG

       260         270         280         290         300
CAUCACACCU UCUACAAUGA GCUCCGUGUU GCCCCAGAGG AGCAUCCCGU

       310         320         330         340         350
CCUCCUUACC GAGGCUCCCC UCAACCCCAA GGCCAACAGG GAAAAGAUGA

       360         370         380   385
CCCAGGUAAG AUUGAGUAAU GCCUACUAAA GCGUC
```

ribozymes and electrophoresed on sequencing gels to determine sizes. Figure 3.11 shows an autoradiograph of a resulting gel with the size standards, *tat-s* RNA incubated with various ribozymes and actin RNA. The measurements from this gel are shown on a standard curve in Figure 3.12. The actin mRNA is used as a standard of 385 nt along with the 1386 nt, 315 nt and 172 nt standard RNAs. The intact *tat-s* RNA is estimated to be 405 nt. The known *tat-s* coding region plus poly-A in the RNA transcript comprise only about 290 nt, leaving over 100 nt to be distributed among the three unknown sequence regions of the *tat-s* transcript as indicated in Figure 3.3.

Ribozyme cleavage produces a 5′ product of discrete size and a 3′ product of variable size. The latter heterogeneous distribution is the result of irregular termination of the RNA polymerase (Melton *et al.*, 1984) which adds a few indeterminate nucleotides at the end of the transcript, producing full length transcripts with heterogeneous ends. This size variation has little impact on the migration of the larger intact transcript but generates a diffuse band of the relatively smaller 3′ cleavage product seen in the lower part of the gel in Figure 3.11. The 5′ cleavage product, as designated in the right hand margin of Figure 3.11 is estimated to be 218 nt for the R1 ribozyme, 202 nt for the RZ2 ribozyme, and 205 nt for the $RZ3_{10}$ - $RZ5_{14}$ ribozymes. These sizes are 17 or 18 nt longer than the length of the *tat-s* coding region 5′ of the predicted cleavage sites for the ribozymes and suggest that this number of unknown nucleotides precede the start codon of the *tat-s* sequence in

Figure 3.11. Sizes of the full-length *tat-s* transcripts and the ribozyme cleavage products. Lanes **M1** and **M2** are labeled transcription control products from pT7-0 and Promega, respectively. Lane **M1**, containing the 1728, 315, and 146 nt fragments, lane **M2**, containing the 1386 and 172 nt fragments, and lane **g** containing the 385 nt labeled actin transcript were used to generate the standard curve. Labeled *tat-s* RNA was incubated with 50 pg of each ribozyme construct for 4 hours (lanes **a - e**) at pH 7.5 before gel electrophoresis. Lane **f** contains labeled *tat-s* RNA with no ribozyme incubation. The estimated sizes of the full-length *tat-s* transcript and the *tat-s* cleavage products are shown in parentheses. Full-length *tat-s* RNA is 390 nt. The 5′ cleavage products are estimated as being: 218 nt (RZ1), 205 nt (RZ2), and 202 nt ($RZ3_{10}$- 5_{14}). The 3′ cleavage products are estimated as being: 172 nt (RZ1), 188 nt (RZ2), and 185 nt ($RZ3_{10}$- 5_{14}).

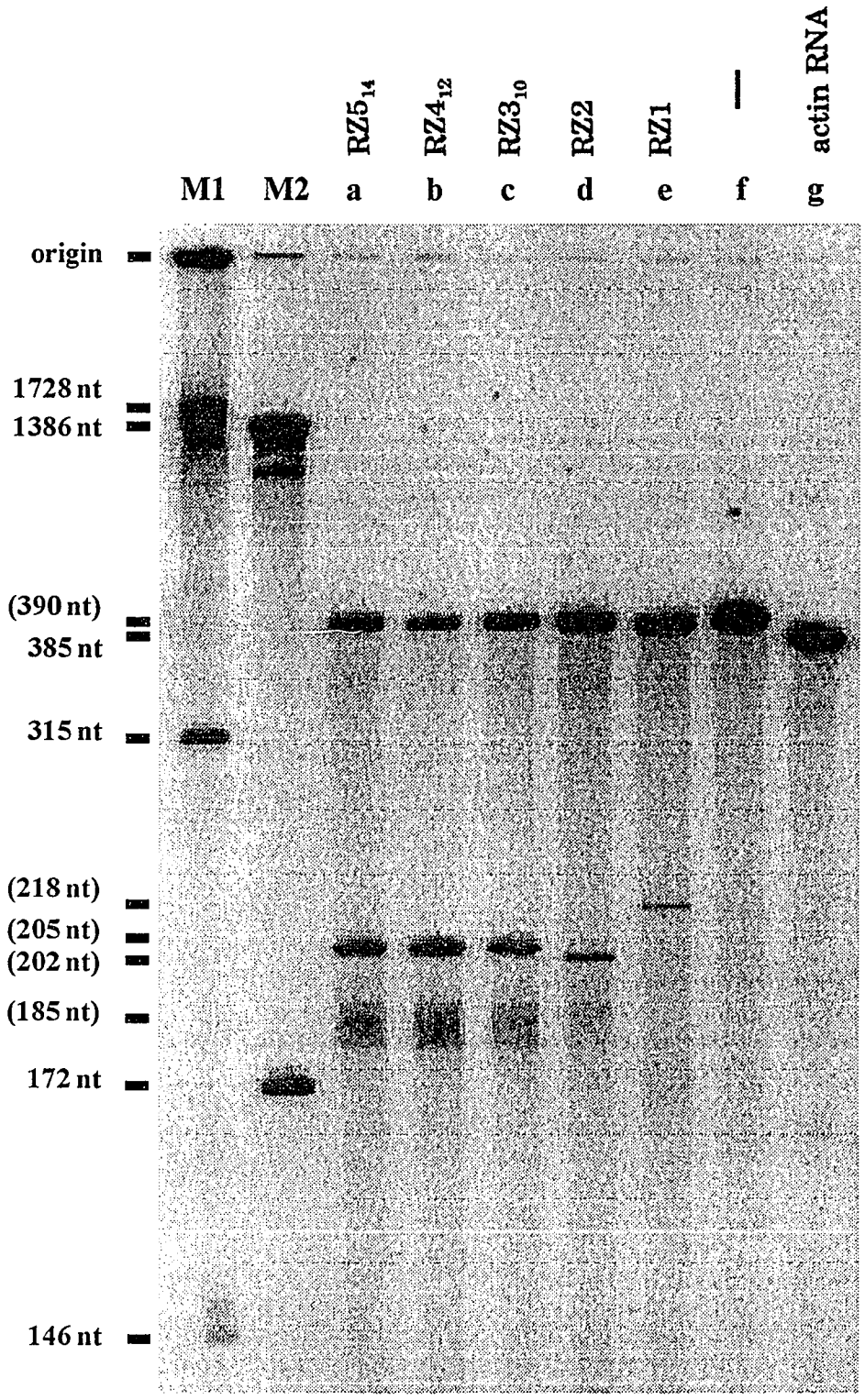
M1
M2
RZ5$_{14}$
a
RZ4$_{12}$
b
RZ3$_{10}$
c
RZ2
d
RZ1
e
—
f
actin RNA
g
origin
1728 nt
1386 nt
(390 nt)
385 nt
315 nt
(218 nt)
(205 nt)
(202 nt)
(185 nt)
172 nt
146 nt

Figure 3.12. Standard curve from the pT7-0, Promega, and actin control transcripts. The solid diamonds represent points used to generate the curve. The open circles represent points from which the sizes of the full-length *tat-s* transcript and the various 5′ and 3′ cleavage products were extrapolated.

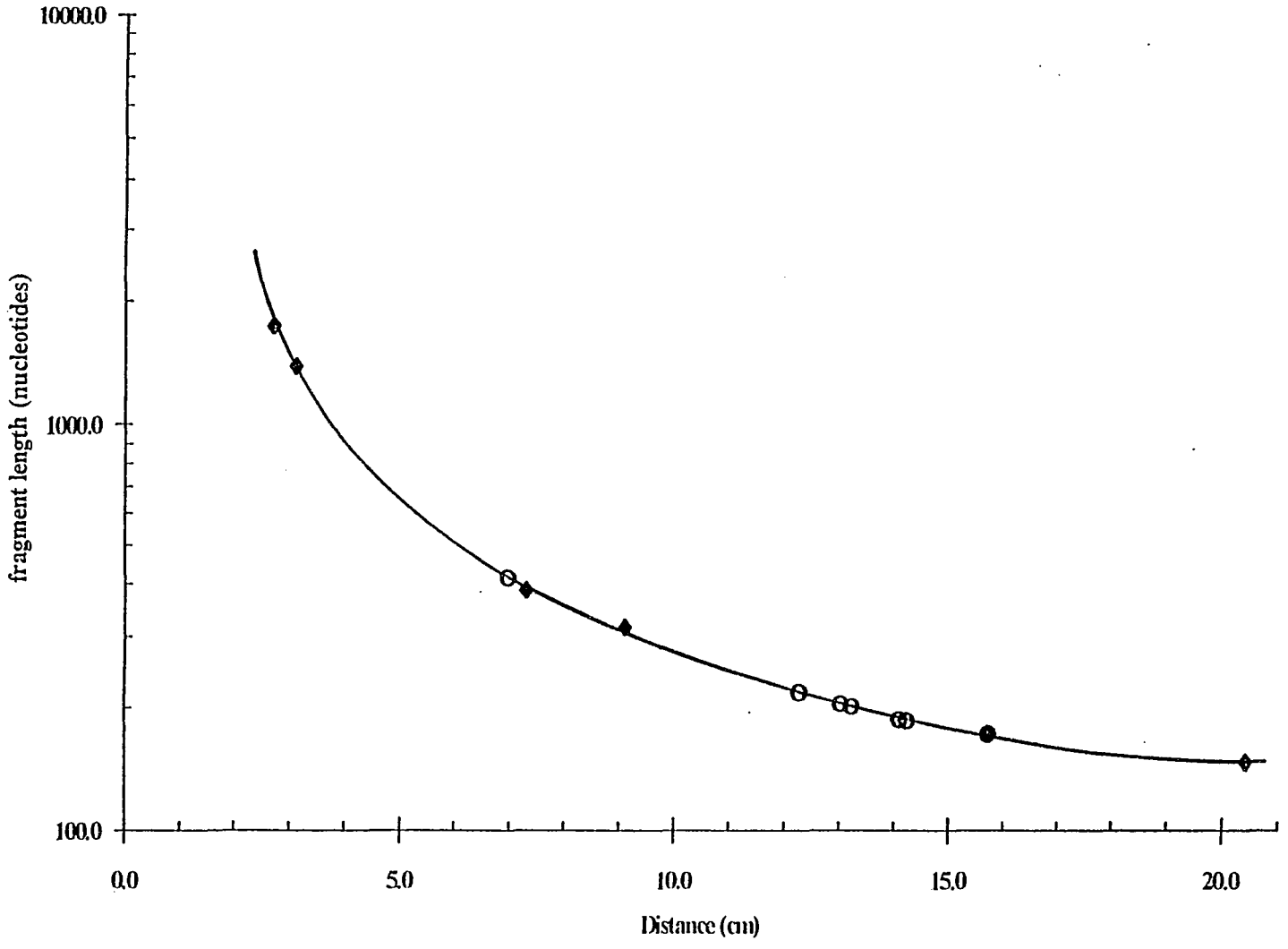
10000.0
1000.0
100.0
fragment length (nucleotides)
0.0
5.0
10.0
15.0
20.0
Distance (cm)

the *tat-s* transcript. The sizes of the 3′ cleavage products, as noted in Figure 3.11, are 172 nt, 188 nt and 185 nt, respectively. These are about 15 nt shorter than would be expected from the 405 nt estimate for the full-length transcript and the sizes of the 5′ cleavage products. The sums of the 5′ and the 3′ cleavage products indicate a size of 390 nt for the full length transcript. This latter size is probably more accurate since the sizes of the smaller RNA molecules are more accurately measured. Using this size, it can be calculated that, in addition to the poly A sequence, about 80 nt of unknown sequence occurs down stream of the *tat--s* coding region.

Ribozymes Do Not Degrade when Incubated at 37°C

Ribozymes RZ1, RZ2 and $RZ3_{12}$ were labeled with ^{32}P and incubated in 10 molar excess with the ^{32}P-labeled *tat-s* RNA transcript. An autoradiograph of an electrophoretic gel of the products of these reactions is shown in Figure 3.13. The size and concentration of all three ribozymes remain constant throughout the incubations with the *tat-s* RNA. At these low concentrations of reactants minimal cleavage of the substrates were observed.

Ribozymes Do Not Catalyze Cleavage of Non-target RNAs

Ribozymes RZ1, RZ2 and $RZ3_{12}$ were incubated in molar excess of ^{32}P-labeled actin RNA transcript for 1, 2 and 4 hours. The actin RNA transcript was also incubated without added ribozyme. The autoradiograph from the electrophoresis of the reaction products of these incubations on a gel is shown in Figure 3.14. There are no

Figure 3.13. Behavior of ribozyme concentration over time. 35 pg of labeled *tat-s* RNA was incubated with 50 pg of labeled ribozyme RZ1 and RZ2 for 0, 1, 2, and 4 hours or with 50 bp of labeled ribozyme $RZ4_{12}$ for 0, 2, and 4 hours. The 218 nt and 205 nt 5′ cleavage products are indicated. The sizes of the ribozymes are predicted and have not been determined empirically.

Figure 3.13

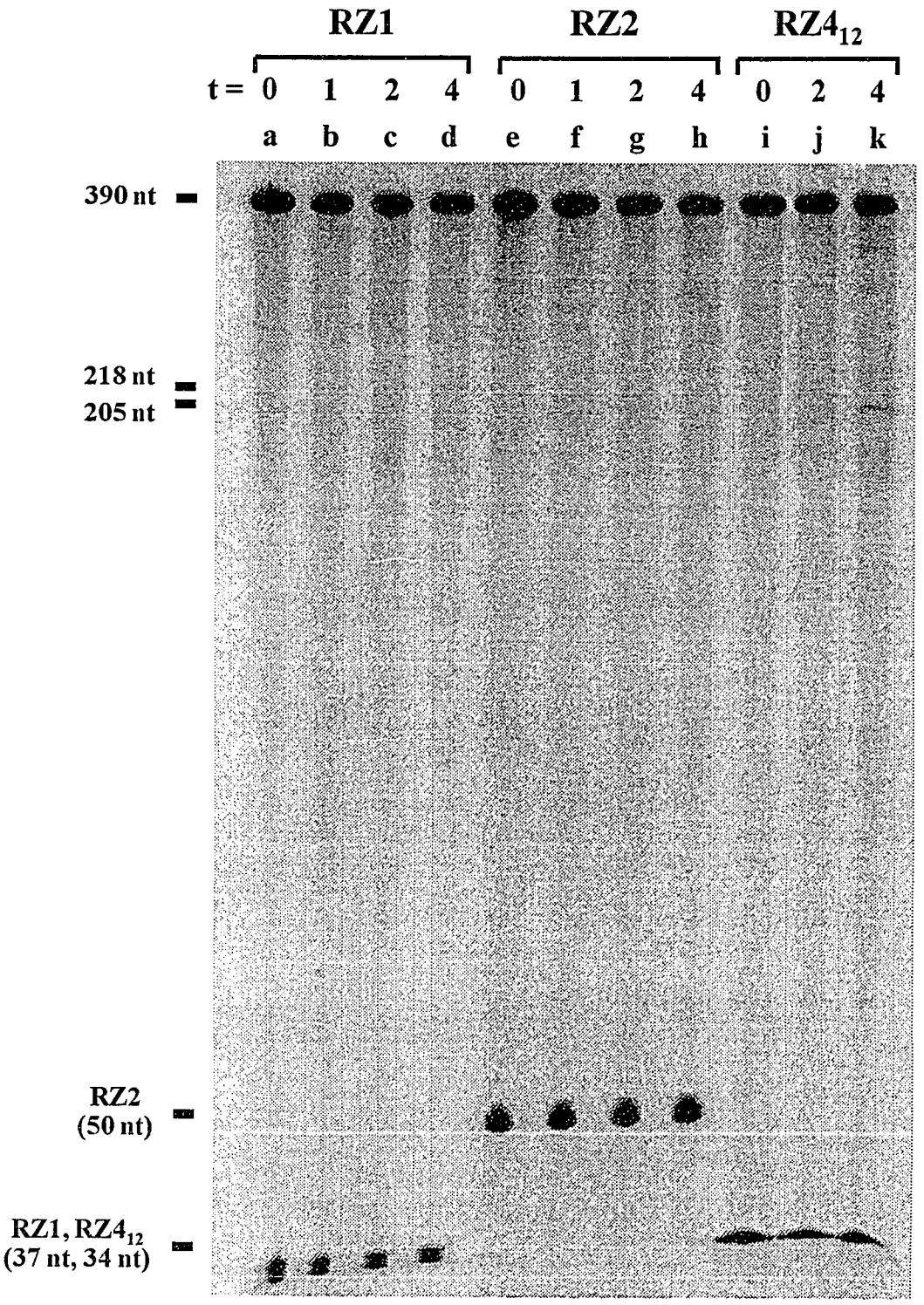
RZ1
RZ2
RZ4$_{12}$
t = 0 1 2 4 0 1 2 4 0 2 4
a b c d e f g h i j k
390 nt
218 nt
205 nt
RZ2
(50 nt)
RZ1, RZ4$_{12}$
(37 nt, 34 nt)

Figure 3.14. Actin RNA treated with ribozymes RZ1, RZ2, and $RZ4_{12}$. 35 pg of labeled actin RNA was incubated for 1, 2, and 4 hours with 50 pg of either ribozyme RZ1, RZ2, or $RZ4_{12}$ at pH 7.5. The 385 nt band indicated is the full-length actin RNA.

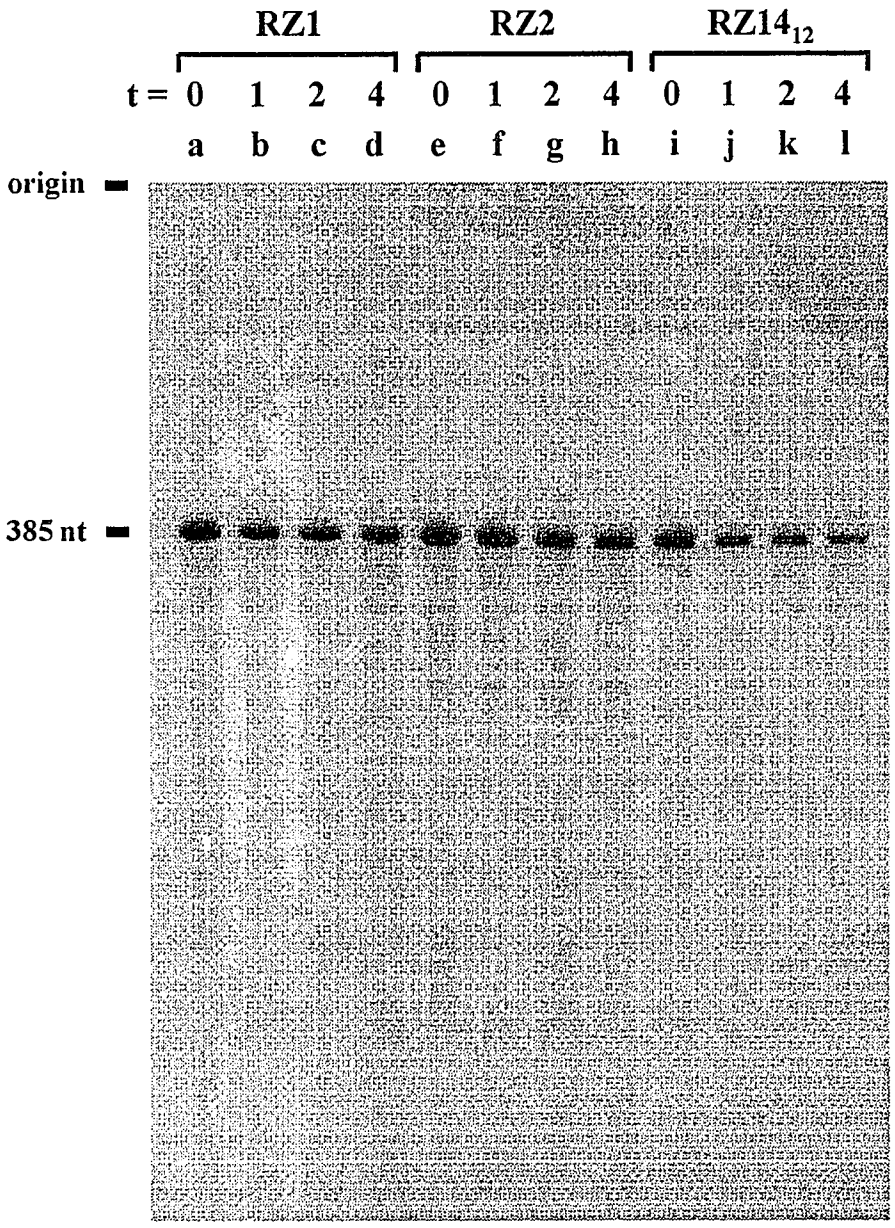
RZ1
RZ2
RZ14$_{12}$
t = 0 1 2 4 0 1 2 4 0 1 2 4
a b c d e f g h i j k l
origin
385 nt

cleavage products evident in any of the lanes and the intensities of the bands of full length RNA transcripts are equivalent in all lanes irrespective of the presence or absence of ribozyme. The ribozymes do not appear to catalyze appreciably the cleavage of RNA molecules which do not include specific recognition sequences.

Ribozyme Cleavage of Substrate RNA at Various pH

The effect of pH on the rate of ribozyme cleavage of substrate RNA was tested by incubating 70 pg of labeled *tat-s* RNA with 1 μg of either ribozyme $RZ3_{10}$ or $RZ4_{12}$ for 2 hours in cleavage buffers at pH 8.0, pH 7.5, or pH 7.2. The products of these reactions were electrophoresed on a gel; an autoradiograph of the gel is shown in Figure 3.15. A slightly higher level of non-specific RNA degradation appears to have occurred at pH 8.0 as judged by seemingly higher levels of background in the pH 8.0 lanes (**a** - **e**) than in the lanes of reactions performed at pH 7.5 and pH 7.2 (**f** - **j**; **k** - **o**, respectively). When the intensities of bands of the products of ribozyme $RZ3_{10}$ digestion are compared at different pH values (lanes **b**, **f**, **k**), no significant differences are observed. The ribozyme $RZ4_{12}$ products at the different pH values also displayed no significant differences in band intensity (lanes **c**, **g**, **l**). When the bands resulting from incubation of *tat-s* RNA with ribozyme $RZ3_{10}$ at all pH levels are compared with the bands resulting from incubation with ribozyme $RZ4_{12}$ at all pH levels, it is evident that ribozyme $RZ4_{12}$ is more active. The bands of the full-length transcript is much much weaker and the bands of the cleavage products much stronger in the lanes of samples incubated with ribozyme $RZ4_{12}$.

Figure 3.15. Effect of pH on ribozyme activity. 70 pg of labeled *tat-s* RNA was incubated with 1 μg of ribozyme $RZ3_{10}$ or $RZ4_{12}$ for 2 hours in cleavage buffers at pH 8.0, pH 7.5 or pH 7.2. The *tat-s* RNA in lanes **a**, **f**, and **k** were incubated for 2 hours in the absence of ribozyme. Parallel reactions were also performed using 500 ng of ribozyme and are indicated with an asterisk (*). Lane **p** contains untreated *tat-s* RNA.

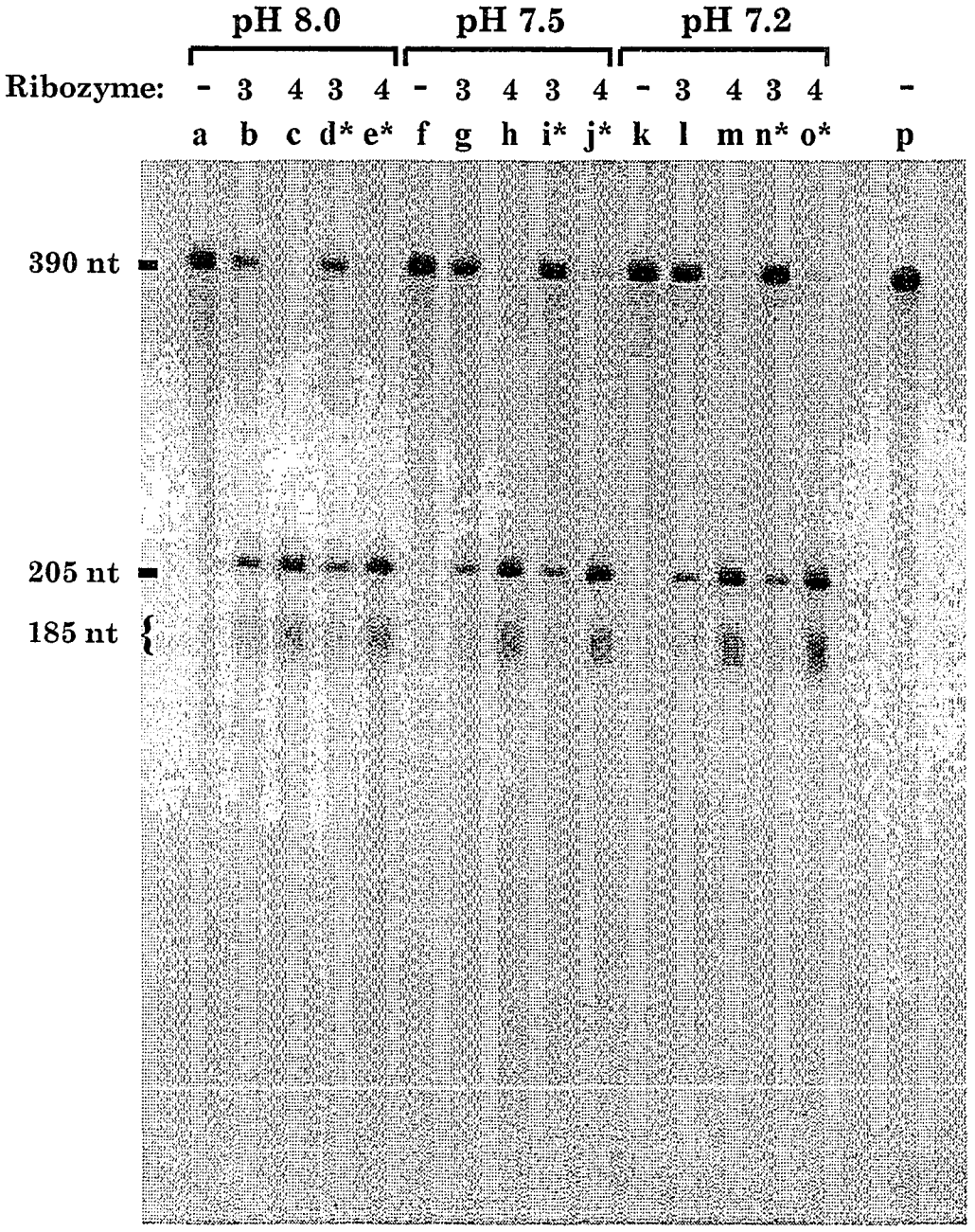
pH 8.0
pH 7.5
pH 7.2
Ribozyme: - 3 4 3 4 - 3 4 3 4 - 3 4 3 4 -
a b c d* e* f g h i* j* k l m n* o* p
390 nt
205 nt
185 nt

When the experiment described above was performed using half as much ribozyme (500 ng ribozyme $RZ3_{10}$ or $RZ4_{12}$), similar results were obtained (lanes **d, e, i, j, n** and **o**; Figure 3.15). Comparisons between reactions containing 1 μg of ribozyme and reactions containing 500 ng of ribozyme resulted in no significant differences in band intensities between the two sets of experiments indicating that the reaction of ribozyme and substrate was at/or near saturation with 500 ng of ribozyme. However even at "saturation" under these conditions where there is a 10,000 fold molar excess of ribozyme over substrate a large proportion of the substrate remains uncleaved after 2 hours.

Concentration Dependence of the Rate of Substrate Cleavage on the Concentration of Ribozyme

To test more fully the dependence of rate of cleavage of substrate on the concentration of ribozyme, 70 pg of labeled *tat-s* RNA was incubated for 2 hours with various amounts of $RZ3_{10}$ and $RZ4_{12}$ ribozymes decreasing in ten-fold increments from 50 ng to 5 pg. Note that at 5 pg of ribozyme the molar ratio of ribozyme and substrate is about 1:1. The results are shown in Figure 3.16. Again $RZ4_{12}$ is more active than $RZ3_{10}$. With both ribozymes, however, the rate of substrate cleavage decreases with decreasing ribozyme concentration. The extent of cleavage with 50 ng of ribozyme approximates those observed with 500 and 1000 ng (see Figure 3.15) and suggests that this amount of ribozyme provides a concentration of ribozyme to produce an optimal rate of reaction under these incubation conditions of minimal concentrations of substrate. As the ribozyme is reduced further the reaction appears to enter a region

Figure 3.16. *Tat-s* RNA cleavage using ribozyme $RZ3_{10}$ or ribozyme $RZ4_{12}$ at varying ribozyme concentrations. 70 pg *tat-s* RNA was incubated with 50 ng (lanes **c** and **h**), 5 ng (lanes **d** and **i**), 500 pg (lanes **e** and **j**), 50 pg (lanes **f** and **k**), and 5 pg (lanes **g** and **l**) of ribozyme $RZ3_{10}$ and $RZ4_{12}$ for 2 hours. Lane **a** contains 70 pg *tat-s* RNA that was not incubated in buffer. Lane **b** contains 70 pg *tat-s* RNA that was incubated for 2 hours without ribozyme.

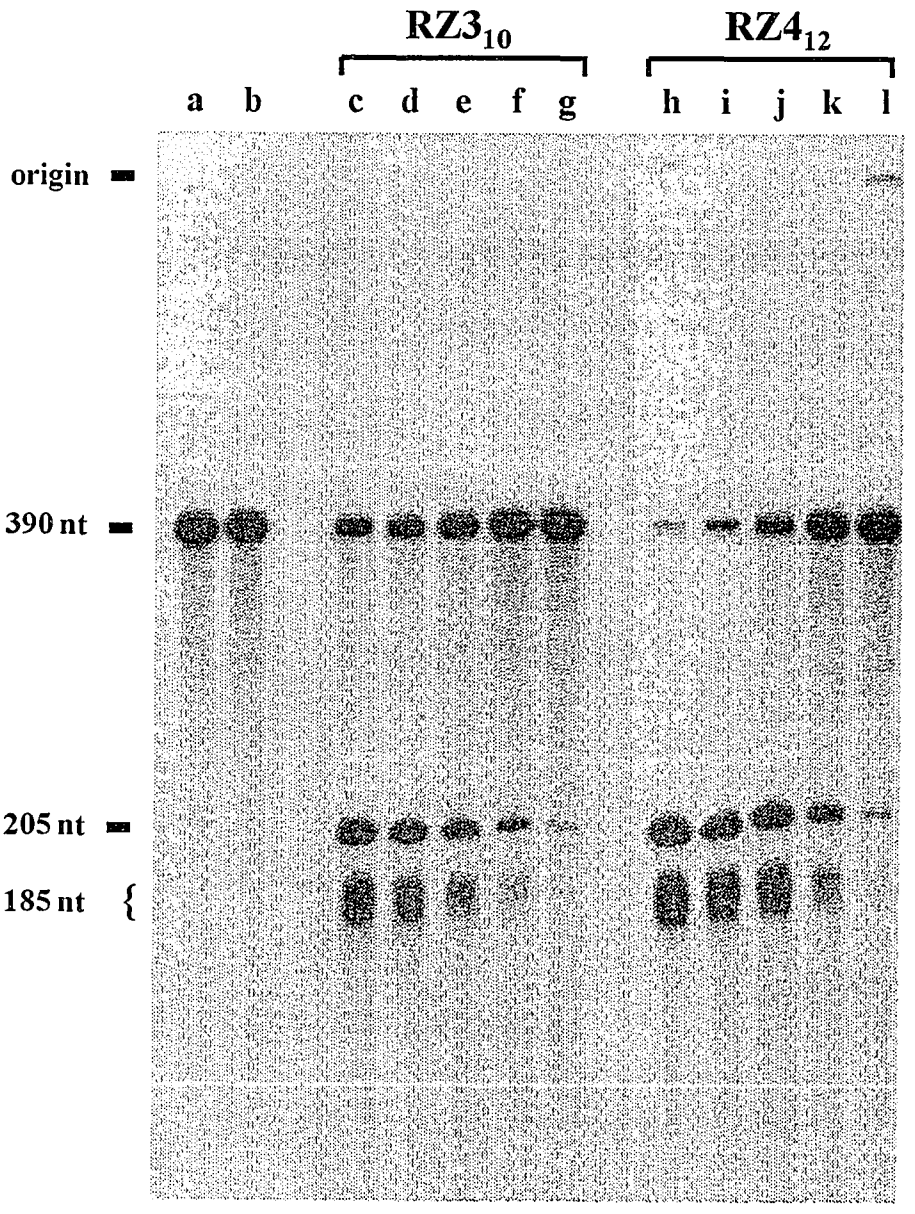
RZ3$_{10}$
RZ4$_{12}$
a b c d e f g h i j k l
origin
390 nt
205 nt
185 nt

where rate of cleavage is dependent on the ribozyme concentration and the extent of cleavage decreases in proportion to the reduction in ribozyme added although only at the lowest concentration, where there is equimolar ribozyme and substrate, can the ribozyme definitely be considered limited. This result suggests that the limiting event in these reactions is the second order reaction of the binding of ribozyme to substrate.

The Effects of Substrate Concentration on the Rate of Ribozyme Cleavage

The concentration of *tat-s* RNA substrate was raised in a set of reaction mixtures with 50 pg of each of ribozyme $RZ3_{10}$ (Figure 3.18), $RZ4_{12}$ (Figure 3.19) and $RZ5_{14}$ (Figure 3.20) to determine the effect of substrate concentration on the rate of the cleavage reaction. These reactions were examined by studying the initial rate of the cleavage reaction. The cleavage products were determined in samples taken from the reaction mixtures at 1, 2, and 4 minutes. A typical gel of these reactions is shown in Figure 3.17. Products were determined for each gel by radioactive counts in bands cut out after autoradiography from electrophoretic gels of the reaction samples (Method I in Figures 3.18 to 3.20) and by densitometric scans of autoradiographs of the gels (Method II in Figures 3.18 to 3.20)

In all of these reactions it is evident that increased concentrations of the substrate considerably enhances the rate at which ribozyme can cleave substrate. Again this result suggests that only a very small proportion of the ribozyme is bound to the substrate and that this second order binding reaction is likely to be the limiting event in the overall cleavage of the substrate by ribozyme.

Figure 3.17. A typical autoradiograph from an initial reaction kinetics experiment. 70 pg of labeled *tat-s* RNA was supplemented with cold *tat-s* RNA to obtain final substrate-to-ribozyme molar ratios of 1:1, 5:1, and 10:1. Cleavage reactions were performed using 50 pg of ribozyme $RZ4_{12}$ at pH 7.5 for 1, 2, 3, and 4 minutes.

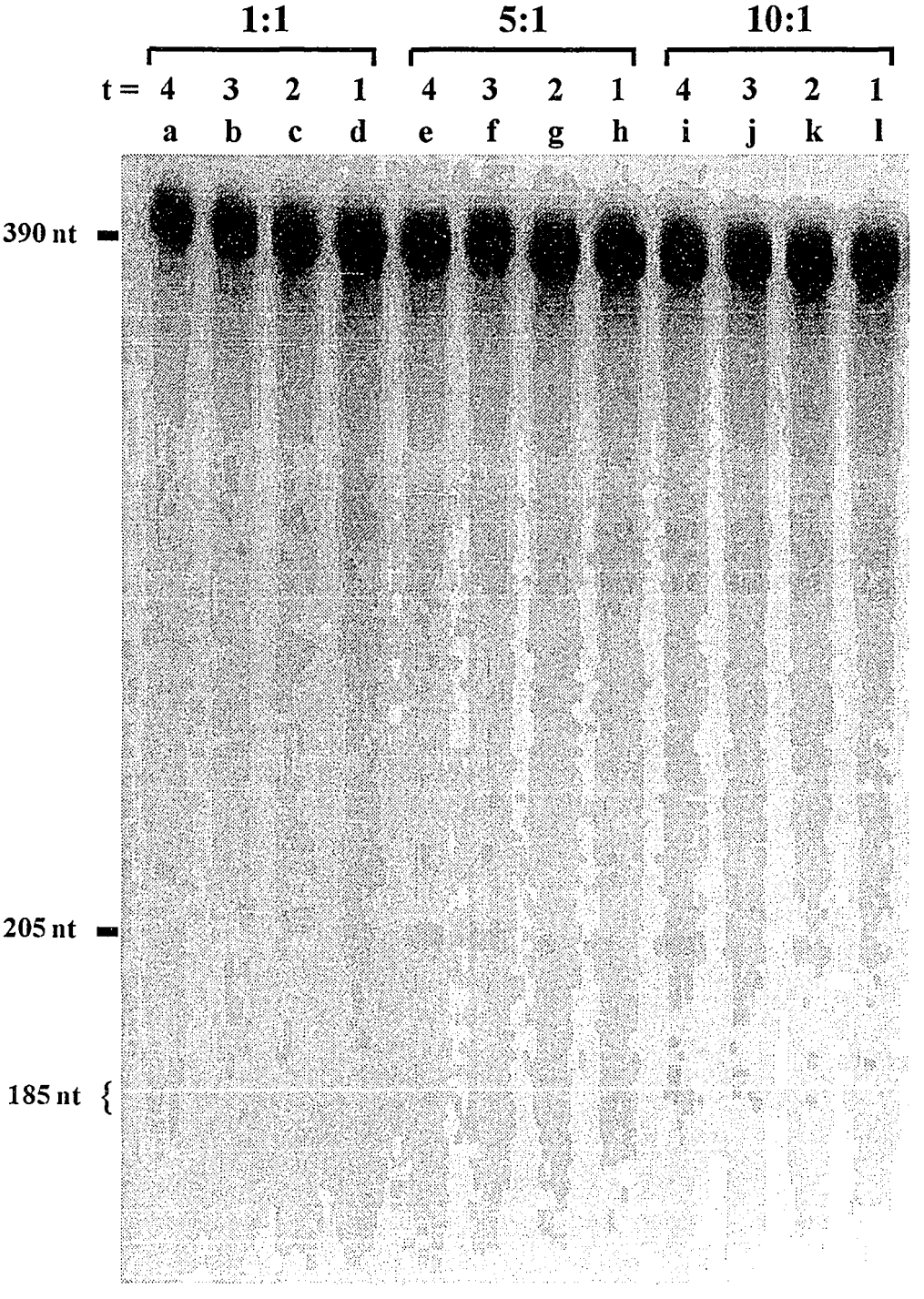
1:1
5:1
10:1
t = 4 3 2 1 4 3 2 1 4 3 2 1
a b c d e f g h i j k l
390 nt
205 nt
185 nt

Figure 3.18. Plot of an initial reaction kinetics experiment performed with ribozyme $RZ3_{10}$. 70 pg of labeled *tat-s* RNA was supplemented with cold *tat-s* RNA to obtain final substrate-to-ribozyme molar ratios of 10:1, 5:1, and 1:1. Cleavage reactions were performed using 50 pg of ribozyme $RZ3_{10}$ at pH 7.5 for 0, 1, 2, 3, and 4 minutes. P1/R was determined using Method I - Radioactive measurements (Panel A) or Method II - Densitometric measurements (Panel B) as described in Chapter 2.

A

Method I

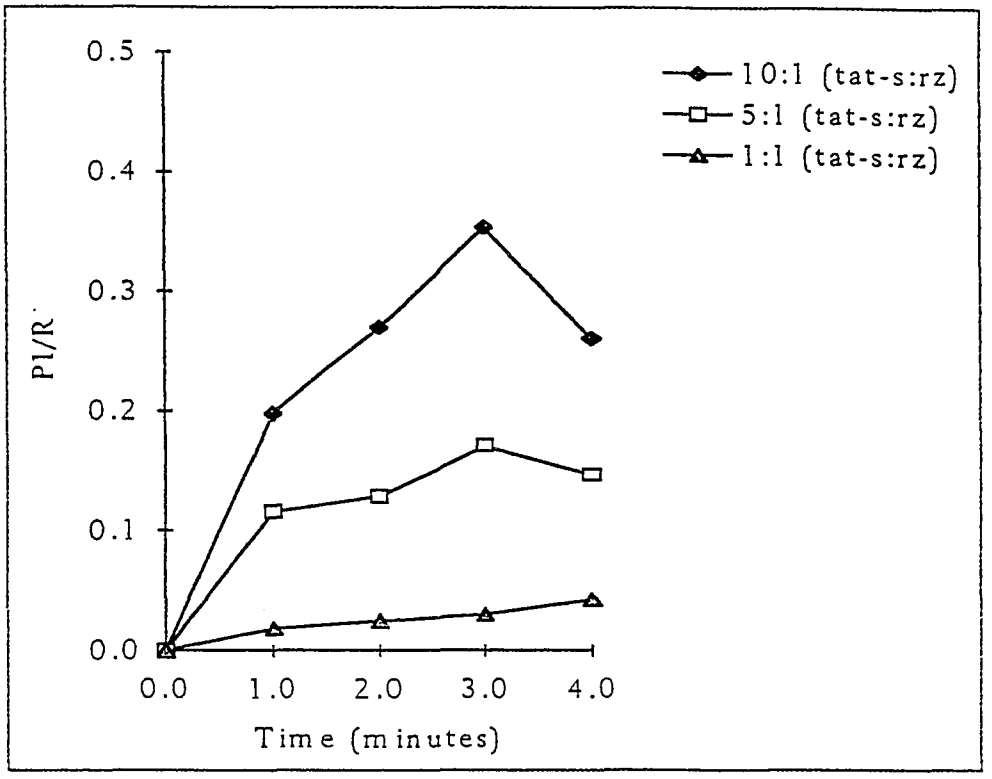

B

Method II

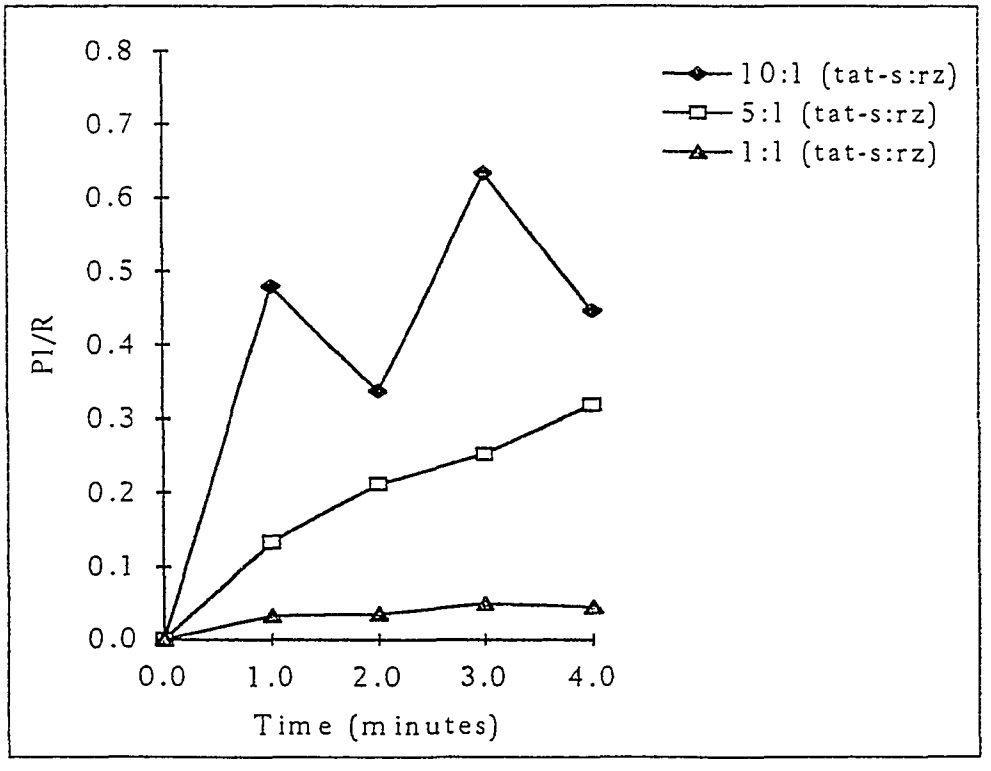

Figure 3.19. Plot of an initial reaction kinetics experiment performed with ribozyme $RZ4_{12}$. 70 pg of labeled *tat-s* RNA was supplemented with cold *tat-s* RNA to obtain final substrate-to-ribozyme molar ratios of 10:1, 5:1, and 1:1. Cleavage reactions were performed using 50 pg of ribozyme $RZ4_{12}$ at pH 7.5 for 0, 1, 2, 3, and 4 minutes. P1/R was determined using Method I - Radioactive measurements (Panel A) or Method II - Densitometric measurements (Panel B) as described in Chapter 2.

A

Method I

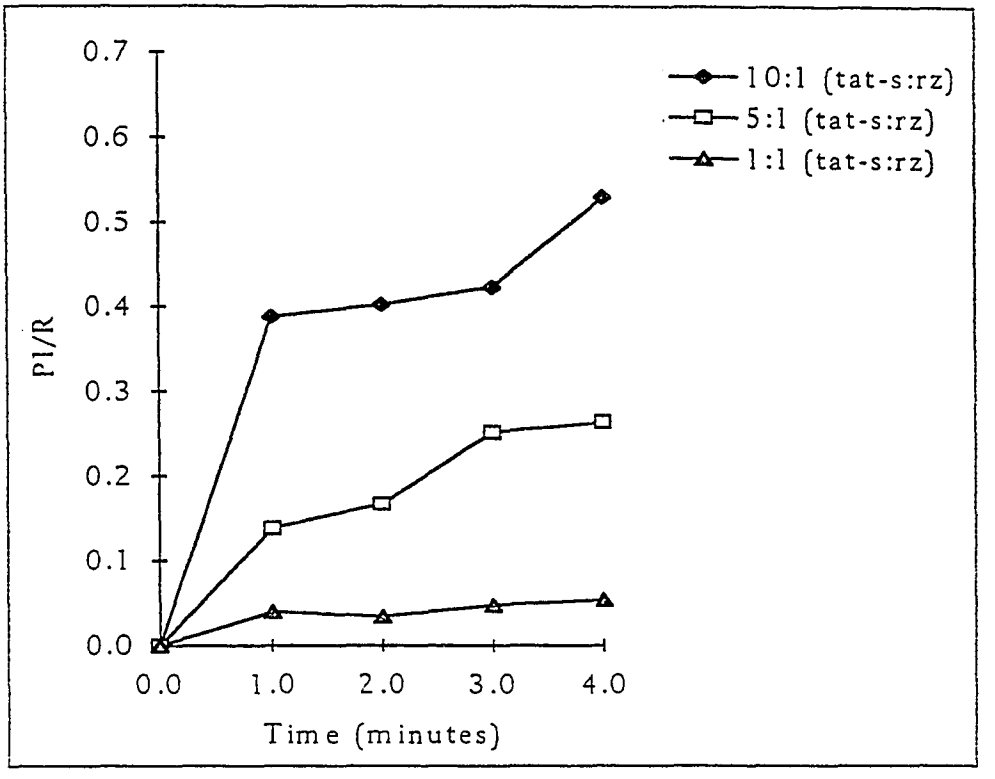

B

Method II

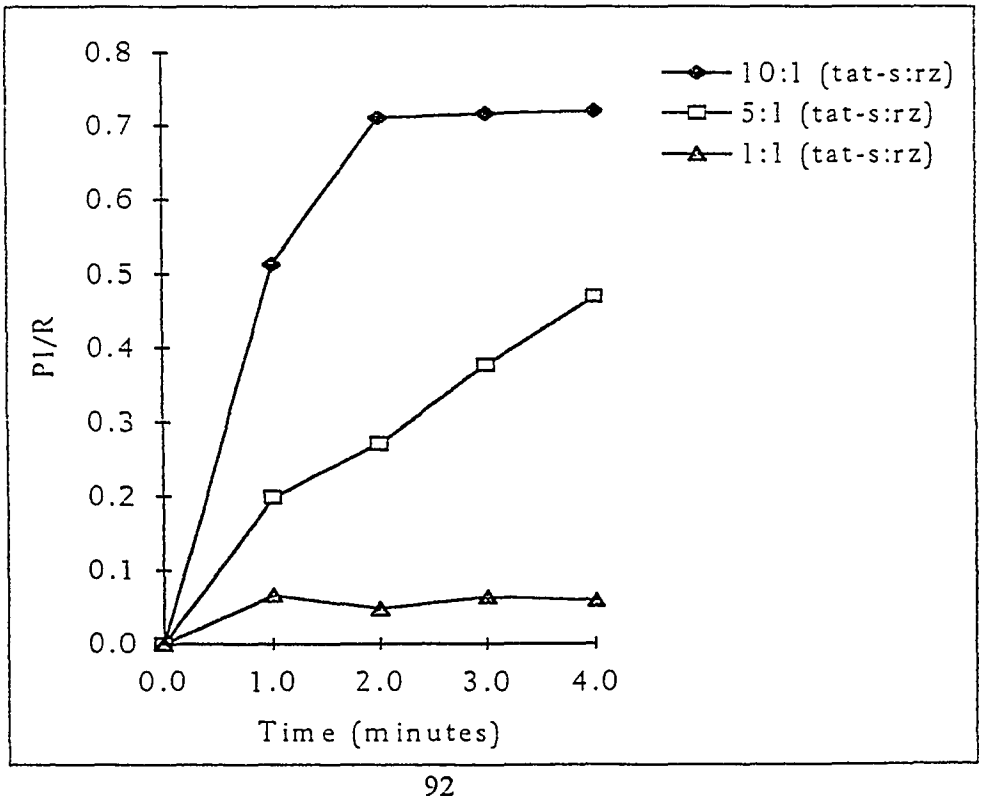

Figure 3.20. Plot of an initial reaction kinetics experiment performed with ribozyme $RZ5_{14}$. 140 pg of labeled *tat-s* RNA was supplemented with cold *tat-s* RNA to obtain final substrate-to-ribozyme molar ratios of 10:1, 5:1, and 1:1. Cleavage reactions were performed using 50 pg of ribozyme $RZ5_{14}$ at pH 7.5 for 0, 0.5, 1.0, 1.5, and 2.0 minutes. P1/R was determined using Method I - Radioactive measurements (Panel A) or Method II - Densitometric measurements (Panel B) as described in Chapter 2.

A

Method I

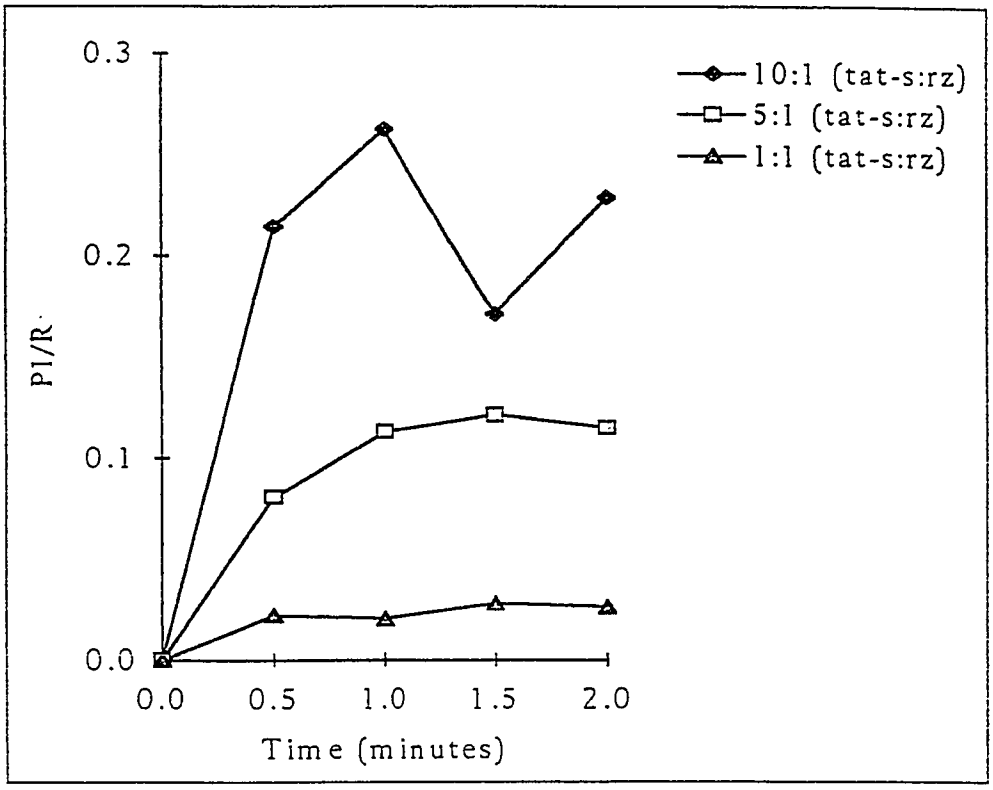

B

Method II

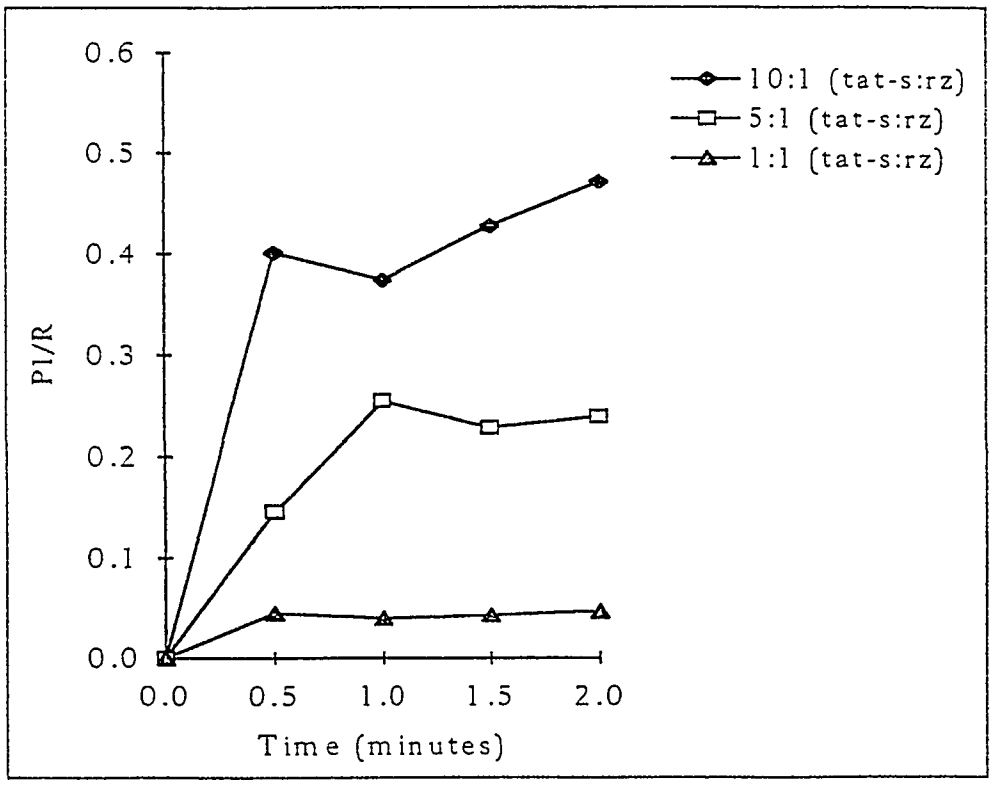

CHAPTER 4

DISCUSSION

Knowledge of the HIV life cycle has been valuable in the development of potential anti-HIV agents. For those millions of people worldwide who are already infected, anti-HIV treatments based on intracellular immunization which work to prevent HIV from actively replicating once it has entered the host cell genome are of key importance. One particular strategy is to target the function of the *tat* gene using ribozymes expressed by constructs transfected into T lymphocyte stem cells. In this study, ribozyme activity was examined *in vitro* to determine parameters which might make ribozyme-mediated *tat* RNA cleavage possible *in vivo*. Since an *in vitro tat-s* expression vector was available, the experiments were performed using the *tat-s* transcript. Ribozymes were also synthesized *in vitro* using synthetic oligonucleotides as template.

The *tat-s* transcript contains seven obligatory hammerhead "GUH" sequences and two obligatory hairpin "GUC" sequences at which ribozyme-mediated cleavage can potentially occur (Figure 4.1). Site VI was chosen for ribozymes RZ2, $RZ3_{10}$, $RZ4_{12}$, and $RZ5_{14}$ primarily because both the hammerhead and the hairpin motifs can cleave at site VI and because the resulting cleavage fragments would be easily distinguishable from the substrate. Additionally, site VI is also present in the first exon of the *rev* gene (Robert-Guroff *et al.*, 1990). Although a *nef* transcript was not used in this study, ribozymes RZ2, $RZ3_{10}$, $RZ4_{12}$, and $RZ5_{14}$ also have the potential of cleaving a *nef* transcript. Ribozyme RZ1 was target to a modified region of the *tat-s*

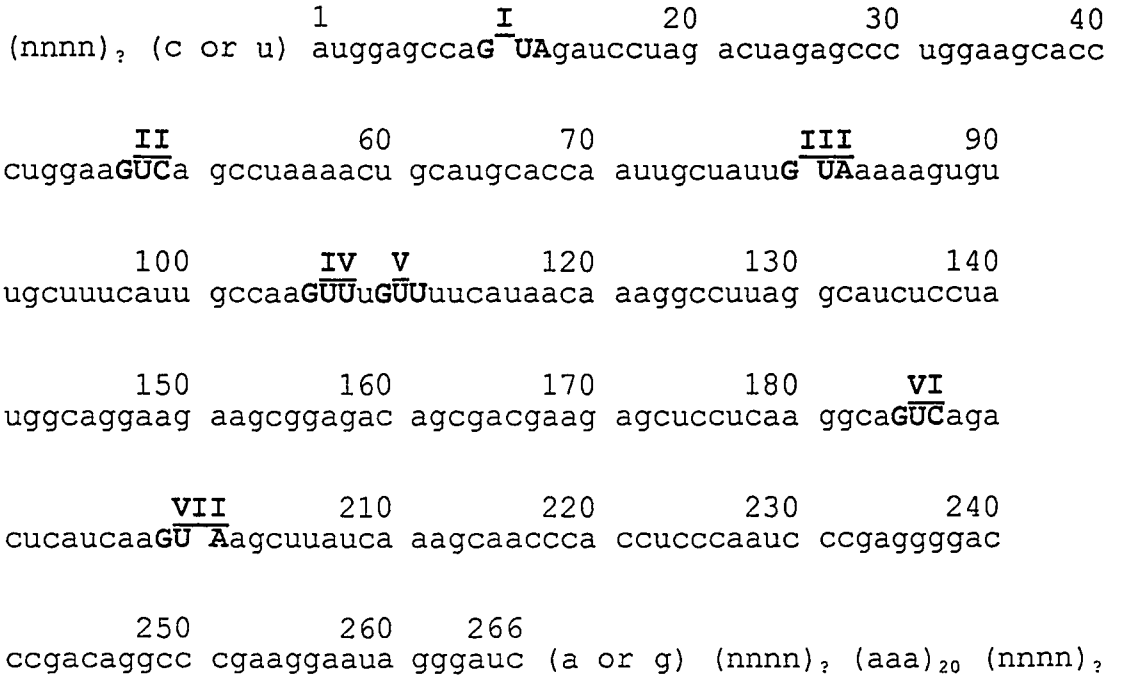

Figure 4.1. Locations of obligatory cleavage sequences in the HIV-1 *tat-s* transcript. The obligatory sequences are denoted in bold, uppercase letters with a corresponding Roman numeral above. Sites I - VII are obligatory hammerhead sequences and sites II and VI are also obligatory hairpin cleavage sequences. $(nnnn)_?$ denotes the positions of nucleotides of unknown sequence and number.

transcript (site VII). The cleavage results obtained using the *tat-s* transcript, with the exception of ribozyme RZ1 should be comparable to those obtained using a native *tat* transcript because both substrates contain the target sequences which the ribozymes recognize.

The *in vitro* cleavage conditions in these experiments do not differ markedly from those of the cell. Cleavage reactions were performed at 37°C at near physiological pH. RNA concentrations, whether it be ribozyme or substrate, ranged from 17.8 μM (1 μg ribozyme/5μl) to 89.0 pM (5.0 pg ribozyme/5μl). These concentrations range from about 10^6 to about 30 molecules per average sized T-cell (see below). Evidence indicates that the ribozyme cleavage reaction requires the presence of a divalent cation (in these experiments, the magnesium ion, Mg^{++}). It has been demonstrated that no cleavage occurs in reactions containing up to 1.0 M NaCl in the absence of Mg^{++} (Uhlenbeck, 1987). Therefore, intracellular concentrations of monovalent cations would be expected to play a minor role in ribozyme cleavage activity. Nuclear magnetic resonance studies indicate that the magnesium ion primarily serves a catalytic role in RNA cleavage (Heus and Pardi, 1991), although the stabilizing effect of Mg^{++} on nucleic acid basepairs can not be ruled out. Second in abundance to the potassium ion, the intracellular Mg^{++} concentration is estimated to be 10 mM (Henry, 1979). Although the cleavage reactions performed in this dissertation used 20 mM $MgCl_2$, it has been demonstrated by another group that ribozyme cleavage rates do not differ significantly at 10 mM $MgCl_2$ than at 20 mM $MgCl_2$ in the absence of Na^+ (Uhlenbeck, 1987).

Control RNA molecules, which contain sixteen GUH/GUC obligatory cleavage sequences but none of the complementary ribozyme flanking sequences, are not cleaved when incubated with molar excess of ribozymes RZ1, RZ2 or $RZ4_{12}$ for up to 4 hours (Figure 3.14). Incubation of the target substrate, *tat-s*, with ribozymes $RZ3_{10}$ or $RZ4_{12}$ at pH 8.0, pH 7.5, and pH 7.2 for two hours resulted in similar degrees of *tat-s* cleavage for each of the ribozymes irrespective of pH (Figure 3.15). These experiments demonstrate the ability of the ribozymes, under near physiological pH conditions, to cleave the substrate to which they are targeted.

As observed in Figure 3.16, in conditions where ribozyme concentrations ranged from 4 x 10^4-fold molar excess to roughly equimolar amounts relative to the substrate concentrations, the extent of *tat-s* cleavage decreases proportionally with the decrease in ribozyme concentration. In conditions where the substrate concentrations ranged from roughly equimolar to 10-fold molar excess relative to the ribozyme concentration (Figures 3.18 – 3.20), a proportional increase in the extent of *tat-s* cleavage was also observed. These data indicate that the cleavage of *tat-s* is dependent on the concentration of both reactants, suggesting that the limiting event is the bimolecular binding of the ribozyme to its substrate.

A R_0t calculation of ribozyme reaction with substrate can be performed with the caveat that quantitative studies of rates of nucleic acid reassociation, specifically R_0t determinations, have not been performed under conditions that use Mg^{++} buffers, although it is known that the stabilizing effects of divalent cations on nucleic acid duplexes is more effective than Na^+ at equivalent concentrations. From Lewin (1987),

one can use the reaction of excess ovalbumin RNA to its cDNA as a standard for calculating the $R_o t_{1/2}$ at a representative ribozyme concentration (eg. 50 pg of ribozyme/5 μl) for the reactions shown in Figures 3.18 – 3.20):

$$\frac{\text{Complexity of ribozyme}}{\text{Complexity of ovalbumin RNA}} = \frac{R_o t_{1/2} \text{ of ribozyme}}{R_o t_{1/2} \text{ of ovalbumin RNA}}$$

Since the Complexity of $RZ4_{12}$ = 34 nt, and the values for ovalbumin are known, $R_o t_{1/2}$ of $RZ4_{12}$ is:

$$R_o t_{1/2}\ RZ4_{12} = \frac{\text{Complexity } RZ4_{12}}{\text{Complexity ovalbumin RNA}} (R_o t_{1/2} \text{ ovalbumin RNA})$$

$$= \frac{34 \text{ bp}}{2000 \text{ bp}} (0.0008)$$

$$= 1.36 \times 10^{-5} \text{ nt-moles-l}^{-1}\text{-sec}^{-1}$$

The initial concentration of ribozyme $RZ4_{12}$ is $R_o = 1.068 \times 10^{-8}$ nt-mole-l^{-1}, thus solving for $t_{1/2}$, one obtains a value of:

$$t_{1/2} = \frac{1.36 \times 10^{-5}}{1.068 \times 10^{-8}}$$

$$\cong 1273 \text{sec.}$$

$$\cong 21 \text{ minutes}$$

Thus at the concentrations of $RZ4_{12}$ used, one would expect 50% of the ribozyme molecules present in the reaction to be bound to the substrate after 21 minutes. At higher concentrations, these reactions should be completed considerably faster. By two hours of incubation even at the low concentration, most of the ribozyme molecules should be bound to the substrate and first-order cleavage kinetics should

probably be expected. Since the observed data support second-order kinetics, one must assume that complete binding is not being achieved due to the dissociation of the ribozyme:substrate complex before the substrate is cleaved.

To give perspective to the concentration of ribozymes used in these studies, the number of molecules required in a cell to achieve equivalent concentrations was calculated. Non-activated T and B lymphocytes are 6 – 10 μm in diameter while activated lymphocytes are slightly larger at 12 – 15 μm in diameter (Henry, 1979). Thus the volume of a 10 μm T lymphocyte would be approximately:

$$\text{volume}_{\text{sphere}} = \pi \frac{D^3}{6} = \pi \frac{(10^{-5}\ \text{m})^3}{6}$$

$$= 5.24 \times 10^{-16}\ \text{m}^3$$

$$\cong 0.5\ \text{pl}$$

The concentration of ribozymes used in the studies illustrated in Figures 3.18 – 3.20 was typically 8.9×10^{-10} M. Therefore, in a 10 μm T lymphocyte with a volume of 0.5 pl, the equivalent number of ribozyme molecules per cell using the typical 8.9×10^{-10} M ribozyme *in vitro* cleavage conditions would be:

$$\frac{0.5\ \text{pl}}{\text{cell}} \left(\frac{8.9 \times 10^{-10}\ \text{mole}}{10^{12}\ \text{pl}}\right) \left(\frac{6.022 \times 10^{23}\ \text{molecules}}{\text{mole}}\right) \cong \frac{268\ \text{molecules of ribozyme}}{\text{cell}}$$

This concentration of 286 molecules/cell is a relatively modest one that can be easily achieved and surpassed using *in vivo* expression strategies such as tRNA gene cassettes (Cotten and Birnstiel, 1989), SV40 early promoter expression plasmids (Cameron and Jennings, 1989), or retroviral vectors (Weerasinghe *et al.*, 1991; Lo *et al.*, 1992).

Furthermore, as seen in Figures 3.18 – 3.20, at this concentration, at least 5% of the substrate is cleaved in four minutes irrespective of substrate concentration. In the case of equimolar concentrations of ribozyme and substrate, about 13 molecules of substrate/cell are cleaved in four minutes or about 200 molecules of substrate/cell are cleaved in an hour. While the actual abundance of *tat* RNA in latent HIV-infected cells has not been determined to date, the observation that the frequency of $CD4^+$ T cells that contain HIV-1 DNA is at least 1/100 cells in patients with AIDS compared to 1/10,000 cells in asymptomatic HIV-seropositive individuals and the observation that these HIV-infected cells contain predominantly one copy of viral DNA per cell (Schnittman *et al.*, 1989) suggest that the abundance of *tat* RNA is not excessive. Thus, the cleavage rates observed would be sufficient in infected cells with the virus still in its quiescent state.

Sequences encoding a ribozyme targeted to a conserved region of the HIV-1 5′ leader sequence were placed under the control of a herpes simplex virus thymidine kinase promoter, an SV40 promoter, a cytomegalovirus promoter, or a fusion thymidine kinase-TAR promoter, which allowed constitutive and *tat*-inducible expression, in Moloney retroviral vectors (Weerasinghe *et al.*, 1991). The vectors were used to transform a human $CD4^+$ lymphocyte-derived MT_4 cell line. The stable MT_4 transformants were challenged with HIV-1 and assayed for HIV-1 through the measurement of HIV-1 p24 antigen (a *gag* gene product) levels in the cell culture supernatant. The transformed cells containing ribozyme-derived vectors showed delayed production of p24 from 3 days to 22 days relative to p24 antigen levels in

control cells. The construct most effective at delaying p24 antigen production contained the thymidine kinase-TAR promoter.

In another study comparing the relative effectiveness of a *tat*-antisense RNA and an anti-*tat* ribozyme in inhibiting HIV-1 production, sequences coding for a *tat*-antisense RNA or an anti-*tat* ribozyme were inserted into the 3′ noncoding region of a neomycin-resistance gene on a Moloney retroviral vector (Lo *et al.*, 1992). Stable transformed human $CD4^+$ T-cell lines containing these constructs were challenged with HIV-1 and assayed for p24 antigen production in cell culture supernatants. The production of viral antigens was delayed for 8 days with cells expressing the anti-*tat* ribozyme and delayed for 12 days with cells expressing the *tat*-antisense RNA relative to p24 production in control cells.

These studies confirm our *in vitro* data indicating that ribozymes should be effective for intracellular immunization against HIV-1. Since only relatively short delays are achieved in these tests of ribozymes in cultured cells, further *in vivo* work must be performed to establish the important parameters to make this approach effective. There are considerable data suggesting that the intracellular regulatory parameters of HIV-1 in these transformed test cell lines are significantly different from those of normal T-cells. The strict dependence of HIV transcription on *tat* and *rev* may be lacking in these cells. Thus, ribozymes will have to be fully tested in normal human T-cells before their potential can be fully evaluated. Although extensive studies are needed, our results and those of others obtained to date are encouraging

and support the concept that ribozymes may provide a technology for intracellular immunization as a viable course for anti-HIV treatment.

APPENDIX A. Initial Reaction Kinetics Experiment #1 – Method I.

Substrate:R	Time (min)	R (mol RZ)	mol tat-s	CPM(c) Uncut	CPM(c) P1	% cleaved	mol P1 present	P1/R
10:R3	1	4.20E-15	4.2000E-14	1774.60	19.00	1.9801	8.3165E-16	0.1980
	2	4.20E-15	4.2000E-14	1554.17	22.90	2.7049	1.1361E-15	0.2705
	3	4.20E-15	4.2000E-14	1600.18	31.20	3.5483	1.4903E-15	0.3548
	4	4.20E-15	4.2000E-14	1518.50	21.60	2.6137	1.0978E-15	0.2614
10:R4	1	4.45E-15	4.4500E-14	2417.02	51.80	3.8865	1.7295E-15	0.3886
	2	4.45E-15	4.4500E-14	2539.90	56.50	4.0281	1.7925E-15	0.4028
	3	4.45E-15	4.4500E-14	2282.09	53.50	4.2359	1.8850E-15	0.4236
	4	4.45E-15	4.4500E-14	2081.48	61.90	5.3129	2.3642E-15	0.5313
5:R3	1	4.20E-15	2.1000E-14	1745.93	21.90	2.3120	4.8551E-16	0.1156
	2	4.20E-15	2.1000E-14	1678.61	23.50	2.5735	5.4043E-16	0.1287
	3	4.20E-15	2.1000E-14	1793.20	33.70	3.4245	7.1914E-16	0.1712
	4	4.20E-15	2.1000E-14	1822.15	29.20	2.9349	6.1632E-16	0.1467
5:R4	1	4.45E-15	2.2250E-14	2721.16	40.90	2.7577	6.1359E-16	0.1379
	2	4.45E-15	2.2250E-14	2681.68	49.00	3.3327	7.4152E-16	0.1666
	3	4.45E-15	2.2250E-14	2334.85	65.60	5.0343	1.1201E-15	0.2517
	4	4.45E-15	2.2250E-14	2536.43	74.90	5.2776	1.1743E-15	0.2639
1:R3	1	4.20E-15	4.2000E-15	2019.10	20.10	1.8437	7.7434E-17	0.0184
	2	4.20E-15	4.2000E-15	2210.53	29.60	2.4642	1.0350E-16	0.0246
	3	4.20E-15	4.2000E-15	1993.48	33.00	3.0288	1.2721E-16	0.0303
	4	4.20E-15	4.2000E-15	1808.31	42.60	4.2557	1.7874E-16	0.0426
1:R4	1	4.45E-15	4.4500E-15	3068.99	67.00	3.9562	1.7605E-16	0.0396
	2	4.45E-15	4.4500E-15	2622.54	48.70	3.3851	1.5064E-16	0.0339
	3	4.45E-15	4.4500E-15	2213.95	57.80	4.6946	2.0891E-16	0.0469
	4	4.45E-15	4.4500E-15	1908.89	57.40	5.3689	2.3892E-16	0.0537

APPENDIX B. Initial Reaction Kinetics Experiment #1 – Method II.

Substrate:R	Time (min)	R (mol RZ)	mol tat-s	g Peak A	g Peak B	% cleaved	mol P1 present	P1/R
10:R3	1	4.20E-15	4.2000E-14	0.0524	0.0014	4.7991	2.0156E-15	0.4799
	2	4.20E-15	4.2000E-14	0.0540	0.0010	3.3761	1.4180E-15	0.3376
	3	4.20E-15	4.2000E-14	0.0474	0.0017	6.3381	2.6620E-15	0.6338
	4	4.20E-15	4.2000E-14	0.0524	0.0013	4.4717	1.8781E-15	0.4472
10:R4	1	4.45E-15	4.4500E-14	0.0663	0.0019	5.1297	2.2827E-15	0.5130
	2	4.45E-15	4.4500E-14	0.0666	0.0027	7.1056	3.1620E-15	0.7106
	3	4.45E-15	4.4500E-14	0.0611	0.0025	7.1668	3.1892E-15	0.7167
	4	4.45E-15	4.4500E-14	0.0632	0.0026	7.2030	3.2053E-15	0.7203
5:R3	1	4.20E-15	2.1000E-14	0.0550	0.0008	2.6711	5.6093E-16	0.1336
	2	4.20E-15	2.1000E-14	0.0554	0.0013	4.2398	8.9035E-16	0.2120
	3	4.20E-15	2.1000E-14	0.0461	0.0013	5.0519	1.0609E-15	0.2526
	4	4.20E-15	2.1000E-14	0.0555	0.0020	6.3664	1.3369E-15	0.3183
5:R4	1	4.45E-15	2.2250E-14	0.0729	0.0016	3.9764	8.8476E-16	0.1988
	2	4.45E-15	2.2250E-14	0.0626	0.0019	5.4165	1.2052E-15	0.2708
	3	4.45E-15	2.2250E-14	0.0578	0.0025	7.5451	1.6788E-15	0.3773
	4	4.45E-15	2.2250E-14	0.0673	0.0037	9.3983	2.0911E-15	0.4699
1:R3	1	4.20E-15	4.2000E-15	0.0563	0.0010	3.2426	1.3619E-16	0.0324
	2	4.20E-15	4.2000E-15	0.0618	0.0012	3.5342	1.4844E-16	0.0353
	3	4.20E-15	4.2000E-15	0.0581	0.0016	4.9393	2.0745E-16	0.0494
	4	4.20E-15	4.2000E-15	0.0569	0.0014	4.4364	1.8633E-16	0.0444
1:R4	1	4.45E-15	4.4500E-15	0.0723	0.0027	6.5823	2.9291E-16	0.0658
	2	4.45E-15	4.4500E-15	0.0615	0.0016	4.6790	2.0822E-16	0.0468
	3	4.45E-15	4.4500E-15	0.0587	0.0021	6.3232	2.8138E-16	0.0632
	4	4.45E-15	4.4500E-15	0.0519	0.0017	5.8205	2.5901E-16	0.0582

APPENDIX C. Initial Reaction Kinetics Experiment #2 – Method I.

Substrate:R	Time (min)	R (mol RZ)	mol tat-s	CPM(c) Uncut	CPM(c) P1	% cleaved	mol P1 present	P1/R
10:R3	1	4.20E-15	4.2000E-14	3598.21	101.40	5.0487	2.1204E-15	0.5049
	2	4.20E-15	4.2000E-14	3505.15	101.70	5.1903	2.1799E-15	0.5190
	3	4.20E-15	4.2000E-14	3186.53	109.70	6.0993	2.5617E-15	0.6099
	4	4.20E-15	4.2000E-14	3014.34	85.40	5.0743	2.1312E-15	0.5074
10:R4	1	4.45E-15	4.4500E-14	3853.15	120.60	5.5762	2.4814E-15	0.5576
	2	4.45E-15	4.4500E-14	2877.77	97.20	5.9911	2.6660E-15	0.5991
	3	4.45E-15	4.4500E-14	3000.94	117.90	6.9012	3.0710E-15	0.6901
	4	4.45E-15	4.4500E-14	2705.14	118.90	7.6580	3.4078E-15	0.7658
5:R3	1	4.20E-15	2.1000E-14	3571.91	97.20	4.8837	1.0256E-15	0.2442
	2	4.20E-15	2.1000E-14	3287.72	111.10	5.9938	1.2587E-15	0.2997
	3	4.20E-15	2.1000E-14	3006.99	101.20	5.9708	1.2539E-15	0.2985
	4	4.20E-15	2.1000E-14	2793.28	99.70	6.3096	1.3250E-15	0.3155
5:R4	1	4.45E-15	2.2250E-14	3021.74	108.30	6.3340	1.4093E-15	0.3167
	2	4.45E-15	2.2250E-14	2940.45	115.00	6.8721	1.5290E-15	0.3436
	3	4.45E-15	2.2250E-14	2619.37	110.10	7.3480	1.6349E-15	0.3674
	4	4.45E-15	2.2250E-14	2681.14	116.60	7.5832	1.6873E-15	0.3792
1:R3	1	4.20E-15	4.2000E-15	3340.53	97.10	5.1992	2.1837E-16	0.0520
	2	4.20E-15	4.2000E-15	3095.68	94.80	5.4624	2.2942E-16	0.0546
	3	4.20E-15	4.2000E-15	2880.66	99.50	6.1184	2.5697E-16	0.0612
	4	4.20E-15	4.2000E-15	2859.39	99.60	6.1669	2.5901E-16	0.0617
1:R4	1	4.45E-15	4.4500E-15	3425.50	129.60	6.6628	2.9650E-16	0.0666
	2	4.45E-15	4.4500E-15	3368.65	116.40	6.1206	2.7237E-16	0.0612
	3	4.45E-15	4.4500E-15	3132.00	108.40	6.1300	2.7278E-16	0.0613
	4	4.45E-15	4.4500E-15	2948.34	101.80	6.1162	2.7217E-16	0.0612

APPENDIX D. Initial Reaction Kinetics Experiment #2 – Method II.

Substrate:R	Time (min)	R (mol RZ)	mol tat-s	g Peak A	g Peak B	% cleaved	mol P1 present	P1/R
10:R3	**1**	**4.20E-15**	**4.2000E-14**	**0.0674**	**0.0028**	**7.2686**	**3.0528E-15**	**0.7269**
	2	**4.20E-15**	**4.2000E-14**	**0.0652**	**0.0049**	**12.4189**	**5.2159E-15**	**1.2419**
	3	**4.20E-15**	**4.2000E-14**	**0.0543**	**0.0045**	**13.5220**	**5.6793E-15**	**1.3522**
	4	**4.20E-15**	**4.2000E-14**	**0.0506**	**0.0038**	**12.4110**	**5.2126E-15**	**1.2411**
10:R4	1	4.45E-15	4.4500E-14	0.0652	0.0035	9.1970	4.0927E-15	0.9197
	2	4.45E-15	4.4500E-14	0.0510	0.0023	7.8418	3.4896E-15	0.7842
	3	4.45E-15	4.4500E-14	0.0566	0.0043	12.5372	5.5790E-15	1.2537
	4	4.45E-15	4.4500E-14	0.0545	0.0042	12.6946	5.6491E-15	1.2695
5:R3	**1**	**4.20E-15**	**2.1000E-14**	**0.0680**	**0.0028**	**7.2091**	**1.5139E-15**	**0.3605**
	2	**4.20E-15**	**2.1000E-14**	**0.0547**	**0.0030**	**9.3776**	**1.9693E-15**	**0.4689**
	3	**4.20E-15**	**2.1000E-14**	**0.0508**	**0.0039**	**12.6525**	**2.6570E-15**	**0.6326**
	4	**4.20E-15**	**2.1000E-14**	**0.0580**	**0.0034**	**9.9590**	**2.0914E-15**	**0.4979**
5:R4	1	4.45E-15	2.2250E-14	0.0569	0.0030	9.0479	2.0131E-15	0.4524
	2	4.45E-15	2.2250E-14	0.0563	0.0035	10.4982	2.3359E-15	0.5249
	3	4.45E-15	2.2250E-14	0.0486	0.0035	11.9625	2.6617E-15	0.5981
	4	4.45E-15	2.2250E-14	0.0539	0.0047	14.1281	3.1435E-15	0.7064
1:R3	**1**	**4.20E-15**	**4.2000E-15**	**0.0543**	**0.0024**	**7.6975**	**3.2329E-16**	**0.0770**
	2	**4.20E-15**	**4.2000E-15**	**0.0559**	**0.0029**	**8.9157**	**3.7446E-16**	**0.0892**
	3	**4.20E-15**	**4.2000E-15**	**0.0569**	**0.0033**	**9.8634**	**4.1426E-16**	**0.0986**
	4	**4.20E-15**	**4.2000E-15**	**0.0567**	**0.0035**	**10.4319**	**4.3814E-16**	**0.1043**
1:R4	1	4.45E-15	4.4500E-15	0.0582	0.0030	8.8637	3.9443E-16	0.0886
	2	4.45E-15	4.4500E-15	0.0572	0.0047	13.4224	5.9730E-16	0.1342
	3	4.45E-15	4.4500E-15	0.0565	0.0043	12.5566	5.5877E-16	0.1256
	4	4.45E-15	4.4500E-15	0.0508	0.0055	16.9627	7.5484E-16	0.1696

APPENDIX E. Initial Reaction Kinetics Experiment #3 – Method I.

Substrate:R	Time (sec)	R (mol RZ)	mol tat-s	CPM(c) Uncut	CPM(c) P1	% cleaved	mol P1 present	P1/R
10:R3	15	4.20E-15	4.2000E-14	3586.99	25.60	1.3287	5.5805E-16	0.1329
	30	4.20E-15	4.2000E-14	3902.06	21.00	1.0052	4.2219E-16	0.1005
	45	4.20E-15	4.2000E-14	3977.01	24.50	1.1490	4.8257E-16	0.1149
	60	4.20E-15	4.2000E-14	3357.24	18.60	1.0345	4.3450E-16	0.1035
10:R4	15	4.45E-15	4.4500E-14	4228.52	28.70	1.2644	5.6267E-16	0.1264
	30	4.45E-15	4.4500E-14	4982.30	44.20	1.6463	7.3260E-16	0.1646
	45	4.45E-15	4.4500E-14	4512.83	37.00	1.5234	6.7791E-16	0.1523
	60	4.45E-15	4.4500E-14	4548.29	45.10	1.8365	8.1726E-16	0.1837
5:R3	15	4.20E-15	2.1000E-14	3922.31	34.30	1.6232	3.4087E-16	0.0812
	30	4.20E-15	2.1000E-14	3972.23	24.00	1.1271	2.3670E-16	0.0564
	45	4.20E-15	2.1000E-14	4126.49	28.00	1.2641	2.6546E-16	0.0632
	60	4.20E-15	2.1000E-14	3834.03	23.80	1.1577	2.4311E-16	0.0579
5:R4	15	4.45E-15	2.2250E-14	4414.31	37.10	1.5610	3.4732E-16	0.0780
	30	4.45E-15	2.2250E-14	4206.80	31.60	1.3975	3.1094E-16	0.0699
	45	4.45E-15	2.2250E-14	4116.16	40.00	1.8005	4.0062E-16	0.0900
	60	4.45E-15	2.2250E-14	4151.05	47.00	2.0916	4.6539E-16	0.1046
1:R3	15	4.20E-15	4.2000E-15	4173.94	28.40	1.2675	5.3236E-17	0.0127
	30	4.20E-15	4.2000E-15	5001.80	33.50	1.2479	5.2413E-17	0.0125
	45	4.20E-15	4.2000E-15	5420.01	29.30	1.0097	4.2407E-17	0.0101
	60	4.20E-15	4.2000E-15	3957.18	25.50	1.2012	5.0452E-17	0.0120
1:R4	15	4.45E-15	4.4500E-15	4839.50	32.10	1.2360	5.5003E-17	0.0124
	30	4.45E-15	4.4500E-15	1876.58	30.60	2.9848	1.3282E-16	0.0298
	45	4.45E-15	4.4500E-15	3526.44	40.00	2.0953	9.3242E-17	0.0210
	60	4.45E-15	4.4500E-15	3294.03	43.40	2.4256	1.0794E-16	0.0243

APPENDIX F. Initial Reaction Kinetics Experiment #3 – Method II.

Substrate:R	Time (sec)	R (mol RZ)	mol tat-s	g Peak A	g Peak B	% cleaved	mol P1 present	P1/R
10:R3	15	4.20E-15	4.20E-14	0.0306	0.0004	2.4070	1.0110E-15	0.2407
	30	4.20E-15	4.20E-14	0.0352	0.0007	3.6164	1.5189E-15	0.3616
	45	4.20E-15	4.20E-14	0.0437	0.0007	2.9337	1.2321E-15	0.2934
	60	4.20E-15	4.20E-14	0.0356	0.0005	2.5816	1.0843E-15	0.2582
10:R4	15	4.45E-15	4.45E-14	0.0372	0.0008	3.8994	1.7352E-15	0.3899
	30	4.45E-15	4.45E-14	0.0416	0.0007	3.0772	1.3694E-15	0.3077
	45	4.45E-15	4.45E-14	0.0396	0.0006	2.7793	1.2368E-15	0.2779
	60	4.45E-15	4.45E-14	0.0374	0.0009	4.3432	1.9327E-15	0.4343
5:R3	15	4.20E-15	2.10E-14	0.0385	0.0008	3.7727	7.9227E-16	0.1886
	30	4.20E-15	2.10E-14	0.0375	0.0010	4.7904	1.0060E-15	0.2395
	45	4.20E-15	2.10E-14	0.0340	0.0007	3.7393	7.8526E-16	0.1870
	60	4.20E-15	2.10E-14	0.0352	0.0009	4.6022	9.6646E-16	0.2301
5:R4	15	4.45E-15	2.23E-14	0.0392	0.0005	2.3501	5.2289E-16	0.1175
	30	4.45E-15	2.23E-14	0.0373	0.0003	1.4948	3.3260E-16	0.0747
	45	4.45E-15	2.23E-14	0.0335	0.0006	3.2689	7.2732E-16	0.1634
	60	4.45E-15	2.23E-14	0.0353	0.0009	4.5897	1.0212E-15	0.2295
1:R3	15	4.20E-15	4.20E-15	0.0330	0.0008	4.3740	1.8371E-16	0.0437
	30	4.20E-15	4.20E-15	0.0424	0.0009	3.8508	1.6173E-16	0.0385
	45	4.20E-15	4.20E-15	0.0400	0.0010	4.5045	1.8919E-16	0.0450
	60	4.20E-15	4.20E-15	0.0358	0.0004	2.0646	8.6714E-17	0.0206
1:R4	15	4.45E-15	4.45E-15	0.0417	0.0003	1.3392	5.9596E-17	0.0134
	30	4.45E-15	4.45E-15	0.0187	0.0000	0.0000	0.0000E+00	0.0000
	45	4.45E-15	4.45E-15	0.0357	0.0004	2.0703	9.2128E-17	0.0207
	60	4.45E-15	4.45E-15	0.0362	0.0009	4.4807	1.9939E-16	0.0448

APPENDIX G. Initial Reaction Kinetics Experiment #4 – Method I.

Substrate:R	Time (sec)	R (mol RZ)	mol tat-s	CPM(c) Uncut	CPM(c) P1	% cleaved	mol P1 present	P1/R
10:R4	30	4.45E-15	4.45E-14	1440.23	34.10	4.2763	1.9029E-15	0.4276
	60	4.45E-15	4.45E-14	1587.51	37.60	4.2777	1.9036E-15	0.4278
	90	4.45E-15	4.45E-14	1470.56	35.80	4.3916	1.9543E-15	0.4392
	120	4.45E-15	4.45E-14	1489.75	42.10	5.0621	2.2526E-15	0.5062
10:R5	30	4.20E-15	4.20E-14	2269.27	26.40	2.1479	9.0211E-16	0.2148
	60	4.20E-15	4.20E-14	1860.43	26.60	2.6268	1.1033E-15	0.2627
	90	4.20E-15	4.20E-14	2046.12	18.90	1.7130	7.1945E-16	0.1713
	120	4.20E-15	4.20E-14	2239.48	27.90	2.2966	9.6458E-16	0.2297
5:R4	30	4.45E-15	2.23E-14	1725.27	28.80	3.0535	6.7939E-16	0.1527
	60	4.45E-15	2.23E-14	1349.43	39.40	5.2213	1.1617E-15	0.2611
	90	4.45E-15	2.23E-14	1878.85	40.90	3.9452	8.7782E-16	0.1973
	120	4.45E-15	2.23E-14	1770.85	56.60	5.6876	1.2655E-15	0.2844
5:R5	30	4.20E-15	2.10E-14	2016.66	17.50	1.6109	3.3830E-16	0.0805
	60	4.20E-15	2.10E-14	2152.46	26.40	2.2618	4.7498E-16	0.1131
	90	4.20E-15	2.10E-14	2551.59	33.60	2.4243	5.0911E-16	0.1212
	120	4.20E-15	2.10E-14	1963.16	24.50	2.3005	4.8311E-16	0.1150
1:R4	30	4.45E-15	4.45E-15	2294.81	52.50	4.1379	1.8414E-16	0.0414
	60	4.45E-15	4.45E-15	2197.94	43.80	3.6237	1.6125E-16	0.0362
	90	4.45E-15	4.45E-15	2145.45	61.60	5.1389	2.2868E-16	0.0514
	120	4.45E-15	4.45E-15	1563.97	44.00	5.0406	2.2431E-16	0.0504
1:R5	30	4.20E-15	4.20E-15	2294.34	27.10	2.1800	9.1561E-17	0.0218
	60	4.20E-15	4.20E-15	2088.01	22.80	2.0187	8.4785E-17	0.0202
	90	4.20E-15	4.20E-15	1802.38	27.10	2.7587	1.1586E-16	0.0276
	120	4.20E-15	4.20E-15	1862.50	26.30	2.5952	1.0900E-16	0.0260

APPENDIX H. Initial Reaction Kinetics Experiment #4 – Method II.

Substrate:R	Time (sec)	R (mol RZ)	mol tat-s	g Peak A	g Peak B	% cleaved	mol P1 present	P1/R
10:R4	30	4.45E-15	4.45E-14	0.0506	0.0021	7.2619	3.2316E-15	0.7262
	60	4.45E-15	4.45E-14	0.0487	0.0016	5.8371	2.5975E-15	0.5837
	90	4.45E-15	4.45E-14	0.0475	0.0020	7.3597	3.2751E-15	0.7360
	120	4.45E-15	4.45E-14	0.0382	0.0019	8.5794	3.8178E-15	0.8579
10:R5	30	4.20E-15	4.20E-14	0.0542	0.0012	4.0099	1.6842E-15	0.4010
	60	4.20E-15	4.20E-14	0.0485	0.0010	3.7446	1.5727E-15	0.3745
	90	4.20E-15	4.20E-14	0.0507	0.0012	4.2749	1.7954E-15	0.4275
	120	4.20E-15	4.20E-14	0.0496	0.0013	4.7122	1.9791E-15	0.4712
5:R4	30	4.45E-15	2.23E-14	0.0459	0.0016	6.1712	1.3731E-15	0.3086
	60	4.45E-15	2.23E-14	0.0490	0.0017	6.1438	1.3670E-15	0.3072
	90	4.45E-15	2.23E-14	0.0423	0.0020	8.1903	1.8224E-15	0.4095
	120	4.45E-15	2.23E-14	0.0455	0.0023	8.7072	1.9373E-15	0.4354
5:R5	30	4.20E-15	2.10E-14	0.0503	0.0008	2.9134	6.1182E-16	0.1457
	60	4.20E-15	2.10E-14	0.0598	0.0017	5.0907	1.0691E-15	0.2545
	90	4.20E-15	2.10E-14	0.0551	0.0014	4.5747	9.6069E-16	0.2287
	120	4.20E-15	2.10E-14	0.0526	0.0014	4.7817	1.0042E-15	0.2391
1:R4	30	4.45E-15	4.45E-15	0.0591	0.0026	7.6644	3.4107E-16	0.0766
	60	4.45E-15	4.45E-15	0.0489	0.0018	6.4942	2.8899E-16	0.0649
	90	4.45E-15	4.45E-15	0.0479	0.0021	7.6400	3.3998E-16	0.0764
	120	4.45E-15	4.45E-15	0.0468	0.0026	9.4877	4.2220E-16	0.0949
1:R5	30	4.20E-15	4.20E-15	0.0567	0.0014	4.4514	1.8696E-16	0.0445
	60	4.20E-15	4.20E-15	0.0555	0.0012	3.9196	1.6463E-16	0.0392
	90	4.20E-15	4.20E-15	0.0548	0.0013	4.2842	1.7994E-16	0.0428
	120	4.20E-15	4.20E-15	0.0546	0.0014	4.6147	1.9382E-16	0.0461

APPENDIX I. Initial Reaction Kinetics Experiment #5 – Method I.

Substrate:R	Time (min.)	R (mol RZ)	mol tat-s	CPM(c) Uncut	CPM(c) P1	% cleaved	mol P1 present	P1/R
10:R4	0.5	4.45E-15	4.45E-14	1271.30	24.80	3.5500	1.5798E-15	0.3550
	1	4.45E-15	4.45E-14	1499.80	49.30	5.8399	2.5988E-15	0.5840
	2	4.45E-15	4.45E-14	1843.80	23.30	2.3288	1.0363E-15	0.2329
	4	4.45E-15	4.45E-14	1242.30	14.80	2.1984	9.7828E-16	0.2198
	15	4.45E-15	4.45E-14	1652.30	16.80	1.8823	8.3763E-16	0.1882
10:R5	0.5	4.20E-15	4.20E-14	1682.80	15.80	1.7407	7.3109E-16	0.1741
	1	4.20E-15	4.20E-14	1730.80	17.80	1.9035	7.9947E-16	0.1903
	2	4.20E-15	4.20E-14	1785.80	27.30	2.8035	1.1775E-15	0.2804
	4	4.20E-15	4.20E-14	2096.30	19.80	1.7509	7.3538E-16	0.1751
	15	4.20E-15	4.20E-14	2223.30	25.30	2.1019	8.8282E-16	0.2102
5:R4	0.5	4.45E-15	2.23E-14	1546.30	27.30	3.2238	7.1729E-16	0.1612
	1	4.45E-15	2.23E-14	1380.30	29.30	3.8509	8.5683E-16	0.1925
	2	4.45E-15	2.23E-14	903.30	25.30	5.0194	1.1168E-15	0.2510
	4	4.45E-15	2.23E-14	1672.30	32.30	3.5161	7.8234E-16	0.1758
	15	4.45E-15	2.23E-14	1241.30	27.80	4.0543	9.0209E-16	0.2027
5:R5	0.5	4.20E-15	2.10E-14	2426.80	15.30	1.1756	2.4687E-16	0.0588
	1	4.20E-15	2.10E-14	2380.30	19.30	1.5068	3.1643E-16	0.0753
	2	4.20E-15	2.10E-14	2388.30	16.30	1.2714	2.6698E-16	0.0636
	4	4.20E-15	2.10E-14	1969.80	21.30	1.9994	4.1988E-16	0.1000
	15	4.20E-15	2.10E-14	1869.30	14.30	1.4228	2.9880E-16	0.0711
1:R4	0.5	4.45E-15	4.45E-15	2054.30	20.80	1.8746	8.3419E-17	0.0187
	1	4.45E-15	4.45E-15	2165.30	23.80	2.0317	9.0412E-17	0.0203
	2	4.45E-15	4.45E-15	1951.30	16.80	1.5985	7.1133E-17	0.0160
	4	4.45E-15	4.45E-15	1665.30	29.30	3.2130	1.4298E-16	0.0321
	15	4.45E-15	4.45E-15	1696.30	30.30	3.2604	1.4509E-16	0.0326

APPENDIX I (continued). Initial Reaction Kinetics Experiment #5 – Method I.

Substrate:R	Time (min.)	R (mol RZ)	mol tat-s	CPM(c) Uncut	CPM(c) P1	% cleaved	mol P1 present	P1/R
1:R5	0.5	4.20E-15	4.20E-15	1917.30	14.80	1.4355	6.0293E-17	0.0144
	1	4.20E-15	4.20E-15	2228.30	14.80	1.2377	5.1982E-17	0.0124
	2	4.20E-15	4.20E-15	2408.30	8.80	0.6847	2.8758E-17	0.0068
	4	4.20E-15	4.20E-15	1872.80	16.80	1.6644	6.9904E-17	0.0166
	15	4.20E-15	4.20E-15	1477.80	26.30	3.2488	1.3645E-16	0.0325

APPENDIX J. Initial Reaction Kinetics Experiment #5 – Method II.

Substrate:R	Time (min.)	R (mol RZ)	mol tat-s	g Peak A	g Peak B	% cleaved	mol P1 present	P1/R
10:R4	0.5	4.45E-15	4.45E-14	0.1453	0.0149	16.2117	7.2142E-15	1.6212
	1	4.45E-15	4.45E-14	0.1452	0.0197	20.3816	9.0698E-15	2.0382
	2	4.45E-15	4.45E-14	0.1374	0.0173	19.1962	8.5423E-15	1.9196
	4	4.45E-15	4.45E-14	0.1358	0.0134	15.6956	6.9846E-15	1.5696
	15	4.45E-15	4.45E-14	0.1141	0.0188	23.7155	1.0553E-14	2.3716
10:R5	0.5	4.20E-15	4.20E-14	0.1069	0.0031	5.1877	2.1788E-15	0.5188
	1	4.20E-15	4.20E-14	0.1129	0.0060	9.1134	3.8276E-15	0.9113
	2	4.20E-15	4.20E-14	0.1220	0.0076	10.5176	4.4174E-15	1.0518
	4	4.20E-15	4.20E-14	0.1221	0.0090	12.2095	5.1280E-15	1.2210
	15	4.20E-15	4.20E-14	0.1144	0.0102	14.4003	6.0481E-15	1.4400
5:R4	0.5	4.45E-15	2.23E-14	0.1278	0.0086	11.2663	2.5067E-15	0.5633
	1	4.45E-15	2.23E-14	0.1209	0.0105	14.0794	3.1327E-15	0.7040
	2	4.45E-15	2.23E-14	0.1259	0.0141	17.4447	3.8814E-15	0.8722
	4	4.45E-15	2.23E-14	0.1143	0.0217	26.3737	5.8681E-15	1.3187
	15	4.45E-15	2.23E-14	0.0804	0.0303	41.5569	9.2464E-15	2.0778
5:R5	0.5	4.20E-15	2.10E-14	0.1100	0.0064	9.8918	2.0773E-15	0.4946
	1	4.20E-15	2.10E-14	0.1132	0.0071	10.5819	2.2222E-15	0.5291
	2	4.20E-15	2.10E-14	0.1200	0.0061	8.7518	1.8379E-15	0.4376
	4	4.20E-15	2.10E-14	0.1231	0.0075	10.3103	2.1652E-15	0.5155
	15	4.20E-15	2.10E-14	0.1156	0.0102	14.2721	2.9971E-15	0.7136
1:R4	0.5	4.45E-15	4.45E-15	0.1112	0.0110	15.7287	6.9993E-16	0.1573
	1	4.45E-15	4.45E-15	0.1277	0.0130	16.1128	7.1702E-16	0.1611
	2	4.45E-15	4.45E-15	0.1147	0.0137	18.3915	8.1842E-16	0.1839
	4	4.45E-15	4.45E-15	0.1134	0.0182	23.2433	1.0343E-15	0.2324
	15	4.45E-15	4.45E-15	0.1105	0.0327	35.8297	1.5944E-15	0.3583

APPENDIX J (continued). Initial Reaction Kinetics Experiment #5 – Method II.

Substrate:R	Time (min.)	R (mol RZ)	mol tat-s	g Peak A	g Peak B	% cleaved	mol P1 present	P1/R
1:R5	0.5	4.20E-15	4.20E-15	0.1089	0.0063	9.8411	4.1333E-16	0.0984
	1	4.20E-15	4.20E-15	0.0874	0.0071	13.2904	5.5820E-16	0.1329
	2	4.20E-15	4.20E-15	0.0937	0.0090	15.3424	6.4438E-16	0.1534
	4	4.20E-15	4.20E-15	0.1022	0.0055	9.2180	3.8716E-16	0.0922
	15	4.20E-15	4.20E-15	0.1092	0.0075	11.4721	4.8183E-16	0.1147

BIBLIOGRAPHY

Ahmad, N. and S. Venkatesan. (1988). *Nef* protein of HIV-I is a transcriptional repressor of HIV-I LTR. *Science.* **241:**1481-1485.

Alizon, M., P. Sonigo, F. Barré-Sinoussi, J.-C. Chermann, P. Tiolais, L. Montagnier, and S. Wain-Hobson. (1984). Molecular cloning of lymphadenopathy-associated virus. *Nature.* **312:**757-760.

Allan, J.S., J.E. Coligan, T.H. Lee, M.F. McLane, P.J. Kanki, J.F. Groopman, and M. Essex. (1985). A new HTLV-III/LAV encoded antigen detected by antibodies from AIDS patients. *Science.* **230:**810-813.

Arya, S.K. and R.C. Gallo. (1986). Three novel genes of human T-lymphotropic virus type III: immune reactivity of their products with sera from acquired immune deficiency syndrome patients. *Proc. Natl. Acac. Sci. USA.* **83:**2209-2213.

Arya, S.K., C. Guo, S.F. Josephs, and F. Wong-Staal. (1985). *Trans*-activator of human T-lymphtropic virus type III (HTLV-III). *Science.* **229:**69-73.

Baltimore, D. (1988). Gene therapy: intracelluler immunization. *Nature.* **335:**395-396.

Barré-Sinoussi, F., J.-C. Chermann, F. Rey, M.T. Nugeyre, S. Chamaret, J. Gruest, C. Dauguet, C. Axler-Blin, F. Vezinet-Brun, C. Rouzioux, W. Rozenbaum, and L. Montagnier. (1983). Isolation of a T-lymphotropic retrovirus from a patient at risk for acquired immune deficiency syndrome (AIDS). *Science.* **220:**868-871.

Bedinger, P., A. Moriarity, R.C. von Borstel, N.J. Donovan, K.S. Steimer, and D.R. Littman. (1988). Internalization of the human immunodeficiency virus does not require cytoplasmic domain of CD4. *Nature.* **334:**162-165.

Berkhout, B., R.H. Silverman, K.-T. Jeang. (1989). Tat *trans*-activates the human immunodeficiency virus through a nascent RNA target. *Cell.* **59:**273-282.

Blattner, W.A. (1991). HIV epidemiology: past, present, and future. *FASEB J.* **5:**2340-2348.

Buzayan, J.M., W.L. Gerlach, and G. Bruening. (1986). Satellite tobacco ringspot virus RNA: a subset of the RNA sequence is sufficient for autolytic processing. *Proc. Natl. Acad. Sci. USA.* **83:**8859-8862.

Cameron, F.H. and P.A. Jennings. (1989). Specific gene expression by engineered ribozymes in monkey cells. *Proc. Natl. Acad. Sci. USA*. **86**:9139-9143.

Cech, T.R. (1988). Conserved sequences and structure of group I introns: building an active site for RNA catalysis – a review. *Gene*. **73**:259-271.

Chang, D.D. and P.A. Sharp. (1989). Regulation by HIV Rev depends upon recognition of splice sites. *Cell*. **59**:789-795.

Chang, P.S., E.M. Cantin, J.A. Zaia, P.A. Ladne, D.A. Stephens, N. Sarver, and J.J. Rossi. (1990). Ribozyme-mediated site specific cleavage of the HIV-1 genome. *Clin. Biotech*. **2**:23-31.

Cochrane, A.W., A. Perkins, and C.A. Rosen. (1990). Identification of sequences important in the nucleolar localization of human immunodeficiency virus rev: relevance of nucleolar localization to function. *J. Virol*. **64**:881-885.

Cotten, M. and M.L. Birnstiel. (1989). Ribozyme mediated destruction of RNA *in vivo*. *EMBO J*. **8**:3861-3866.

Cotten, M., G. Schaffner, and M.L. Birnstiel. (1989). Ribozyme, antisense RNA, and antisense DNA inhibition of U7 small nuclear ribonucleoprotein-mediated histone pre-mRNA processing in vitro. *Mol. Cell. Biol*. **9**:4479-4487.

Cullen, B.R. (1990). The HIV-1 Tat protein: an RNA sequence-specific processivity factor? *Cell*. **63**:655-657.

Cullen, B.R. (1991). Regulation of HIV-1 gene expression. *FASEB J*. **5**:2361-2368.

Cullen, B.R. and W.C. Greene. (1989). Regulatory pathways governing HIV-I replication. *Cell*. **58**:423-426.

Dingwall, C., I. Ernberg, M.J. Gait, S.M. Green, S. Heaphy, J. Karn, A.D. Lowe, M. Singh, M.A. Skinner, and R. Valerio. (1989). Human immunodeficiency virus 1 tat protein binds trans-activation-responsive region (TAR) RNA *in vitro*. *Proc. Natl. Acad. Sci. USA*. **86**:6925-6929.

Fauci, A.S. (1988). The human immunodeficiency virus: infectivity and mechanisms of pathogenesis. *Science*. **239**:617-622.

Feinberg, M.B., R.F. Jarrett, A. Aldovini, R.C. Gallo, and F. Wong-Staal. (1986). HTLV-III expression and production involve complex regulation at the levels of splicing and translation of viral RNA. *Cell*. **46**:807-817.

Felber, B.K., M. Hadzopoulou-Cladaras, C. Cladaras, T. Copeland, and G.N. Pavlakis. (1989). rev protein of human imunodeficiency virus type 1 affects the stability and transport of the viral mRNA. *Proc. Natl. Acad. Sci. USA*. **86:**1495-1499.

Ferguson, B.Q., B.K. Friedland, E. Hendrickson, L. Strehl, S.R. Petteway, and G.J. Jonak. (1989). Chemical synthesis and expression of a gene encoding HIV-1 TAT protein. *Bioch. and Bioph. Res. Comm.* **160:**1429-1437.

Fisher, A.G., M.B. Feinberg, S.F. Josephs, M.E. Harper, L.M. Marselle, G. Reyes, M.A. Gonda, A. Aldovini, C. Debouk, R.C. Gallo, and F. Wong-Staal. (1986). The *trans*-activator gene of HTLV-III is essential for virus replication. *Nature.* **320:**367-371.

Forster,A.C. and R.H. Symons. (1987). Self-cleavage of virusoid RNA is performed by the proposed 55-nucleotide active site. *Cell.* **50:**9-16.

Franchini, G., M. Robert-Guroff, J. Ghrayeb, N.T. Chang, and F. Wong-Staal. (1986). Cytoplasmic localization of the HTLV-III 3′ *orf* protein in cultured T cells. *Virol.* **155:**593-599.

Frankel, A.D., D.S. Bredt, and C.O. Pabo. (1988). Tat protein from human immunodeficiency virus forms a metal-linked dimer. *Science.* **240:**70-73.

Gallo, R.C., S.Z. Salahuddin, M. Popovic, G.M. Shearer, M. Kaplan, B.F. Haynes, T.J. Palker, R. Redfield, J. Oleska, B. Safai, G. White, P. Foster, and P.D. Markham. (1984). Frequent detection and isolation of cytopathic retroviruses (HTLV-III) from patients with AIDS and at risk for AIDS. *Science.* **224:**500-503.

Gartner, S., P. Markovits, D.M. Markovitz, M.H. Kaplan, R.C. Gallo, and M. Popovic. (1986). The role of mononuclear phagocytes in HTLV-III/LAV infection. *Science.* **233:**215-219.

Gatignol, A., A. Kumar, A. Rabson, and K.-T. Jeang. (1989). Identification of cellular proteins that bind to the human immunodeficiency virus type 1 trans-activation-responsive TAR element RNA. *Proc. Natl. Acad. Sci. USA*. **86:**7828-7832.

Gaynor, R., E. Soultanakis, M. Kuwabara, J. Garcia, and D.S. Sigman. (1989). Specific binding of a HeLa cell nuclear protein to RNA sequences in the human immunodeficiency virus transactivating region. *Proc. Natl. Acad. Sci. USA*. **86:**4858-4862.

Gilman, A.G. (1987). G proteins: transducers of receptor-generated signals. *Ann. Rev. Bioch.* **56**:615-649.

Goodchild, J. and V. Kohli. (1991). Ribozymes that cleave an RNA sequence from human immunodeficiency virus: the effect of flanking sequence on rate. *Arch. Bioch. and Bioph.* **284**:386-391.

Guy, B., M.B. Kieny, Y. Riviere, C. LePeuch, K. Dott, M. Girard, L. Montagnier, and J.P. Lecocq. (1987). HIV F/3′ *orf* encodes a phosphorylated GTP-binding protein resembling an oncogene product. *Nature.* **330**:266-269.

Guyader, M., M. Emerman, P. Sonigo, F. Clavel, L. Montagnier, and M. Alizon. (1987). Genome organization and transactivation of the human immunodeficiency virus type 2. *Nature.* **326**:662-669.

Hahn, B.H., G.M. Shaw, S.K. Arya, M. Popovic, R.C. Gallo, and F. Wong-Staal. (1984). Molecular cloning and characterization of the HTLV-III virus associated with AIDS. *Nature.* **312**:166-169.

Hammarskjöld, M.-L., J. Heimer, B. Hammarskjöld, I. Sangwan, L. Albert, and D. Rekosh. (1989). Regulation of human immunodeficiency virus env expression by the rev gene product. *J. Virol.* **63**:1959-1966.

Hammarskjöld, M.-L. and D. Rekosh. (1989). The molecular biology of the human inmmunodeficiency virus. *Biochim. et Biophys. Acta.* **989**:269-280.

Hammes, S.R., E.P. Dixon, M.H. Malim, B.R. Cullen, and W.C. Greene. (1989). Nef protein of human immunodeficiency virus type 1: evidence against its role as a transcriptional inhibitor. *Proc. Natl. Acad. Sci. USA.* **86**:9549-9553.

Hampel, A. and R. Tritz. (1989). RNA catalytic properties of the minimum (-)sTRSV sequence. *Biochemistry.* **28**:4929-4933.

Hampel, A. and R. Tritz. (1990). Ribozymes: a new motif--the 'hairpin'. *Comments.* **17(1)**:29.

Haseloff, J. and W.L. Gerlach. (1988). Simple RNA enzymes with new and highly specific endoribonuclease activities. *Nature.* **344**:585-591.

Haseltine, W.A. (1991). Molecular biology of the human immunodeficiency virus type 1. *FASEB J.* **5**:2349-2360.

Hauber, J. and B.R. Cullen. (1988). Mutational analysis of the *trans*-activation-responsive region of the human immunodeficiency virus type I long terminal repeat. *J. Virol.* **62**:673-679.

Hauber, J., A. Perkins, E.P. Heimer, and B.R. Cullen. (1987). Trans-activation of human immunodeficiency virus gene expression is mediated by nuclear events. *Proc. Natl. Acad. Sci. USA.* **84**:6364-6368.

Henry, J.B. (1979). *Clinical Diagnosis and Management by Laboratory Methods.* 16th ed. Vol. 1. Philadelphia: W.B. Saunders Company.

Heus, H.A. and A. Pardi. (1991). Nuclear magnetic resonance studies of the hammerhead ribozyme domain. Secondary structure formation and magnesium ion dependence. *J. Mol. Biol.* **217**:113-124.

Ho, D.D., R.J. Pomerantz, and J.C. Kaplan. (1987). Pathogenesis of infection with human immunodeficiency virus. *N. Engl. J. Med.* **317**:278-286.

Ho, D.D., T.R. Rotan, and M.S. Hirsch. (1986). Infection of monocyte/macrophages by human T lymphotropic viruses type III. *J. Clin. Invest.* **77**:1712-1715.

Holt, J. and R. Lechner. (1990). Sequence-specific anti-RNA reagents for cell physiology. *Comments.* **16(14)**:1.

Jakobovits, A., D.H. Smith, E.B. Jakobovits, and D.J. Capon. (1988). A discrete element 3′ of human immunodeficiency virus 1 (HIV-1) and HIV-2 mRNA initiation sites mediates transcriptional activation by an HIV *trans* activator. *Mol. Cell. Biol.* **8**:2555-2561.

Keshet, E., and H.M. Temin. (1979). Cell-killing by spleen necrosis virus is correlated with a transient accumulation of spleen necrosis virus DNA. *J. Virol.* **31**:376-388.

Kim, S., K. Ikeuchi, R. Byrn, J. Groopman, and D. Baltimore. (1989). Lack of a negative influence on viral growth by the *nef* gene of human immunodeficiency virus type 1. *Proc. Natl. Acad. Sci. USA.* **86**:9544-9548.

Klatzmann, D., F. Barré-Sinoussi, M.T. Nugeyre, C. Dauguet, E. Vilmer, C. Griscelli, F. Brun-Vezinet, C. Rouzioux, J.C. Gluckman, J.-C. Chermann, and L. Montagnier. (1984). Selective tropism of lymphadenopathy associated virus (LAV) for helper-induced T lymphocytes. *Science.* **225**:59-63.

Kong, L.I., S.W. Lee, J.C. Kappes, J.S. Parkin, D. Decker, J.A. Hoxie, B.H. Hahn, and G.M. Shaw. (1988). West African HIV-2-related human retrovirus with attenuated cytopathicity. *Science.* **240:**1525-1529.

Kruger, K., P.J. Grabowski, A.J. Zaug, J. Sands, D.E. Gottschling, and T.R. Cech. (1982). Self-splicing RNA: autoexcision and autocyclization of the ribozomal RNA intervening sequence of Tetrahymena. *Cell.* **31:**147-157.

Laspia, M.F., A.P. Rice, and M.B. Mathews. (1990). Synergy between HIV-1 Tat and adenovirus E1A is principaly due to stabilization of transcriptional elongation. *Genes Dev.* **4:**2397-2408.

Lazinski, D., E. Grzadzielska, and A. Das. (1989). Sequence-specific recognition of RNA hairpins by bacteriophage antiterminators requires a conserved arginine-rich motif. *Cell.* **59:**207-218.

Lewin, B. (1990). *Genes IV.* New York: Oxford University Press.

Levy, J.A. (1989). Pathogenesis of human immunodeficiency virus infection. *Annals NY Acad. Sci.* **567:**58-68.

Levy, J.A., A.D. Hoffman, S.M. Kramer, J.A. Landis, J.M. Shimabukuro, and L.S. Oshiro. (1984). Isolation of lymphocytopathic retroviruses from San Francisco patients with AIDS. *Science.* **225:**840-842.

Lo, K.M.S., M.A. Biasolo, G. Dehni, G. Palú, and W.A. Haseltine. (1992). Inhibition of replication of HIV-1 by retroviral vectors expressing *tat*-antisense and anti-*tat* ribozyme RNA. *Virology.* **190:**176-183.

Lorentzen, E.U., U. Wieland, J.E. Kühn, and R.W. Braun. (1991). In vitro cleavage of HIV-1 vif RNA by a synthetic ribozyme. *Virus Genes.* **5:**17-23.

Luciw, P.A., C. Cheng-Mayer, and P.A. Levy. (1987). Mutational analysis of the human immunodeficiency virus: the *orf-B* region down-regulates virus replication. *Proc. Natl. Acad. Sci. USA.* **84:**1434-1438.

Luciw, P.A., S.J. Potter, K. Steimer, D. Dina, and J.A. Levy. (1984). Molecular cloning of AIDS-associated virus. *Nature.* **312:**760-763.

Maddon, P.J., A.G. Dalgleish, J.S. McDougal, P.R. Clapham, R.A. Weiss, and R. Axel. (1986). The T4 gene encodes the AIDS virus receptor and is expressed in the immune system and the brain. *Cell.* **47:**333-348.

Malim, M.H., S. Böhnlein, J. Hauber, and B.R. Cullen. (1989a). Functional dissection of the HIV-1 Rev *trans*-activator-derivation of a *trans*-dominant repressor of Rev function. *Cell.* **58**:205-214.

Malim, M.H., J. Hauber, R. Fenrick, and B.R. Cullen. (1988). Immunodeficiency virus *rev trans*-activator modulates the expression of the viral regulatory genes. *Nature.* **335**:181-183.

Malim, M.H., J. Hauber, S.-Y. Le, J.V. Maizel, and B.R. Cullen. (1989b). The HIV-1 *rev trans*-activator acts through a structural target sequence to activate nuclear export of unspliced viral mRNA. *Nature.* **338**:254-257.

Maniatis, T., E.F. Fritsch, and J. Sambrook. (1982). *Molecular Cloning. A laborotory manual.* New York: Cold Spring Harbor Press.

Marciniak, R.A., B.J. Calnan, A.D. Frankel, and P.A. Sharp. (1990a). HIV-1 Tat protein *trans*-activates transcription in vitro. *Cell.* **63**:791-802.

Marciniak, R.A., M.A. Garcia-Blanco, and P.A. Sharp. (1990b). Identification and characterization of a HeLa nuclear protein that specifically binds to the trans-activation-response (TAR) element of human immunodeficiency virus. *Proc. Natl. Acad. Sci. USA.* **87**:3624-3628.

McClure, M.O., M. Marsh, and R.A. Weiss. (1988). Human immunodeficiency virus infection of CD4-bearing cells occurs by a pH-independent mechanism. *EMBO J.* **7**:513-518.

McDougal, J.S., M.S. Kennedy, J.M. Sligh, S.P. Cort, A. Mawle, and J.K.A. Nicholson. (1986). Binding of HTLV-III/LAV to $T4^+$ T cells by a complex of the 110K viral protein and the T4 molecule. *Science.* **231**:382-385.

Melton, D.A., P.A. Krieg, M.R. Rebagliati, T. Maniatis, K. Zinn, and M.R. Green. (1984). Efficient *in vitro* synthesis of biologically active RNA and RNA hybridization probes from plasmids containing a bacteriophage SP6 promoter. *Nucl. Acids Res.* **12**:7035-7056.

Milligan, J.F., D.R. Groebe, G.W. Witherell, and O.C. Uhlenbeck. (1987). Oligoribonucleotide synthesis using T7 RNA polymerase and synthetic DNA templates. *Nucl. Acids Res.* **15**:8783-8798.

Mitsuya, H., K.J. Weinhold, P.A. Furman, M.H. St. Clair, S. Nusinoff Lehrman, R.C. Gallo, D. Bolognesi, D.W. Barry, and S. Broder. (1985). 3'-Azido-3'-deoxythymidine (BW A509U): an antiviral agent that inhibits the infectivity and cytopathic effect of human T-lymphotropic virus type III/lymphadenopathy-associated virus *in vitro*. *Proc. Natl. Acad. Sci. USA*. **82:**7096-7100.

Mitsuya, H., R. Yarchoan, and S. Broder. (1990). Molecular targets for AIDS therapy. *Science*. **249:**1533-1544.

Muesing, M.A., D.H. Smith, C.D. Cabradilla, C.V. Benton, L.A. Lasky, and D.J. Capon. (1985). Nucleic acid structure and expression of the human AIDS/lymphadenopathy retrovirus. *Nature*. **313:**450-458.

Muesing, M.A., D.H. Smith, and D.J. Capon. (1987). Regulation of mRNA accumulation by a human immunodeficiency virus trans-activator protein. *Cell*. **48:**691-701.

Nelbock, P., P.J. Dillon, A. Perkins, and C.A. Rosen. (1990). A cDNA for a protein that interacts with the human immunodeficiency virus Tat transactivator. *Science*. **248:**1650-1653.

Niederman, T.M.J., B.J. Thielan, and L. Ratner. (1989). Human immunodeficiency virus type 1 negative factor is a transcriptional silencer. *Proc. Natl. Acad. Sci. USA*. **86:**1128-1132.

Perkins, A., A.W. Cochrane, S.M. Ruben, and C.A. Rosen. (1989). Structural and functional characterization of the human immunodeficiency virus *rev* protein. *J. Acq. Immun. Def. Syn.* **2:**256-263.

Popovic, M., M.G. Sarngadharan, E. Read, and R.C. Gallo. (1984). Detection, isolation, and continuous production of cytopathic retroviruses (HTLV-III) from patients with AIDS and pre-AIDS. *Science*. **224:**497-500.

Prody, G.A., J.T. Bakos, J.M. Buzayan, I.R. Schneider, and G. Bruening. (1986). Autolytic processing of dimeric plant virus satellite RNA. *Science*. **231:**1577-1580.

Rabson, A.B. and M.A. Martin. (1985). Molecular organization of the AIDS retrovirus. *Cell*. **40:**477-480.

Ratner, L., W. Haseltine, R. Patarca, K.L. Livak, B. Starcich, S.F. Josephs, E.R. Doran, J.A. Rafalski, E.A. Whitehorn, K. Baumeister, L. Ivanoff, S.R. Petteway, Jr., M.L. Pearson, J.A. Lautenberger, T.S. Papas, J. Ghrayeb, N.T. Chang, R.C. Gallo, and F. Wong-Staal. (1985). Complete nucleotide sequence of the AIDS virus, HTLV-III. *Nature.* **313**:277-284.

Robert-Guroff, M., M. Popovic, S. Gartner, P. Markham, R.C. Gallo, and M.S. Reitz. (1990). Structure and expression of *tat*-, *rev*-, and *nef*-specific transcripts of human immunodeficiency virus type 1 in infected lymphocytes and macrophages. *J. Virol.* **64**:3391-3398.

Rosen, C.A., J.G. Sodroski, and W.A. Haseltine. (1985). The location of *cis*-acting regulatory sequences in the human T cell lymphotropic virus type III (HTLV-III/LAV) long terminal repeat. *Cell.* **41**:813-823.

Rosenberg, Z.F. and A.S. Fauci. (1989). The immunopathogenesis of HIV infection. *Adv. in Immunol.* **47**:377-431.

Roy, S., U. Delling, C.-H. Chen, C.A. Rosen, and N. Sonenberg. (1990). A bulge structure in HIV-1 TAR RNA is required for Tat binding and Tat-mediated *trans*-activation. *Genes Dev.* **4**:1365-1373.

Sambrook, J., E.F. Fritsch, and T. Maniatis. (1989). *Molecular Cloning. A Laboratory Manual, Second Edition.* (C. Nolan, ed.). New York: Cold Spring Harbor Laboratory Press.

Sanchez-Pescador, R., M.D. Power, P.J. Barr, K.S. Steimer, M.M. Stempien, S.L. Brown-Shimer, W.W. Gee, A. Renard, A. Randolph, J.A. Levy, D. Dina, and P.A. Luciw. (1985). Nucleotide sequence and expression of an AIDS-associated retrovirus (ARV-2). *Science.* **227**:484-492.

Sarver, N., E.M. Cantin, P.S. Chang, J.A. Zaia, P.A. Ladne, D.A. Stephens, and J.J. Rossi. (1990). Ribozymes as potential anti-HIV-1 thrapeutic agents. *Science.* **247**:1222-1225.

Schnittman, S.M., M.C. Psallidopoulos, H.C. Lane, L. Thompson, M. Baseler, F. Massari, C.H. Fox, N.P. Salzman, and A.S. Fauci. (1989). The reservoir for HIV-1 in human peripheral blood is a T cell that maintains expression of CD4. *Science.* **245**:305-308.

Selby, M.J., E.S. Bain, P.A. Luciw, and B.M. Peterlin. (1989). Structure, sequence, and position of the stem-loop in *tar* determine transcriptional elongation by *tat* through the HIV-1 long terminal repeat. *Genes and Dev.* **3**:547-558.

Sharp, P.A. and R.A. Marciniak. (1989). HIV TAR: an RNA enhancer? *Cell.* **59:**229-230.

Shaw, G.M., B.H. Hahn, S.K. Arya, J.E. Groopman, R.C. Gallo, and F. Wong-Staal. (1984). Molecular characterization of human T-cell leukemia (lymphotropic) virus type III in the acquired immune deficiency syndrome. *Science.* **226:**1165-1171.

Sodroski, J., W.C. Goh, C. Rosen, A. Dayton, E. Terwilliger, and W. Haseltine. (1986). A second post-transcriptional *trans*-activator gene required for HTLV-III replication. *Nature.* **321:**412-417.

Sodroski, J., R. Patarca, C. Rosen, F. Wong-Staal, and W. Haseltine. (1985a). Location of the *trans*-activating region on the genome of human T-cell lymphotropic virus type III. *Science.* **229:**74-77.

Sodroski, J., C. Rosen, F. Wong-Staal, S.Z. Salahuddin, M. Popovic, S. Arya, R.C. Gallo, and W.A. Haseltine. (1985b). *Trans*-acting transcriptional regulation of human T-cell leukemia virus type III long terminal repeat. *Science.* **227:**171-173.

Stein, B.S., S.D. Gowda, J.D. Lifson, R.C. Penhallow, K.G. Bensch, and E.G. Engleman. (1987). pH-independent HIV entry into CD4-positive T cells via virus envelope fusion to the plasma membrane. *Cell.* **49:**569-668.

Terwilliger, E., J.G. Sodroski, C.A. Rosen, and W.A. Haseltine. (1986). Effects of mutations within the 3′ *orf* open reading frame region of human T-cell lymphotropic virus type III (HTLV-III/LAV) on replication and cytopathogenicity. *J. Virol.* **60:**754-760.

Titus, D.E., ed. *Promega Protocols and Applications Guide, Second Edition.* (1991). U.S.A.: Promega Corporation.

Uhlenbeck, O.C. (1987). A small catalytic oligoribonucleotide. *Nature.* **328:**596-600.

Varmus, H. (1989). Retroviruses. *Science.* **240:**1427-1435.

Vaishnav, Y.N. and F. Wong-Staal. (1991). The biochemistry of AIDS. *Ann. Rev. Biochem.* **60:**577-630.

Wain-Hobson, S., P. Sonigo, O. Danos, S. Cole, and M. Alizon. (1985). Nucleotide sequence of the AIDS virus, LAV. *Cell.* **40:**9-17.

Wang, A.V.T. (1987). Molecular characterization of a cytoplasmic actin gene developmentally regulated during sea urchin embryogenesis. Doctoral dissertation, Univ. of Hawaii, Dept. of Bioch. & Bioph.

Waring, R.B. and R.W. Davies. (1984). Assessment of a model for intron RNA secondary structure relevant to RNA self-splicing – a review. *Gene.* **28:**277-291.

Weeks, K.M., C. Ampe, S.C. Schultz, T.A. Steitz, and D.M. Crothers. (1990). Fragments of the HIV-1 Tat protein specifically bind TAR RNA. *Science.* **249:**1281-1285.

Weerasinghe, M., S.E. Liem, S. Asad, S.E. Read, and S. Joshi. (1991). Resistance to human immunodeficiency virus type 1 (HIV-1) infection in human $CD4^+$ lymphocyte-derived cell lines conferred by using retroviral vectors expressing an HIV-1 RNA-specific ribozyme. *J. Virol.* **65:**5531-5534.

Zaug, A.J., M.D. Been, and T.R. Cech. (1986). The *Tetrahymena* ribozyme acts like an RNA restriction endonuclease. *Nature.* **324:**429-433.